ADAPTIVE DEFIBRILLATOR DESIGN

A THESIS SUBMITTED FOR THE

DEGREE OF MASTER OF ENGINEERING (ELECTRICAL)

BY HOSSIEN MAHDAVIAN

B.E. (ELECTRONICS)

DEPARTMENT OF ELECTRICAL AND ELECTRONIC ENGINEERING,

VICTORIA UNIVERSITY OF TECHNOLOGY, FOOTSCRAY CAMPUS,

MAY 1993

TABLE OF CONTENTS

CHAPTER 2

LITERATURE SURVEY

CHAPTER 3

ADAPTIVE DEFIBRILLATOR DESIGN

CHAPTER 4

EXPERIMENTAL METHODS AND RESULTS

CHAPTER 5

CONCLUSION

APPENDICES

ACKNOWLEDGEMENTS

I wish to show my appreciation to :

1- Professor Packer for his guidance during this research, without whom, the task of completing this thesis would have been difficult.

Professor Packer's suggestions which originate from his insight into Biomedical Engineering have been very valuable for me.

2- Dr. Zayegh who originally introduced and made contribution to the subject of this research program, and I am grateful for his support and supervision.

3- Dr. Malyniak for his helpful and constructive comments on the thesis.

4- Dr. Kalam for his guidance during Dr. Zayegh's absence and corrections in the writing up stage.

5- Dr. Williamson (M.D.) for correcting physiological aspects of the thesis.

LIST OF FIGURES

LIST OF TABLES

ABSTRACT

Defibrillators are medical equipments which are widely used to resume the normal pacemaking activities of the heart in patients with myocardium abnormalities.

Electrical defibrillation is usually achieved by passing an electrical current pulse transthoracically through the heart of the patient. The source of this electrical current is usually a high voltage capacitor. This capacitor is charged to a voltage between 3000 and 6000 volts and then discharged via a relay through the transthoracic cavity of the patient. An inductor is used in series with the capacitor to generate an electrical current pulse with a damped sinusoidal shape (Lown waveform) and a duration of 5-10 msec.

The successful operation of defibrillators depends on two parameters, Transthoracic Resistance (TTR) and the peak defibrillation current.

Transthoracic Resistance is the electrical resistance, measured at the defibrillator electrodes. Peak defibrillator current is the maximum current which passes through the defibrillator electrodes and hence, through the transthoracic cavity of the patient.

During defibrillation, high TTRs cause low current and low TTRs cause high current to pass through the myocardium tissues. While high current through the heart damages its tissues, low current through the heart, may not be enough to defibrillate the heart.

So far, control of this peak current during defibrillation by measurement and adjustment of the TTR has not been attempted (adaptive defibrillation). In this thesis, a method is described for implementing such an adaptive defibrillator by control of the defibrillator current. In this method, during the early stages of the electrical discharge of the capacitor, the TTR of the patient is measured and the

current through the TTR is adjusted by switching in a by-passing network consisting of a power switch and a power resistor.

In this project, to simulate the operation of a defibrillator, a hardware device with scaled values was designed and built. Also, the algorithm proposed by this research, for the implementation of the adaptive defibrillator, was successfully tested.

SUMMARY OF CONTENT

In chapter 1, the principal electrical and physiological activities of the heart are discussed. Mechanism of fibrillation, electric shock and defibrillation are also discussed in chapter 1.

The defibrillator's structure and a review of past work in determination of the TTR and defibrillator threshold current is given in chapter 2.

In chapter 3, an outline of the requirements for an adaptive defibrillator is given. Based on this outline, a hardware model which simulates the operation of a defibrillator is designed. Technical considerations in designing this model and their implication in an adaptive defibrillator are described in this chapter. The look-up tables used for calculation of the TTR are also given in chapter 3.

Chapter 4 describes the steps taken in testing the model. The plots and photographs of the resultant waveforms for various test resistors are given in this chapter. The operation of the model and the results are also discussed in chapter 4.

Chapter 5 includes a general description of the project, conclusions, limitations and recommendations for future work.

CHAPTER 1

PHYSIOLOGICAL ASPECTS

In this chapter, the basic information of electro-physiology of a living cell membrane is initially discussed and then used as an introduction to myocardial tissue activities (e.g. rhythmicity and refractory period). Also, several aspects related to the heart and defibrillator functions are included. Some of these aspects are the electrocardiogram, the cardiac cycle, causes of fibrillation and electric shock.

1.1 MEMBRANE POTENTIALS[1]

Small electric potentials exist across all living cell membranes. Some cells such as nerve and muscle cells are excitable. This means they can generate electrochemical impulses at their membranes and they can use these impulses to transmit signals along the membranes.

There are two basic means by which membrane potentials can develop:

1) Diffusion of ions through the membrane due to ion concentration differences between the two side of the membrane, and

2) Active transport of ions through the membrane.

Both generate an imbalance between negative and positive charges (hence generating a potential across the membrane).

When a concentration difference of a single type of ion across a membrane causes diffusion of ions through the membrane (generating a membrane potential), the magnitude of the potential inside the membrane versus the outside is determined by the following equation (derived for body temperature 38°C) :

$$\text{EMF (millivolts)} = -61 \log \frac{\text{concentration inside}}{\text{concentration outside}}$$

1. Section 1.1 to 1.3 are summaries of a detailed description of membranes given in [15].

This is the Nernst equation and the potential is the Nernst potential. Two conditions are necessary for the Nernst potential to develop as a result of diffusion:

1) The membrane must be selectively permeable, allowing a single type of ion to diffuse through the membrane while other ions do not diffuse.

2) The concentration of the diffused ions must be greater on one side of the membrane than the other side.

When a membrane is permeable to several different ions , the resultant diffusion potential depends on :

a) The polarity of the electrical charge of each ion

b) The permeability of the membrane to each ion, and

c) The concentration of the ions on the inside and outside of the membrane.

The Goldman-Hodgkin-Katz equation calculates the membrane potential when two univalent positive ions, sodium(Na^+) and potassium (K^+) and one univalent negative ion, chloride (Cl^-) are involved [15]:

$$\text{EMF (millivolts)} = -61 \log \frac{C_{Na+i}\, P_{Na+} + C_{k+i}\, P_{K+} + C_{Cl-o}\, P_{Cl-}}{C_{Na+o}\, P_{Na+} + C_{k+o}\, P_{K+} + C_{Cl-i}\, P_{Cl-}}$$

where the C is the concentration in milli-equivalence (mEq) and P is the permeability in milli-mole/m^2/sec.

Sodium, potassium and chloride ions are the most important ions involved in creating membrane potentials in nerve, muscle fibres (skeletal, cardiac and smooth) and neurones.

As briefly discussed before, a potential is also created across a membrane by active transport of ions. Cell membranes have a powerful sodium-potassium pump which pumps three sodium ions to the extracellular fluid and two potassium ions to the inside (active

transport). This is an electrogenic pump. As more positive charges result on the outside than the inside, a positive ion deficit on the inside remains. That is, the intracellular potential is negative.

This sodium-potassium pump causes a concentration gradient for sodium and potassium across the resting membrane. The ratio of the concentration of ions from the inside to the outside is:

$$Na^+ \text{ inside/ } Na^+ \text{ outside} = 13.5/135 = 0.1$$
$$K^+ \text{ inside/ } K^+ \text{ outside} = 140/4 = 35.$$

On the other hand, there exists a channel type of transport protein in the cell membrane through which potassium and sodium ions can leak. These channels are called potassium-sodium "Leak" channels and are 100 times more permeable to potassium than sodium.

The normal concentration of potassium ions inside the nerve fibre is approximately 140 mEq per litre and 4 mEq per litre on the outside. Hence the Nernst potential is :

$$EMF = -61 \log 140/4 = -94 \text{ mV}$$

On the other hand, if there is no pumping of ions through the nerve membrane and if the membrane was only permeable to sodium but not to all other ions, then :

$$EMF = -61 \log 0.1 = +61 \text{ mV}$$

In the resting state, the diffusion potentials alone caused by potassium and sodium diffusion would create a membrane potential of approximately -86 mV. Almost all of this being determined by the potassium diffusion. An additional -4 mV is contributed to the membrane potential by the electrogenic Na^+-K^+ pump giving a total resting membrane potential of -90 mV .

The resting membrane potential in large skeletal muscle fibres is also approximately -90 mV. In small nerve fibres and small muscle fibres (e.g. smooth muscles) the membrane potential is between -40 and -60 mV.

1.2 ACTION POTENTIAL

Action potentials are rapid changes in the membrane potential. Nerve signals are transmitted by these potentials. Each action potential

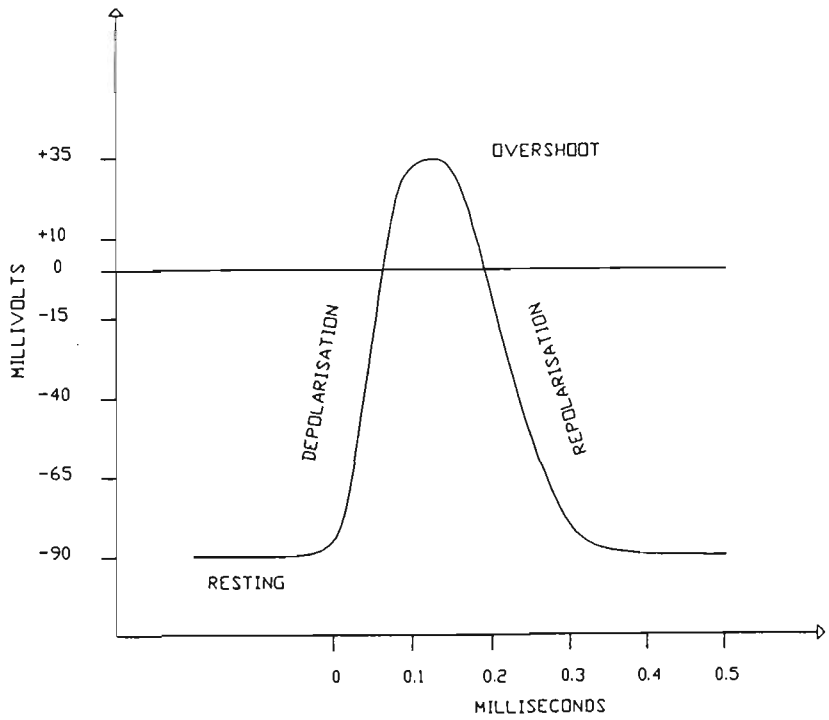

Figure 1.1 A typical action potential

begins by a sudden change from negative resting potential to a positive membrane potential and almost ends with equally rapid change back again to the negative potential. A typical action potential is shown in Figure 1.1.

At the resting stage the membrane is said to be polarised because of the negative membrane potential (-90 mV).

At the depolarisation stage, the membrane suddenly becomes very permeable to sodium ions allowing tremendous numbers of sodium ions to flow to the interior of the axon. In large nerve fibres, the result is that, the resting potential of -90 mV is changed to a positive potential. However, for smaller fibres and central nervous system neurones the potential only approaches the zero level with no overshoot, towards a positive voltage.

At the repolarisation stage, the membrane becomes highly permeable to

potassium ions as the sodium channels close as rapidly as they had opened. Hence the normal resting potential is re-established.

The principal factor in causing both depolarisation and repolarisation of the nerve membrane during the action potential, is the voltage-gated sodium and potassium channels. These two voltage-gated channels are in addition to the Na^+-K^+ pump and Na^+-K^+ leak channels.

As long as the membrane of a nerve fibre remains undisturbed, no action potential is generated. However, if any event causes the resting potential to rise from -90 mV to threshold level, voltage-gated sodium channels are affected and opened. This allows rapid inflow of sodium ions which increases the membrane potential further until all of the voltage-gated sodium channels are opened. But, within another fraction of a millisecond the rising membrane potential causes inactivation of the sodium channels and the action potential terminates.

An action potential occurs only when the initial rise in membrane potential is great enough. Usually a sudden rise of 15 to 30 mV in membrane potential is required to generate an action potential, (e.g. from -90 to -65 mV). The minimum membrane potential required to generate an action potential is called the stimulation threshold (e.g. -65 mV).

The action potential propagates by exciting the adjacent portion of the membrane. In this way depolarisation and repolarisation are transmitted.

A second action potential cannot occur in an excitable fibre as long as the membrane is still depolarised from the preceding action potential. The reason is that the sodium channels are inactivated shortly after initiation of the action potential and no stimulus can open these channels. Only when the membrane potential reaches the resting potential can these channels be reopened. The period during which a second action potential cannot be generated with any stimuli is called the absolute refractory period. This period is about 1/2500 second for large myelinated nerve fibres (fast fibres).

There exists a relative refractory period lasting one quarter to one half of the absolute refractory period during which stronger than normal stimuli can excite the fibre.

1.3 RHYTHMICITY OF EXCITABLE TISSUES

If the threshold for stimulation is reduced, repetitive discharge of excitable tissues can occur. In the heart, most smooth muscles and main neurones of the central nervous system, repetitive discharges occur normally. These rhythmical discharges are the basis of the heart beat, control of breathing and peristalsis.

Rhythmicity occurs if the membrane, even in its natural state is permeable to sodium ions (or to Ca^{++}-Na^{+} slow channels) to allow automatic membrane depolarisation. So for automatic depolarisation the resting potential must be only -60 to -70 mV. This voltage is not negative enough to keep closed the sodium (or Na^{+}-Ca^{++}) channels. As a result sodium and calcium ions flow inward, increasing the permeability of the membrane which increases flow of these ions. Hence a regenerative condition begins until an action potential is created.

At the end of the action potential, the membrane repolarises and shortly after, with a new action potential generated in the same way, the membrane depolarises. The depolarisation-repolarisation cycle continues again and again causing self induced rhythmical excitation.

It must be noted that due to the long refractory period of the excitable tissues, the depolarisation cannot occur immediately after the repolarisation, hence the cycle of depolarisation-repolarisation is sustained.

1.4 THE CIRCULATORY SYSTEM

The primary functions of the circulatory system are to deliver oxygen and nutrients to the body tissues for metabolism and to remove waste products for excretion. The blood, which is pumped by the heart,

carries these substances to all the tissues in the body via the blood vessels. Figure 1.2 illustrates the main features of the circulatory system.

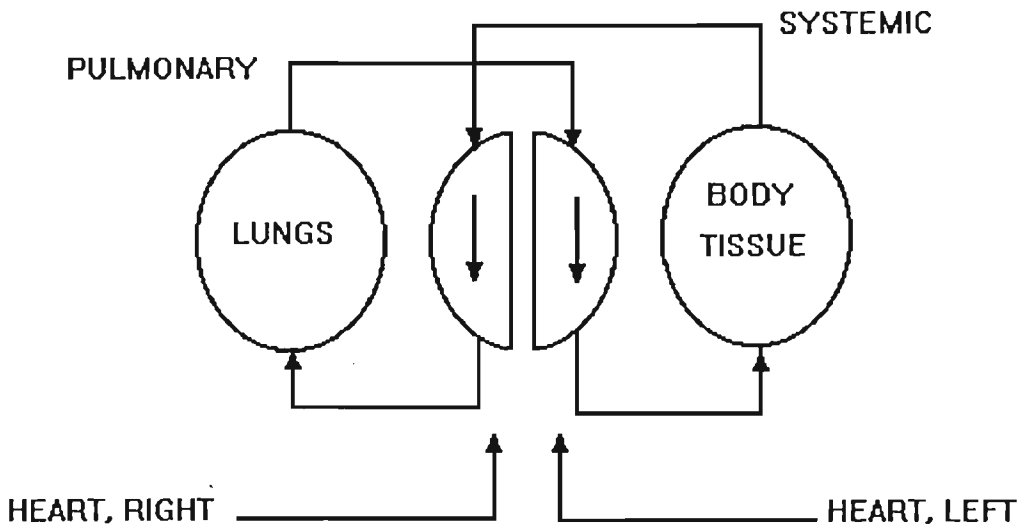

Figure 1.2 Circulatory system of human body

1.5 THE HEART

1.5.1. THE STRUCTURE OF THE HEART

The heart has the cardiac muscle types:

a) Atrial
b) Ventricular
c) Specialised excitatory and conductive muscle.

The atrial and ventricular muscles contract the same way as skeletal muscles except that the duration of a single twitch is much longer. The specialised excitatory and conductive fibres contract only feebly because they contain few contractile fibres. These fibres, however provide an important excitatory system for the heart and a transmission system for rapid conduction of the cardiac excitatory signals through the heart.

The heart is basically a double in line dual pump providing intermittent pressure for pulmonary and systemic circulation. The muscular tissue is the myocardium. The heart is divided into two halves and its operation is shown in Figure 1.2 and Figure 1.3.

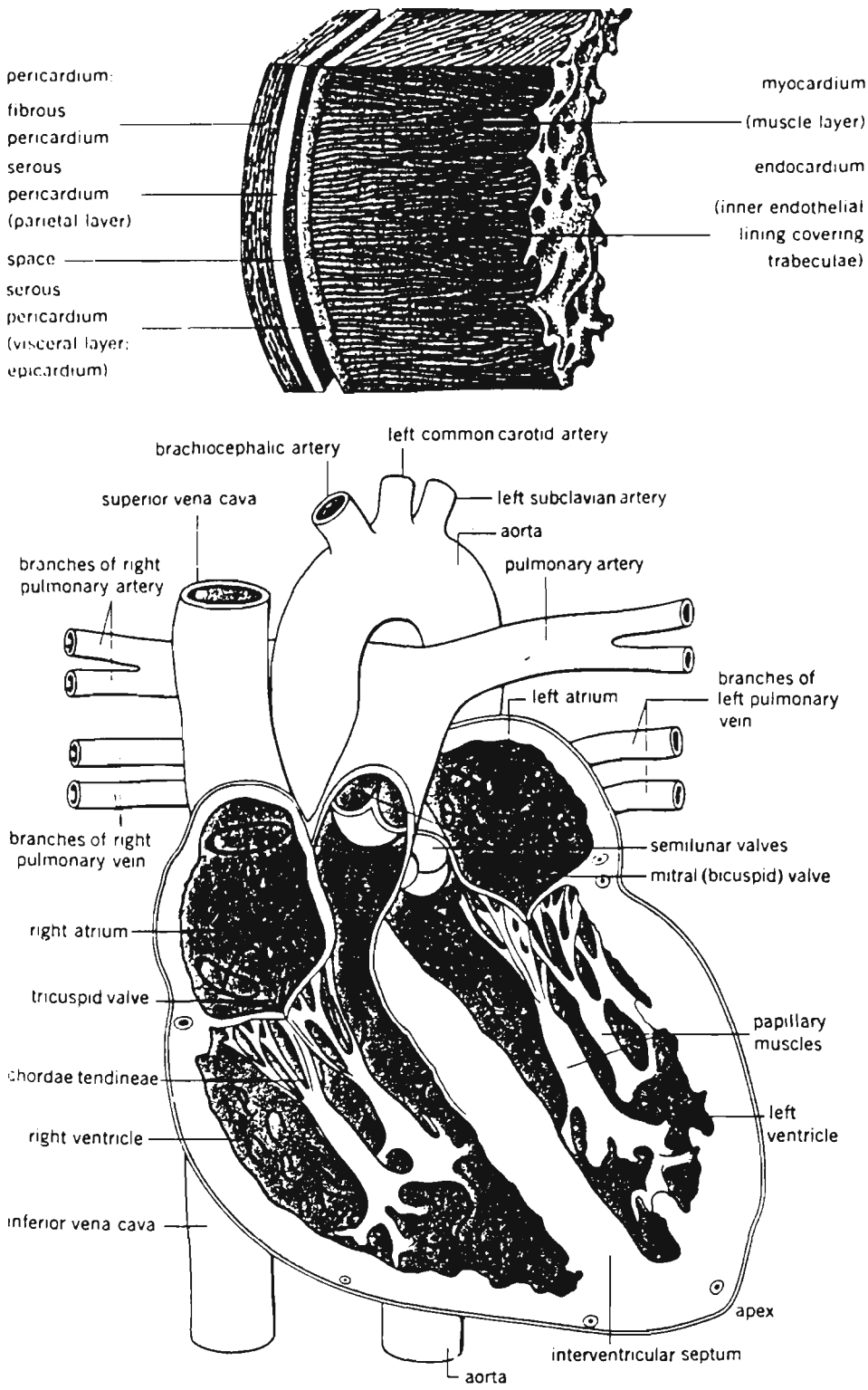

Figure 1.3 Cross sectional diagram of the heart showing the position of the valves and the direction of the blood flow inside the heart [3].

1.5.2. THE CARDIAC CYCLE

The cardiac cycle is a two stage cycle, namely:

a) Diastole (relaxation)

b) Systole (contraction)

Figure 1.4 illustrates the relation of systole and diastole with ventricular and aortic pressure, the valvular mechanics, atrial pressure, the ECG and phonocardiogram.

During diastole, the atria and ventricles are relaxed. Blood returning from the lungs and the body flows into the atria. The tricuspid and mitral valves are both open allowing blood flow into the ventricles. The aortic and pulmonary valves are both closed from pressure in their outflow vessels. Hence, blood cannot flow back into the ventricles (Figure 1.3).

During systole, the heart contracts forcing blood into the arterial system. The cycle starts with atrial systole pumping blood into the

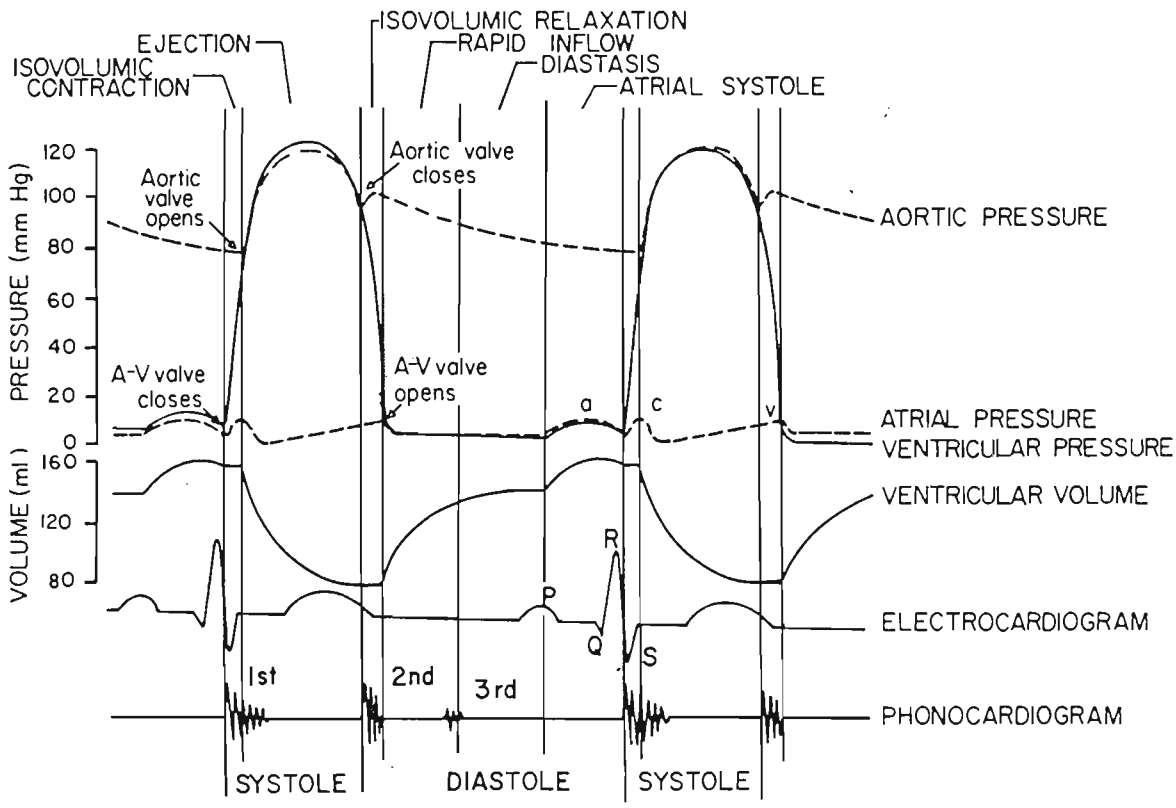

Figure 1.4. Cardiac cycle [15].

ventricles. This, however, accounts for only 10-15% of the ventricles, blood volume capacity. After a brief pause, in order to allow the ventricles to fill completely, ventricular systole begins. The contraction commences at the apex of the heart and spreads towards the base of the heart, thus forcing blood out through the pulmonary and aortic valves into the arteries. Both sides of the heart contract in unison. The blood vessels convert the pulsating output of the heart into a smooth flow of blood through the capillaries.

1.6. ELECTRICAL ACTIVITY OF THE HEART

1.6.1 ELECTRICAL PROPERTIES OF THE MYOCARDIUM

The myocardium cell membrane has the ability to propagate a depolarisation wave to other cells resulting in myocardial contraction. Myocardium structure is a syncytium (e.g. continuous cell membrane for all cells). Once a part is depolarised, it travels to all others (all or nothing effect).

There are three very important differences between the electrical activity of cardiac muscle and skeletal muscle.

1. In skeletal muscle, a depolarisation wave travels at a uniform rate. In the myocardium, there are specialized high speed conductive pathways which conduct a depolarisation wave throughout the heart much more rapidly than others.

2. The duration of depolarisation and hence, of the refractory period in myocardium is approximately 100 times longer than in skeletal muscle.

3. Specialised myocardial cells called pacemakers exist in the SA node (Figure 1.5) whose myocardial cell membrane does not require an external stimulus to reach the threshold. These cells can spontaneously depolarise at periodic intervals without the need for an external stimulus. This activity is called automaticity.

1.6.2 CELL GROUPS WITHIN THE HEART

Figure 1.5 shows some special cells within the myocardium. They have characteristics different from those of normal cells.

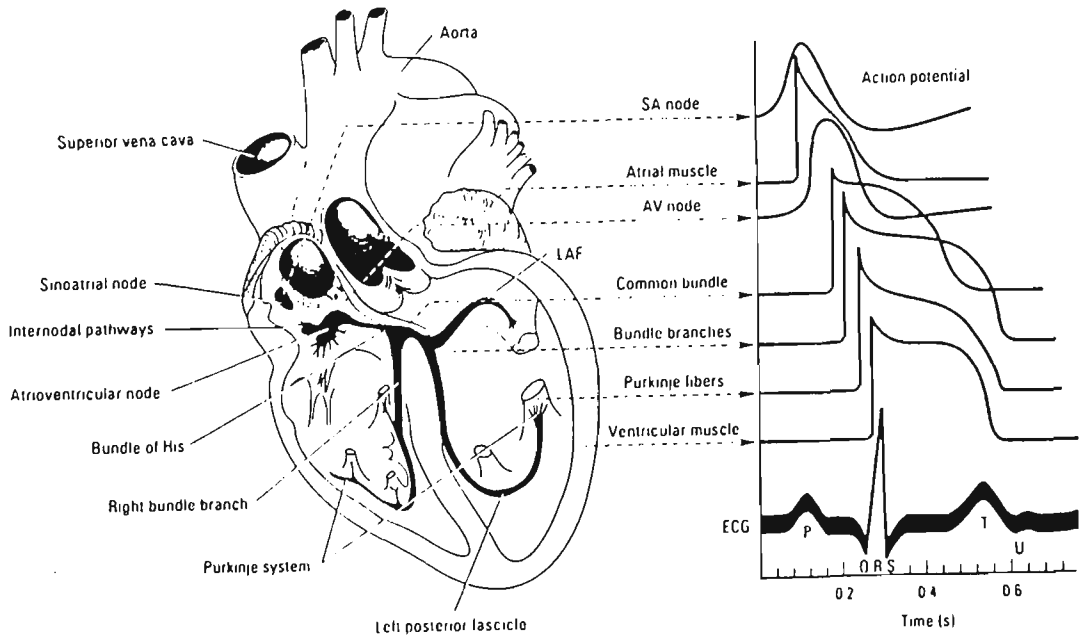

Figure 1.5 Pacemaker cells in the myocardium [9].

The pacemaker cells, which depolarise at the fastest rate, are grouped in the Sino Atrial (SA) node located in the back wall of the right atrium. These cells depolarise at the rate of about 70 to 75 per minute. The next fastest rate is found in the Atrio-Ventricular (AV) node at the junction between the atria and ventricles. The cells in the AV node depolarise at the rate of about 60 per minute.

The highly conductive paths of the heart start with the "Bundle of His" at the AV node which spontaneously depolarise at a rate of 50 to 55 times per minute and terminate in the "Purkinje Network" whose cells automatically depolarise at a rate of 40 to 45 per minute.

The muscle cells, which make up the bulk of the heart (myocardium), depolarise at a rate of 30 to 35 per minute.

1.6.3 ELECTRICAL ACTIVITY OF THE CARDIAC CYCLE

The fact that myocardial cells have such a long refractory period ensures that the first cells to depolarise will control the rate at

which the other cells in the heart depolarise. The cells in the SA node, being the natural pacemaker for the heart, have the highest depolarisation rate. These cells depolarise and initiate a depolarisation wave. From the SA node, the depolarisation wave passes from right to left over both atria, resulting in atrial systole.

The depolarisation wave is stopped by a non-conductive layer of tissue between the atria and ventricles. At about the same time the wave reaches the AV node where specialized cells delay the progress of the wave by about 70 msec. This built-in delay is very important, as it allows atrial systole to reach completion before ventricular systole commences.

From the AV node the depolarisation wave continues in "Bundle of His" and its right and left bundle branches. The depolarisation wave rapidly travels throughout the Purkinje network- a fine mesh of faster conductive fibres which distribute to inner surfaces of both ventricles. Contraction of the ventricles commences at the apex and spreads towards the base of the heart and blood is forced out through the pulmonary and aortic valves. The resultant pressure closes the mitral and tricuspid valves.

Should the SA node stop operating, the group of cells with the next highest depolarisation rate will take over the role of the pacemaker due to their automaticity. Thus a natural back-up system exists.

The natural SA node rate is increased when the body requires more oxygen during periods of physical and emotional stress. The SA node is liberally supplied with nerve endings, which can stimulate its cells more rapidly if called for. A variety of drugs can alter the SA node rate, both speeding it up and slowing it down.

1.7 ELECTROCARDIOGRAM

Electrocardiography is the process of detecting, amplifying and displaying the electrical signals of the heart. These signals result

from the pacemaking activities of the heart.

Three electrodes are usually connected to the human body to detect an ECG signal. The electric potential between two electrodes is measured with respect to the third electrode namely, the reference point (earth). This method of measurement (e.g. measuring the potential of two points with respect to another point) is a differential method which is advantageous in detection of small electrical signals in an electrically noisy environment.

Depending on the position of the electrodes, three types of ECG signals are usually detected. The reference electrode is always connected to the right leg (RL).

If the second electrode is connected to the right arm (RA) and the third electrode is connected to the left arm (LA), the ECG is called Lead I. If the two electrodes are connected to RA and left leg (LL), the ECG is called Lead II, and if the electrodes are connected to the left arm (LA) and left leg the ECG is called Lead III. Figure 1.6 shows a normal Lead II electrocardiogram (ECG).

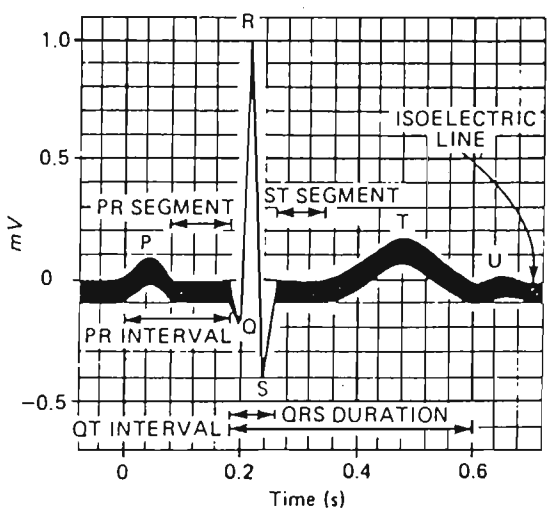

Figure 1.6 Normal Lead II ECG [9].

There are five notable points labeled P, Q, R, S and T and each point corresponds to a certain stage of the cardiac cycle.

The different parts of the Lead II ECG, can be itemised as follows:

P Wave -represents the atrial myocardium depolarisation.

PR Segment -represents the period for which the depolarisation wave is delayed in the AV node, by 70 msec.

QRS Complex -represents ventricular depolarisation.

ST Segment -is the interval between the end of ventricular depolarisation and the beginning of repolarisation. This segment represents the delay caused by the extended refractory period in myocardial cells.

T Wave -as the ventricular myocardium repolarises, the electrical cell potentials are measured as this wave.

1.8 THE MECHANISM OF FIBRILLATION

Fibrillation is characterized by an uncoordinated contraction and relaxation of the myocardial fibres. In a normal cardiac cycle the SA node acts as a pacemaker and the resulting cycle is "Sinus Rhythm". When the ventricular myocardium fibrillates it contracts randomly and synchronous activity is lost. The heart no longer acts as a pump. There are two basic theories employed to explain the mechanism of fibrillation.

As mentioned in section 1.3, the refractory period ensures that a depolarisation wave will not travel back upon itself and cause muscle oscillation. Under certain conditions such an oscillation can occur and is called "Circus Motion" or re-entrant excitation.

Abnormalities in propagation timing of the depolarisation and repolarisation wave of the cardiac muscle may cause circus motion.

These abnormalities can result from a longer propagation pathway and decreased refractory period of the heart muscle. For example, when the heart becomes enlarged, longer propagation pathways are created and any disorder in the Purkinje system causes slower conduction of the wave. Both of these may result in circus motion. A third cause of circus motion may be due to a decreased refractory period. This sometimes results from increased cardiac excitability caused by adrenaline (the adrenal hormone stimulating autonomic adrenergic nerve action), sympathetic activity, or irritation of the heart as a result of disease.

In any of these cases, a resultant circus motion will cause a re-entrant excitation of the cardiac muscle resulting in fibrillation.

Fibrillation will only be sustained under the right circumstances. There is a concept of "Critical Heart Mass" below which the fibrillation will not be sustained. An increase in temperature will cause a decrease in the refractory period which aids the re-entrant excitation.

Multiple site pacemaker activity will also result in fibrillation [37]. Such activity occurs if two or more areas of the latent pacemaker tissue become active at the same time. One cause of this is the stimulation by beta adrenergic neurohumours. In addition, if some cells are damaged, electric potentials may be created between different areas of the cells. Cells which are not normally pacemaker in character may become pacemakers, resulting in ventricular tachycardia. If myocardial mass is large there is a greater likelihood of having multiple pacemaker sites.

In general, anything which alters depolarisation wave conduction velocity, refractory period length, or which changes excitability or automaticity of the pacemaker cells may induce fibrillation. There are many agents which alter, not just one, but many of these factors.

1.9 CAUSES OF FIBRILLATION

1.9.1 MYOCARDIAL INFARCTION

When a coronary artery becomes narrowed or blocked, the myocardial tissue becomes hypoxic (oxygen starved) due to ischaemia (lack of blood flow) . Hypoxic myocardial cells may begin to act as pacemakers. Should some tissue die, it is surrounded by dying tissue which is hyper-excitable and exhibits pacemaking activity. The infarct constitutes a region of non-uniformity and the stage is set for the excitation that can zig-zag around the ventricular mass and become self sustaining (circus motion) and fibrillation occurs.

1.9.2 ELECTRIC SHOCK

The two types of electric shock which cause fibrillation, are macro-shock and micro-shock.

Macro-shock refers to the application of electric current to the surface of the human body. The most common type of macro-shock is electrocution from a power distribution system. Other sources of macro-shock are things such as, lightening strike, and high voltage capacitor.

Power distribution systems, depending on their voltage and energy, cause different damages to living bodies. Burning of living tissue results if the energy delivery of the source is high. Fibrillation due to macro-shock, usually, results from a power distribution system.

1.9.2.1 MACRO-SHOCK

In macro-shock, there is a range of frequencies (45 Hz to 65 Hz) for which, at a constant voltage, less electrical current is required to cause fibrillation. However, dc currents, and ac currents outside 45 Hz and 65 Hz can also cause fibrillation [37].

The curve in Figure 1.7 shows the current above which 50% of adult men cannot control their muscle action (e.g. cannot let go of the electrodes).

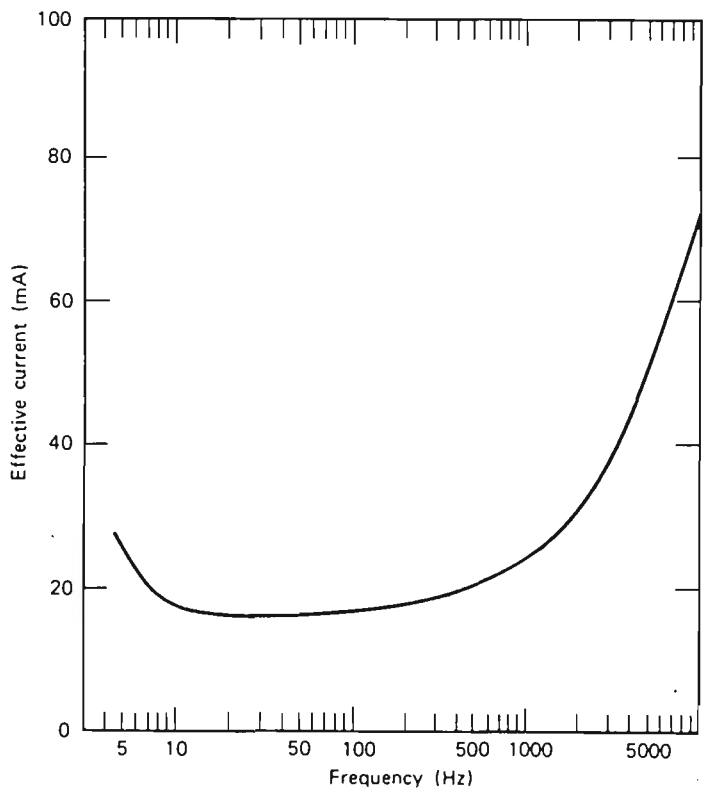

Figure 1.7. Curve of current versus frequency above which 50% of men cannot let go of the electrodes [3].

As illustrated in Figure 1.7, when the frequency of the stimulating voltage increases, a larger current is required to disrupt normal activities of muscles.

In a macro-shock, current can pass through different pathways. For example, when a voltage difference exists between two points, electric shock can occur if the body of a person contacts with these two points in one of the following ways:

a) contact of two hands with two points

b) contact of one hand and two feet with two points

c) contact of the body and hands with two points

d) contact of two or more parts of the body with two points

In any of the above cases, the closer the pathway is to the heart, the greater the risk of fibrillation.

The most common type of macro-shock which results from a power distribution system (e.g., a 240 volts and 50Hz system) is shown in Figure 1.9. As the neutral conductor (also known as the cold conductor) of a power distribution system is usually near ground potential, any contact of the body with the active conductor (the hot or live conductor) will cause an electrical current to pass through the body to the ground. This current results from a direct physical contact with a live conductor or it can be due to the leakage current of equipment.

In all electrical or electronic equipment there is a leakage current flow from the ac power section to the metal case of the equipment. This leakage current usually flows to ground through the ground wire in the power cord. The main source of this leakage current is the stray capacitance of the ac power sections and ground and/or the power transformer and its case. In some equipment, to reduce Electromagnetic Interferences, additional capacitors are placed between power wires and ground. These capacitors increase leakage current and their use has been limited by statuary organisations in terms of the leakage current they generate and based on their place in equipment categories (e.g. maximum 200 μA leakage current for hand held equipment).

If the leakage capacitance C is 20 nF, for a 50 Hz power distribution system, the leakage current calculation is as follows:

$X_C = 1/2\pi fC = 1.6 \times 10^5\ \Omega$

Assuming the stray resistances and inductances are negligible then:

$I = V/X_C = 240/1.6 \times 10^5 = 1.5\ mA$

Figure 1.8 illustrates the leakage capacitances of an electrical

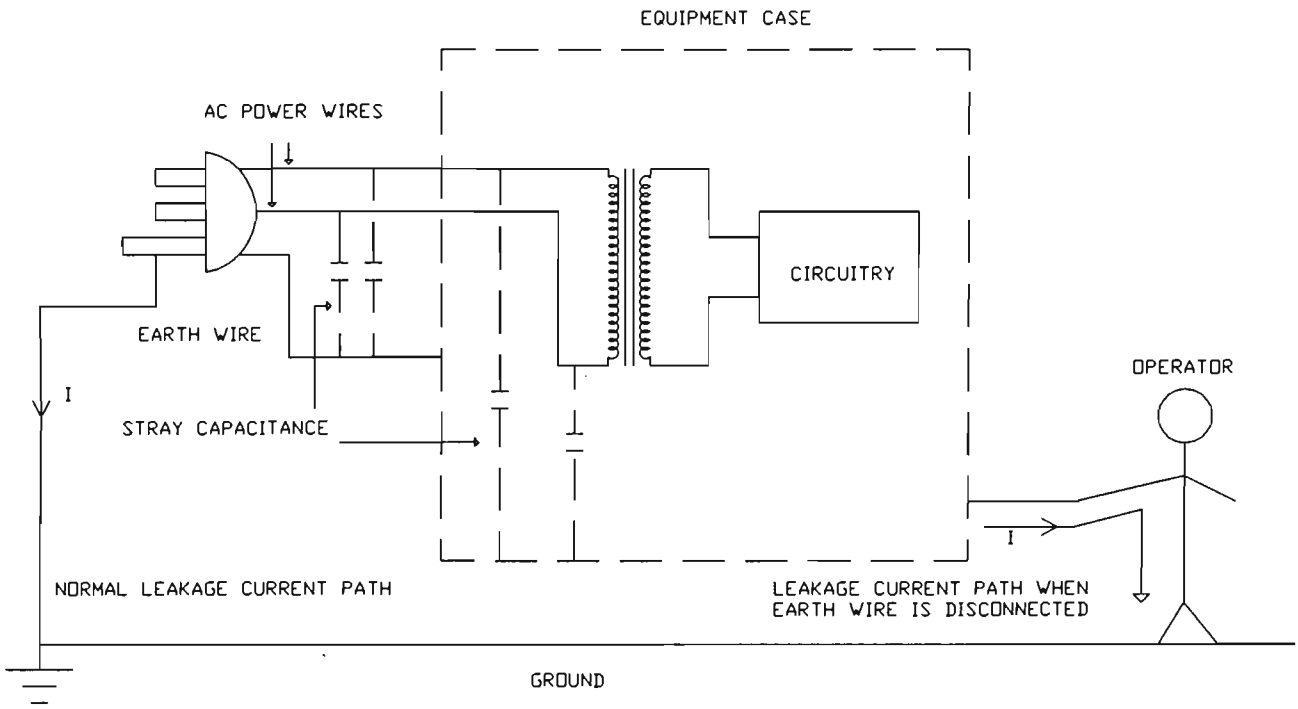

Figure 1.8. Schematic of an electrical instrument showing the leakage capacitances.

instrument. As shown in this figure, if the earth wire is disconnected, the case of the instrument acts as a voltage source which can supply a current equal to its leakage current. Depending on the value of this leakage current, fibrillation can result if the case of the equipment is in contact with the body.

Rechargeable, battery operated instruments, and instruments powered with dc voltage, minimise the generation of the leakage current due to 50 Hz supply. The reason is that for a dc supply f = 0, so $X_C = \infty$, and hence the leakage current is zero. This reduces the risk of macro-shock due to leakage current.

The amount of current passing through the body depends on the voltage of the power distribution system and the impedance of the circuit (loop A, shown in Figure 1.9) consisting of the conductors, ground and body impedance. The amount of 50Hz macro-shock required to precipitate

fibrillation depends on the body size, the path of the current flow and the duration of the shock application. The least current is required when the pathway is in the head-to-foot direction.

Tacker and Geddes [37] state that the threshold of fibrillation caused by a 60Hz current can be estimated from Equation 1.1:

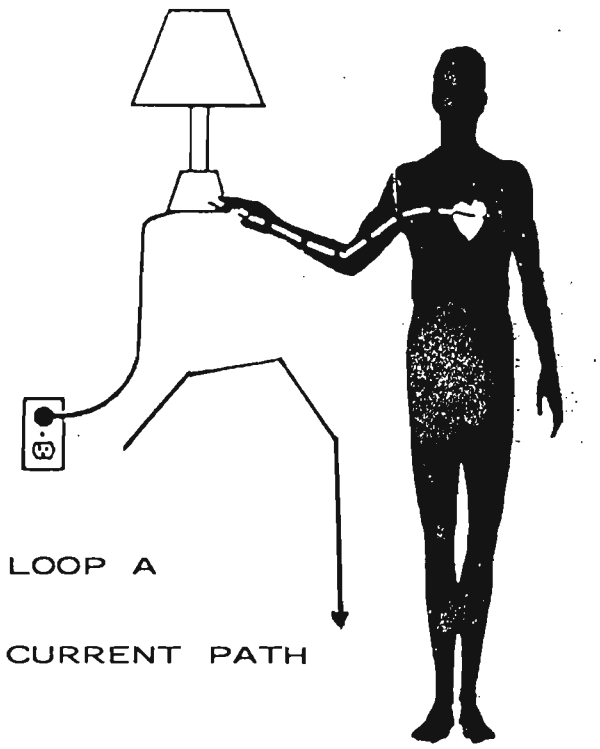

Figure 1.9 Macro-shock

$I = 69.4\ W^{0.533}$ LEAD I

$I = 29.7\ W^{0.51}$ LEAD II Equation 1.1

$I = 33.6\ W^{0.437}$ LEAD III

where I is the RMS current in milliamperes and W is the body weight in kilograms [37].

1.9.2.2 MICRO-SHOCK

Micro-shock is the situation where the heart is affected via intravascular, intracardiac catheters or electrodes. In this case very little current is required to precipitate fibrillation. With an electrode catheter in direct contact with the heart, only 5 to 20mV is required for fibrillation. However, if the circuit connected to the heart includes a peripheral saline or blood-filled catheter, 20 to 100V is required [37].

Micro-shock occurs in medical situations. In an Intensive Care Unit (ICU), patients usually have arterial catheters for blood pressure measurements and venous pressure manometry. These catheters provide low-resistance electrical paths directly to the heart, and they increase the possibility of micro-shock. It has been suggested that micro-shock via internal electrodes may be a significant factor in fatal accidents in operating rooms and ICUs [3]. Micro-shocks of this nature involve very small currents that are well below the perception levels of staff members and thus would not be felt by them.

Macro-shock and micro-shock cause fibrillation by creating a rapid firing pacemaker or by the process of vulnerable period stimulation. The latter refers to the generation of fibrillation by the delivery of a single stimulus during the vulnerable period, i.e., during the first part of the T wave of the ECG. This is due to a lack of uniform recovery from the refractory state, and areas of block (refer to section 1.6.3) probably facilitate re-entry of propagated excitation.

1.9.3 EFFECT OF DRUGS

Several drugs used in cardiac management can also induce fibrillation. For example, large doses of digitalis, adrenaline and adrenergic ß agonist or calcium salts, used to increase the force of muscle contraction may cause fibrillation. These drugs potentiate to cause

fibrillation. Hypothermia increases the excitability of the myocardium and can also cause fibrillation. This is due to the increase in the propagation velocity of the pacemaking wave and the decrease in the refractory period which results in circus motion.

1.10 ATRIAL FIBRILLATION

Atrial fibrillation is the un-coordinated contraction and relaxation of the atria. Hence, they do not force blood into the ventricles. The AV node is not supplied with rhythmic stimulation from the SA node. The ventricles still pump, although not to capacity, and somewhat irregularly. This condition is not life threatening. As shown in Figure 1.10, the P waves are absent and QRS complexes are temporarily irregular.

Atrial fibrillation is often converted to sinus rhythm using drug therapy. Alternatively if drugs fail, or urgency prevails, a stronger measure of "Elective Cardioversion", is applied.

Elective cardioversion is the use of synchronized electric shocks for the treatment of arrhythmias other than ventricular fibrillation.

To prevent an electric shock occurring at the vulnerable period causing ventricular fibrillation, a defibrillator usually senses the QRS complex and after 40 msec an electric shock, with an energy level

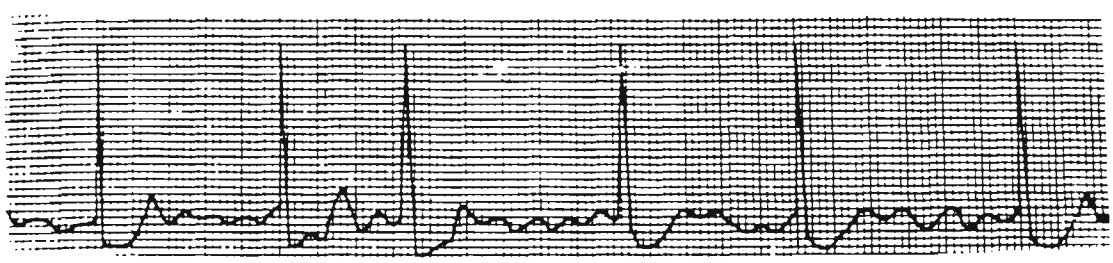

Figure 1.10 ECG diagram of a heart with Atrial Fibrillation.

(approximately 25 Joules) lower than the ventricular defibrillation energy, is applied to the patient.

1.11 VENTRICULAR FIBRILLATION

Ventricular fibrillation (VF) is the most serious arrhythmia. VF is the un-coordinated contraction of ventricular myocardial fibres. When in VF, all pumping action is lost, and if not treated, VF is lethal within a matter of minutes (3 to 16 minutes). Figure 1.11 shows a Lead I ECG of a heart in VF.

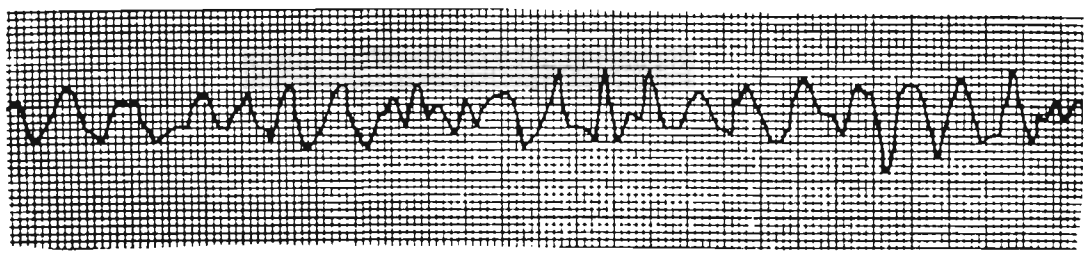

Figure 1.11 ECG of a heart in Ventricular Fibrillation.

1.12 DEFIBRILLATION

Ventricular fibrillation is a very serious condition diagnosed explicitly by ECG as a zero cardiac output and might also be due to asystole (flat ECG). In either, death occurs in a matter of minutes.

In treating fibrillation it is necessary to create conditions which interrupt the self sustaining excitation. If the myocardium can be rendered inexcitable by depolarisation with defibrillation, then hopefully, the natural pacemaker cells in the SA node will then resume pacemaking control and re-establish sinus rhythm.

1.12.1 CHEMICAL DEFIBRILLATION

Potassium Chloride (KCl) as a cardioplegic solution can be injected directly into the coronary arteries. This renders the cells depolarised and after a few moments, fibrillation ceases. The KCl is flushed out with continued cardiac compressions and the excitability of the myocardial cells is restored. To accelerate the restoration of excitability, a small amount of Calcium Chloride ($CaCl_2$) can be introduced by injection ($CaCl_2$ increases the force of contraction). A coordinated pacemaking stimulus can then excite a coordinated contraction. Excess KCl makes the cells hypo-dynamic whereas excess $CaCl_2$ may restart fibrillation. This technique is difficult to perform and direct access to the heart is necessary (suitable for open heart surgery).

1.12.2 ELECTRICAL DEFIBRILLATION

A substantial proportion of the myocardium must be rendered inexcitable to achieve defibrillation.

The most effective and reversible method of making myocardial cells inexcitable is to depolarise or hyperpolarise them by passage of an electric current pulse. Current entering a cell will hyperpolarise it. Current emerging from a cell will depolarise it.

It is very important that the method of achieving defibrillation should not damage the myocardial tissue. If the current duration and intensity is adequate the cells of the myocardium will be rendered inexcitable.

The current intensity, duration and distribution are of great importance to the success of a defibrillation attempt and are addressed in the following description of defibrillators.

CHAPTER 2

LITERATURE SURVEY

2.1 HISTORICAL BACKGROUND

In 1899, Prevost and Battelli [1] reported that a suitable electric discharge through canine ventricles was able to stop fibrillation. This observation initiated broad research activities which led to the first electrical resuscitation of a human by Paul Zoll in 1956. This event occurred after a series of research by scientists such as Hooker, Kouwenhoven, and Langworthy in the area of electrocution threshold, chemical and electrical defibrillation.

With the success of electrical ventricular defibrillation, Kouwenhoven [1] continued to investigate different waveforms for defibrillation. He originally used a 60 Hz sinusoidal current and later on pointed out the safety and portability requirements of defibrillators.

This investigation, in line with the research performed by other scientists such as Lown and others [1], resulted in the realisation of the original version of the modern defibrillator, constructed from a charged capacitor as an energy source with an inductor in series with it to generate a damped sinusoidal waveform which has been widely used till today. Although different defibrillation current pulse waveforms have been proposed by researchers [32], [12], [17], [37], [40], the damped sinusoidal waveform is regarded to be the most efficient waveform in defibrillation.

Today, portable and compact defibrillators are available in the market which have facilities such as Electrocardiogram (ECG), synchronised defibrillation and patient resistance recorders. Although there are

---

1. For more information about the history of defibrillators and the pioneers in this field, refer to [11] and [35].

still wide differences in the components used and the waveforms generated by different defibrillators supplied by different manufacturers (Appendix A), there exists a universal agreement that defibrillation occurs when the electrical current through the heart reaches a threshold level [21], [12], [27].

2.2 CONVENTIONAL DEFIBRILLATORS

2.2.1 DEFIBRILLATOR STRUCTURE

As described earlier, most modern defibrillators generate a damped sinusoidal waveform (Figure 2.2). This type of waveform has proven to be the most effective so far and the generating circuit is relatively simple.

The basis of this type of defibrillator is a simple series RLC circuit (Figure 2.1) and the electric current produced is shown in Figure 2.2.

The capacitor is initially charged to a high voltage by a switched charging circuit (e.g., a switch mode power supply). When the defibrillator is fired, the capacitor discharges through the inductor/body resistance path (Figure 2.1) and generates a damped sinusoidal waveform, the shape of which can be predicted if the circuit parameters (e.g., initial energy, L, C, Rs and TTR) are known. To calculate the current in the circuit shown in Figure 2.1 for various TTRs, the following second order differential equation for the circuit must be solved. The solution to this differential equation will be discussed later.

$$L\, d^2i/dt^2 + (R_s+R_p)\, di/dt + 1/C\, i = 0$$

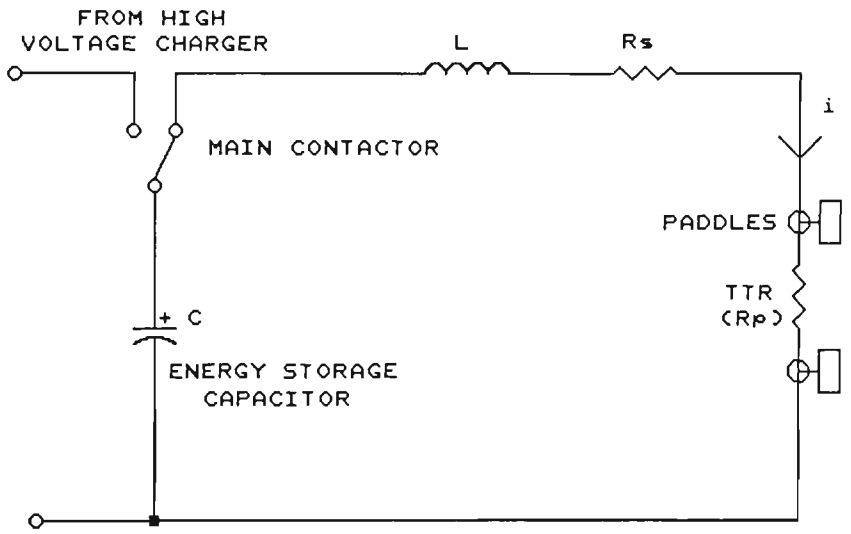

Figure 2.1 The simplified circuit of a defibrillator.

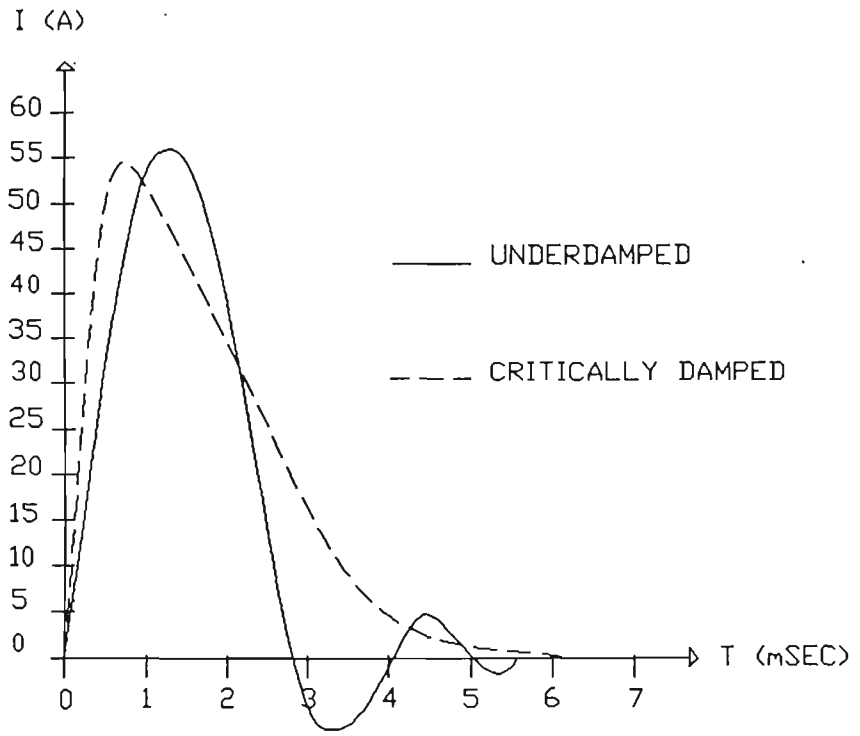

Figure 2.2 The electrical current in the circuit of Figure 2.1.

Depending on the parameters of the circuit, the resultant current waveform of the circuit after the discharge of the capacitor can be overdamped, critically damped or underdamped.

The main components in a defibrillator are the capacitor, inductor and paddles. Also, the energy delivery of a defibrillator is an important parameter in the selection of a good defibrillator.

The capacitor used has a value in the range of 16 to 45 μF. It may be charged up to 6000V. Currently available defibrillators use single mylar or polyvinylidene flouride (K film) capacitors. The recently developed K film capacitors are reduced in size and weight by about 50% relative to older mylar capacitors.

K film capacitors are susceptible to undershoot (negative part of the waveform which occurs in the case of an underdamped situation, e.g., low TTR value) and the life of the capacitor will be severely reduced if it is exposed to undershoot of over 10%. To overcome this, the preferred waveform is a critically damped sinusoid and the RLC parameters are adjustable accordingly.

The inductor (or choke) is introduced to smooth the waveform and eliminate switching spikes. The inductor, however, has a parasitic resistance which absorbs some of the stored energy.

The paddles are the defibrillator's electrodes . There are two types of external paddles.

The Anterior-Anterior paddles (A-A) and Anterior-Posterior paddles (A-P). The A-A type are more commonly used as they are simple to use. They often have the same shape as a steam iron, as shown in Figure 2.3, but in some models the handle is perpendicular to the electrodes in a "plunger" arrangement.

A-P paddles are less commonly used, (although they are thought to be more effective) as a large plate-like electrode must be placed under the patient. This can be inconvenient in an emergency accident scene.

Energy selection is important in passing different currents through different TTRs. For a given defibrillator and a given TTR, the higher the energy setting, the more electrical current passes through the patient's resistance.

Energy of defibrillation is selected based on recommendations from regulatory organizations. For example, the maximum recommended energy level is 360 Joules. Older units might be capable of delivering energies up to 400 Joules.

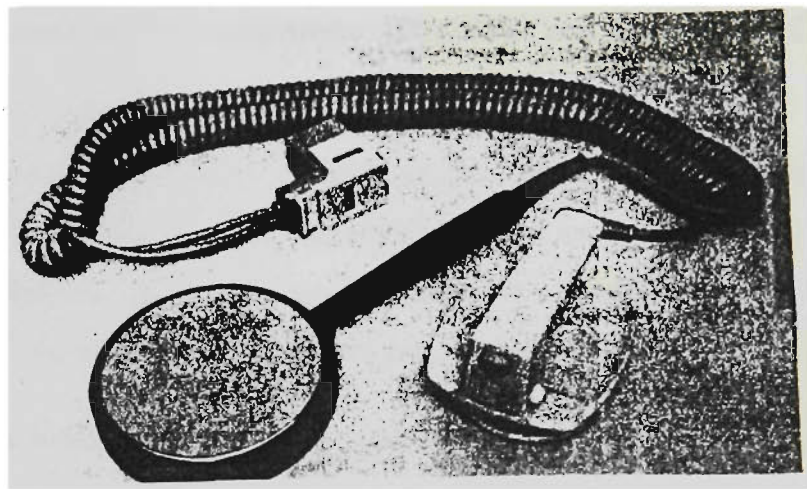

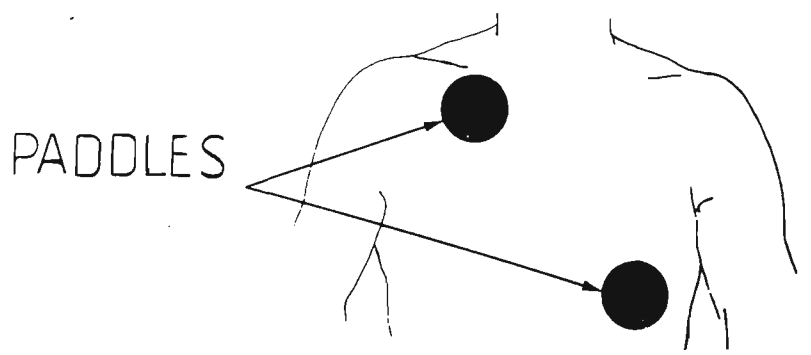

Figure 2.3 a) A-A paddles of a defibrillator, **b)** A-A paddle positions.

It has been proven that higher defibrillation energies cause myocardial damage [13], [36], [38], [8], so new designs of the defibrillators need specific approval from statuary organizations if they can deliver energies of more than 400 Joules to the patient.

2.2.2 EFFECT OF ELECTRICAL CURRENT WAVEFORM

The first defibrillator used to defibrillate a human heart, operated with 60Hz alternating current [11], [35]. This was due to the fact that by 1933 scientists knew that the heart could fibrillate if 60Hz electrical current was passed through it and the effect of electrical current in defibrillating canine heart was known since 1899. Also, as the defibrillator was first developed in the U.S.A., 60Hz power source was used in experiments regarding fibrillation and defibrillation.

Kouwenhoven [35] was the first scientist who proposed a quantitative value of 60 Hz current for fibrillation and defibrillation in dogs. After the first successful defibrillation in a human (by Paul Zoll in 1956), Kouwenhoven started a systematic study about the effect of frequency and current in fibrillating and/or defibrillating dogs.

His main objective was to find the safest operating frequency for the power distribution system and also to find the most effective frequency and current for defibrillation.

By connecting electrodes directly to the apex of the ventricles and applying electrical current to the electrodes, he found that ventricular fibrillation could be most easily precipitated with 0.2-0.4 mA (mean value) pulses in a frequency range from 42 to 120Hz.

Frequencies below and above this level required more current for fibrillation. For a sinusoidal wave, the lowest current (0.2 to 1.4mA) for defibrillation was found in a frequency range extending from 40 to 90Hz.

After Kouwenhoven 's 280lb defibrillator was successfully tested in a human, he pointed out the greater safety and portability of the capacitor-discharge defibrillator. His first capacitor-discharge defibrillator consisted of two 25μF capacitors charged to 2000 volts. When discharged by a relay to the thorax of the patient, one capacitor generated the positive current and the other generated the negative current through the thorax. Later on, as more scientific works were performed for safety of defibrillators, double phase (positive and negative current) defibrillators led to the modern defibrillators with damped sinusoidal waveform.

Defibrillators with a trapezoidal waveform are an important family of defibrillator used clinically. Niebauer et al [27] investigated the efficacy and safety of defibrillation with 10-millisecond trapezoidal waveforms of different tilts. They found that there were no differences in defibrillation threshold current and myocardial depression for waveforms of 10%, 45%, 65% and 80% tilt. However, they confirmed the dose-duration of current for defibrillation.

Other sources such as Tacker [34] and Peleska [29] found a higher incidence of atrioventricular (AV) block after defibrillation with a direct capacitor-discharge (no series inductor) than when a damped-sine waveform was used.

Holmes [16] also found that short-duration, high-peak current trapezoidal wave shocks produced significantly more hemodynamic impairment than longer duration, lower tilt trapezoidal wave shocks.

2.3 ELECTRICAL PROPERTIES OF THE SKIN

In the measurement of skin resistance [22] [43], the voltage at which the measurement is made is of crucial importance.

At low voltages, i.e, less than 1 V, the skin resistance between two

electrodes is in the range of 2kΩ to 20kΩ . The value may be lowered slightly by good skin preparation, which normally involves cleaning the skin with alcohol and abrasion of the stratum corneum with emery paper. This low skin resistance is desirable when measuring ECG, EMG and EEG.

On the other hand, when the resistance between the paddles of a cardiac defibrillator is measured, it has a value of 25Ω to 125Ω at peak defibrillation current [21]. This peak value of current is usually in the range of 25A to 100A. The voltage between the two paddles varies from 3000V to 6000V depending on the defibrillator internal circuitry and patient resistance.

Maxwell [22] showed that this enormous change in resistance was due to a phenomenon known as the skin resistance breakdown. He found that 50μsec after the initiation of the defibrillation pulse, the skin resistance drops to a value not more than 500Ω ,and that there are negligible changes in the skin resistance after 200μsec.

Until this time, little research has been done to understand the behaviour of the TTR during the early stages of a defibrillator pulse.

Some researchers [21] [2] have recorded the TTR during defibrillation, but these records show the TTR at the peak defibrillator current, and do not show the behaviour of the skin resistance at the early stage of application of the defibrillator pulse.

Also, records from different research groups, have some major differences in the measurement of the TTR. Some of the discrepancies in different records from various sources can be explained by studying Maxwell's results. These discrepancies will be discussed and results summarised in the next section.

2.4 REVIEW OF THE PAST WORK IN DETERMINATION OF TTR

The mechanism for measuring the Transthoracic Resistance even in modern

defibrillators has been static for many years. A low voltage ac signal is applied to the chest and the current is measured and hence the TTR can be estimated. For instance, the HP78670A defibrillator uses a 31.25 kHz signal to measure the TTR. This method does not take into account the skin resistance breakdown which is due to a high voltage/current presence during the shock.

Before the evolution of the most recent generation of defibrillators, Geddes et al [14] had first tried to predict the TTR and the threshold current for defibrillation from the physical characteristics of the patients. They had assumed that the TTR and threshold current changed with physical conditions such as weight.

Although they found linearity between current dose and weight, there were some exceptions. Hence, this method did not seem accurate. Other experiments were performed so as to predict the Transthoracic Resistance and the defibrillation threshold current.

They selected 71 dogs and applied a low level sinusoidal signal (1mA constant current, 10-500 kHz) to measure the resistance between the paddles. Then they applied electric shocks to the anaesthetized dogs and calculated the resistances between the paddles by measuring the currents through and voltages across the paddles during the defibrillation.

By comparison of the low level ac voltage measurement of the TTR and the actual resistances measured during the high voltage shock, they concluded that both results were similar if the low level signal frequency was 29 kHz. This might be the reason why the Hewlett-Packard defibrillator uses a 31.25 kHz low level signal to estimate the TTR. This method may also be questionable for the following reasons:

First, because the tests by Geddes et al [14] were performed on dogs and the behaviour of the human TTR might be different.

Second, transthoracic skin resistance breaks down if it is exposed to a high voltage [22], [43].

Maxwell [22] and Tulloh [43] measured the human TTR during actual defibrillations. The method they both employed to measure TTR was similar in principle. They both measured the current and voltage of the paddles during the application of the shock (defibrillation process) and hence calculated the TTR.

Tulloh [43] used sleeves of aluminium foil around the cables which connected the internal circuit of the defibrillator to the paddles. The voltage induced in the capacitance between each paddle and its corresponding sleeve was used as a potential divider to represent the voltage between the paddles. This was done to provide Class B isolation required by safety standards. Tulloh reported difficulties in calibration of the circuit due to the movement of the aluminium sleeves inside the equipment. These difficulties arose from the change in capacitance between each cable and its corresponding sleeve as a result of physical movement of the cable inside the defibrillator enclosure. It seemed that the sleeves were displaced by the high level of Electro-Magnetic Interference (EMI) resulting from the contactor switching (this effect is analogous to the physical movement of a conductor in an electric or magnetic field).

Maxwell [22], however, used optocouplers to sense the voltage across the paddles and hence recorded successful results in the measurement of the TTR. In Maxwell's work, the values of current and voltage of the patient's TTR were converted to digital values using two 8 bit A/D convertors. These values were saved in a battery backed memory array during real defibrillations. Then, they were extracted and taken to a computer for analysis. Some of these results are shown in Figure 2.4 . These results are very valuable for understanding the TTR's behaviour at the early stage of the application of the defibrillation pulse.

At this point it is worthwhile to compare the annotating facilities (recording the various parameters related to the defibrillation, e.g.,

peak current and the patient resistance) of the HP78670A defibrillator with the Maxwell technique in recording the Transthoracic Resistance.

The HP defibrillator uses a look-up table to calculate TTR. The TTR value and other data related to the test condition such as delivered energy and peak defibrillation current is recorded after each defibrillation. This method is based on the peak current measurement of defibrillation and the solution of the second order differential equation based on known parameters of the defibrillator [2]. This method assumes that the patient resistance is linear and does not provide any data in relation to the breakdown of the TTR.

As Maxwell showed the behaviour of the skin resistance during defibrillation, it is necessary to discuss his results in more detail and compare them with results from other sources.

In the 17 records he collected, it is observed that 50μsec after the initiation of the pulse the skin resistance falls to the range of 50-500 ohms and from 200μsec on there is little difference in TTR value.

Maxwell stated that if the skin resistance is measured by an ohm meter (e.g. a digital multimeter, DMM) at any two arbitrary points (e.g. between left and right hands), a value in the kΩ (e.g. 5kΩ) range should be expected (this value depends on pressure on electrodes, skin preparation , etc.). He stated that this high resistance is due to the low voltage/low current measurement . In his work he showed that during the real defibrillation as the transthoracic cavity of all of the 17 patients were exposed to high voltage and current, the value of their TTRs dropped to a value between 25 and 125 ohms. The decrease in TTR occurred in the first 200 μsec after the initiation of the defibrillation pulse and reached a value between 25 and 125 ohms at the peak defibrillator current.

Machin [21] compared the results from two different defibrillators. The records he collected from a modified defibrillator which was similar to Maxwell's, Cardiac Recorders 61A, showed the TTR to be between 25 to 105 ohms with a mean value of 58.2 ohms while the

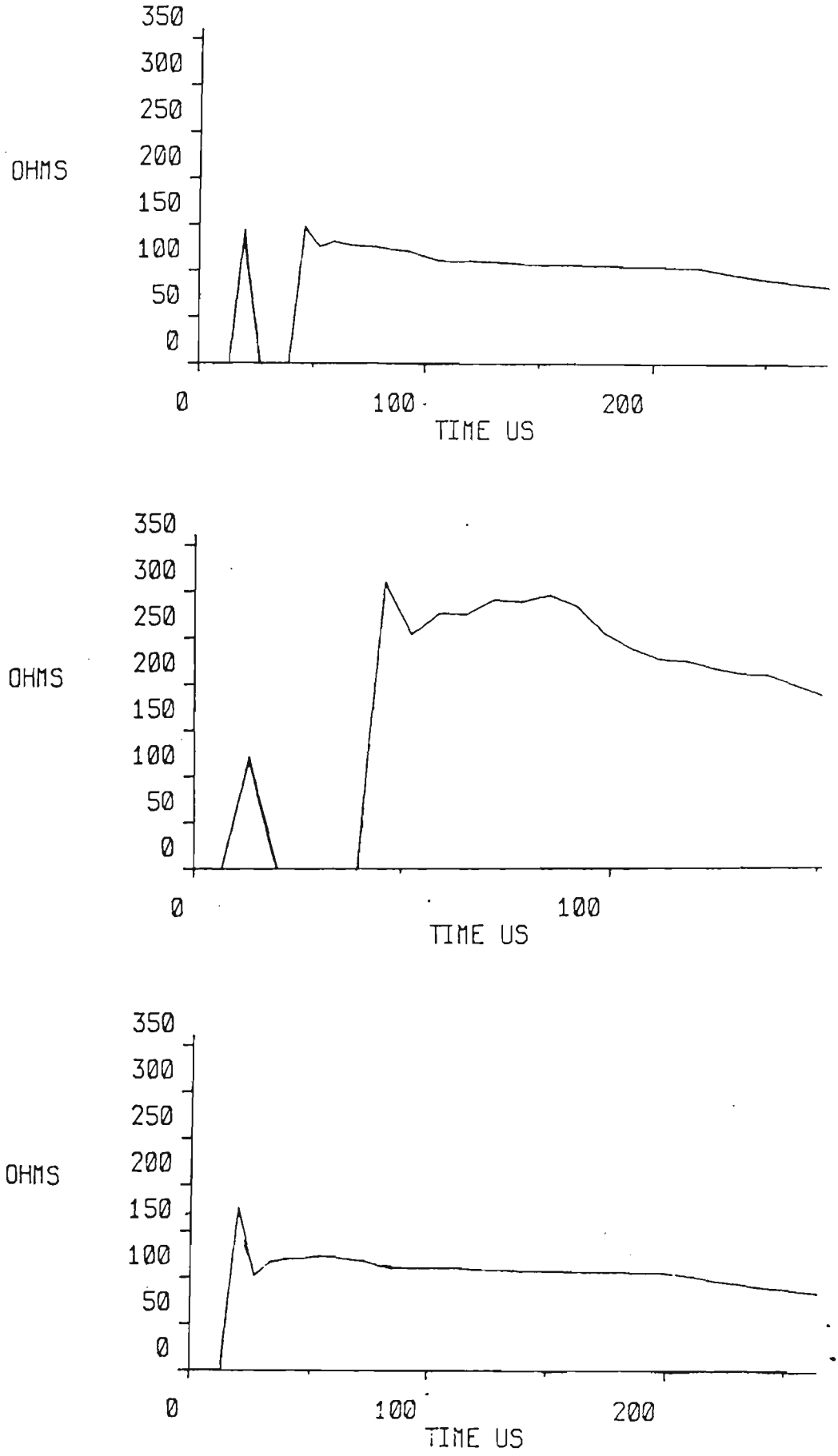

Figure 2.4 Maxwell's results [22] in determination of the TTR value before and after the skin resistance breakdown.

results that he collected from a HP78670A showed a range between 40 and 150 ohms and a mean value of 86.8 ohms. Both results have been reported to be the TTR values at the peak defibrillator current (Figure 2.5).

It can be seen that compared to the Cardiac Recorders 61A, the HP78670A recorded a higher mean value of TTR.

Some of the differences are expected because the HP78670A does not use a conductive gel in the defibrillation process, while the Cardiac Recorders 61A does. It has been reported by Tacker and Paris [37] that using good quality conductive gel can decrease the TTR by 19%.

Other parameters such as pressure on the paddles and physiological characteristics of patients are also important and may have caused the differences in TTR measurements, [39], [24], [18], [17], [6], [7], [40], [5], [10],.

In general, it is difficult to compare the results from different sources in the measurement of the TTR. This is because there are many parameters in defibrillation that affect the TTR measurement. These parameters are, the paddle sizes, skin preparation, pressure applied on paddles, physical conditions of the patients, interface material between the skin and the paddles, number of counter-shocks, energy setting of the defibrillation and the internal parameters of the defibrillator.

Machin and Briwnhill [21] stated that the comparison they made between the HP defibrillator and the Cardiac Recorder defibrillator, was made with fairly identical conditions (e.g., all of the patients were male, paddles were identical). They also stated that the 19% of difference in mean value of TTR in Figure 2.5, was due to the conductive gel which had been used for the Cardiac Recorder defibrillator, and had not been used for the HP defibrillator. However, the difference in mean value of the TTRs measured by the HP and Cardiac Recorder defibrillators was 41% (58.2Ω compared with 86.8Ω), which is much more than 19%.

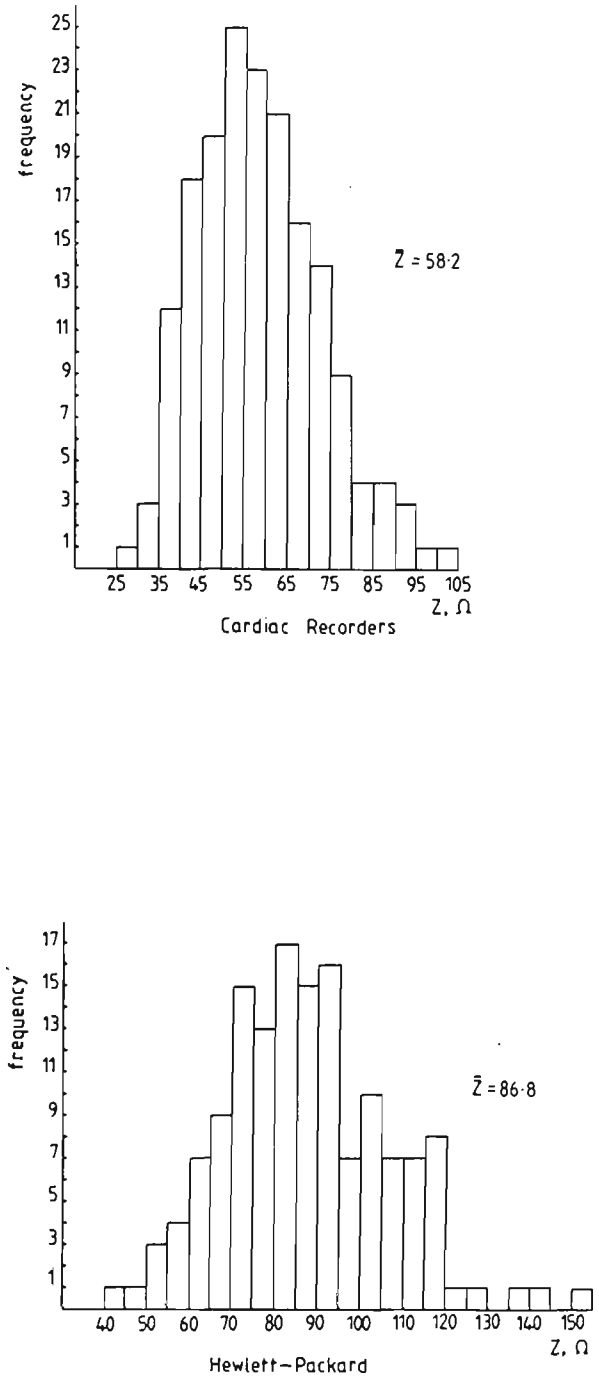

Figure 2.5 The TTR resistances recorded from HP78670A and Cardiac Recordes 61A [21].

In the process of this research, a software program (Appendix C) was developed to determine if the skin resistance breakdown had any effect on this difference in recording of the TTR by the HP and Cardiac Recorder defibrillators. In this software program, based on the data from Maxwell's research, the skin resistance breakdown was simulated and the current in the circuit of Figure 2.1 was calculated (a nonlinear TTR, e.g., TTR value was assumed to be 5000Ω for the first 50 μsec and then 50Ω for the rest of the calculation). The results were compared with the condition that no TTR breakdown occurred (linear TTR, e.g., 50Ω for all time). The comparison showed that, for the calculation of the look-up table values for the adaptive defibrillator, TTR could be assumed linear. However, a skin resistance breakdown coefficient must be considered in calculation of the values tabulated in the look-up tables. It means that the defibrillator current waveform can be approximated by a damped sinusoidal waveform which has been shifted in time by 50 μsec. Hence a linear model (no skin resistance breakdown) can be used to solve a nonlinear process (skin resistance breakdown).

The software simulation also explained why the results from the HP defibrillator and Cardiac Recorder defibrillator, in measurement of the TTR were different.

In chapter 5, a quantitative comparison is given between the linear and non-linear model of the skin resistance (skin resistance breakdown) based on the software simulation.

2.5 DEFIBRILLATION THRESHOLD CURRENT

It is universally accepted that for successful defibrillation, the electrical current passing through the heart has to reach a threshold level, [25], [31], [12], [37], [19], [38].

Geddes et al [12] used an isolated heart of a dog to estimate this threshold current in an experiment shown in Figure 2.6. They applied increments of electrical current through a chemical solution to the

heart and measured the pressure inside the heart ventricles. The pressure and the visual observation of the heart were referred to as a measure of defibrillation. Then they recorded the current at which the defibrillation occurred as the defibrillation threshold current.

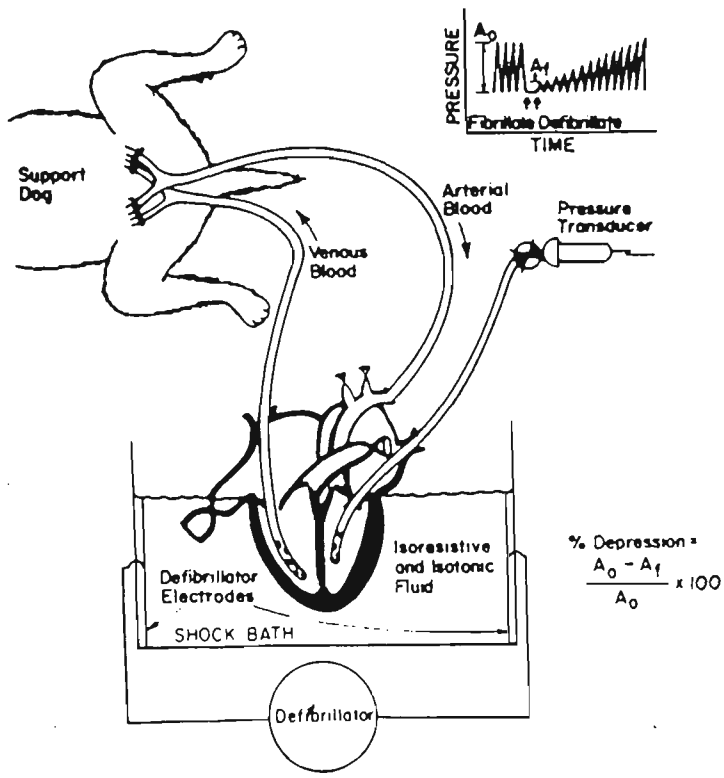

Figure 2.6 The defibrillation threshold current measurement [12].

Ruize et al [31] also investigated the fibrillation threshold current in dogs by using defibrillator paddles and confirmed the dose-duration (e.g. the amount of current and its duration in an electric shock) requirements for fibrillation.

Monzon and Guiller [25] designed a simulated current mode defibrillator on the basis that current defibrillates. They proposed that in a defibrillator the storing element could be an inductor rather than a capacitor. They stated that by switching off the energizing path of an inductor with no path other than the Transthoracic Resistance of the patient, due to the stored energy in the inductor, the defibrillator will act as a current source and no matter what the patient resistance is, the same initial peak current would result from the defibrillation.

The main problem with this technique (the circuit was realized with lower energy capacity than commercial defibrillators) is that the proposed equipment to deliver energy levels up to 400 Joules is bulky and cannot be implemented in practice except in coronary care units as a fixed (non-portable) defibrillator. However, one of the major characteristics of a practical defibrillator is its portability.

In the case of ventricular fibrillation (no blood pumping), death will occur in 3 to 16 minutes. So it is necessary for a current mode defibrillator to be portable so that ambulance personnel can carry the equipment to the victim especially at the scene of an accident.

McDaniel and Schuder [20] introduced an algorithm to determine the defibrillation threshold current. This algorithm was based on computer simulation and basic theory of probability involving an assumed underlying dose-response relationship. They stated that higher accuracy at the expense of a higher number of fibrillation episodes was achieved in determining the defibrillation threshold current.

Church et al [4] modeled defibrillation as a stochastic event in which a given energy determined the probability of defibrillation. They stated that based on their proposed statistical method, the large amount of information that has been collected on the defibrillation threshold current during defibrillation can be used to estimate defibrillation threshold.

Packer and Zayegh [28] proposed an adaptive strategy for controlling the energy delivery of a defibrillator. Based on simulation studies, they demonstrated that by using a digital signal processor, and, switching on a by-passing network, it is possible to implement an adaptive defibrillator. Based on this work and the behaviour of the Transthoracic Resistance during the application of a current pulse, a new technique is proposed for the implementation of an adaptive defibrillator. A summary of this technique which was developed during this research program, is given in section 3.1.

CHAPTER 3

ADAPTIVE DEFIBRILLATOR DESIGN

3.1 DEFINING THE ADAPTIVE ALGORITHM

From the discussion in chapter 2 about the TTR and defibrillation threshold current, the following hypotheses can be made:

a) The Transthoracic Resistance breakdown occurs at approximately 50 μsec after the initiation of the current pulse, and, after 200 μsec, there is a negligible change in TTR value.

b) There are differences in the lower and higher values of the measured TTR from different sources. However, the range of 25 to 125 ohms has been widely recorded.

c) The major factor in effective defibrillation is the peak defibrillation current achieved with a 5-10 msec damped sinusoidal waveform. Hearts of human subjects can be defibrillated with about 1 A (peak)/kg of body weight [37].

d) The peak current flowing through the patient can be modified by switching in an appropriate by-passing resistive network.

Based on the above conclusions, the adaptive defibrillator has to:

a) Measure the TTR before the occurrence of the peak current.

b) Predict from the look-up tables the peak electrical current and the time it flows through the heart. If this peak current exceeds the defibrillation current threshold level, calculate the time that the switching network has to operate in order to by-pass the excess energy.

c) Wait (when required) for the current to reach the threshold level.

d) Switch in the by-passing network.

The defibrillator is set to a level of energy which can deliver the required threshold current density to the patient with the highest Transthoracic Resistance of 125 ohms.

3.2 MEASUREMENT OF THE TTR

The circuit of a Lown (damped sinusoidal) waveform defibrillator is modelled in Figure 3.1 As all the parameters of the circuit are known (i.e., L, C, R_S and V(0)), the patient's TTR (R_p) can be found at any time by measuring the current in the circuit.

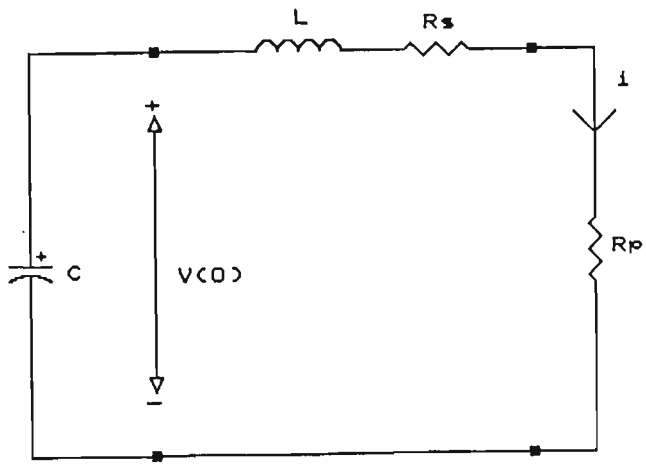

Figure 3.1 The simplified model of a Lown waveform defibrillator.

To calculate the relationship between the current in the circuit and the resistance R_p, the differential equation of Equation 3.1 must be solved.

$$L\, di^2/dt^2 + (R_s+R_p)di/dt + 1/C\, i = 0 \qquad \text{Equation 3.1}$$

with initial condition V(0) which can be calculated from the energy of defibrillator ($W = 1/2\ CV^2(0)$).

Assuming R_p is constant, if i(t) is measured, and since the initial voltage of the capacitor V(0), capacitance C (and hence the energy level), inductance L, and series resistance R_s are known, R_p or the Transthoracic Resistance can be found by solving the above equation.

Alternatively, this equation can be solved for i(t) for a range of TTRs (e.g. 25 to 125 ohms) in increments of say 5 ohms (depending on the required accuracy of the system). A look-up table can then be set up indicating the peak current associated with each TTR.

For instance, if a defibrillator has the following parameters,

C = 33 μF, L = 50 mH, R_s = 11 Ω, V(0) = 4671 V

(from which its energy setting , $W = 1/2.C.V^2$ is 360 Joules), by measuring the current $i(t_1)$ at $t = t_1$ the value of R_p or TTR can be found.

The solution of the differential equation is monolithic and there is just one value of TTR that can result in the measured current at time $t = t_1$.

The second order differential equation can be solved by classical methods (Laplace Transform) or numerical methods. Appendix B gives the classical solution of the above equation.

To investigate the validity of the concept in practice, a simulated defibrillator was designed with low capacitor voltage and energy level. The parameters of this simulated circuit were selected as follows:

C = 30 μF, L = 53.3 mH, Rs = 15 Ω, V(0) = 12 V

Using a numerical method, to solve the differential equation 3.1, a set of tables were obtained and used to fill in the look-up tables of the adaptive controller. Table 3.1 shows the values of the peak current and the times at which they occur for different resistances (TTRs), ranging from 25 to 125 ohms with increments of 5 ohms. If the peak

current of the circuit is measured, then from this table, the TTR can be found. Alternatively, if TTR is known then the peak current can be found.

3.2.1 SINGLE SAMPLING METHOD FOR DETERMINATION OF THE TTR

The algorithm for the operation of the adaptive controller which had been originally proposed, can be summarised as follows:

a) Initiate the defibrillation pulse.

b) Measure the current at a time greater than 50 µsec (after the break down) after the initiation of the pulse and well short of the required threshold current occurrence at the worst case condition (374 µsec, refer to Table 3.3), say at 200 µsec after the initiation of the pulse.

c) Obtain the TTR from a look-up table for t = 200µs.

d) Calculate the time at which the peak current will occur and the time that the controller must wait for the current to reach the threshold value.

e) Switch in the by-passing network to modify the current.

As discussed in the next section, due to bouncing of the relay, it was not possible to identify the initiation time of the pulse, so the current had to be measured at two stages in order to calculate the TTR.

3.2.2 BOUNCING OF THE RELAY

In order to calculate the TTR by measuring the current and comparing it with a look-up table, it is necessary for the controller to know the exact time of initiation of the pulse. However, bouncing of the relay imposes large electrical current spikes in the circuit which

makes it almost impossible to identify the beginning of the defibrillation pulse. This is due to the fact that, the controller starts the sampling after the relay is activated. However, the Lown waveform is not generated exactly after the relay is energized because the relay contact bounces and passes noisy current in the circuit. Tens of microseconds pass before the contacts of the relay are connected together firmly, hence generating the Lown waveform.

The current spikes generated by bouncing of the relay occur randomly in time and amplitude, and although it is possible to minimize them (discussed in section 3.5), they cannot be removed completely.

A Digital Storage Oscilloscope and a plotter, both equipped with a GPIB port (General Purpose Interface Bus, IEEE 488 Bus), was used to record the bouncing of the relay and other waveforms. Figure 3.2 and 3.3 show the bouncing of the relay.

In Figure 3.2, the bouncing of the relay is shown when R_p = 68 Ω. As illustrated in this figure, the duration of the noisy peaks are approximately 300 µsec each and they are 750 µsec apart.

Figure 3.3 illustrates the bouncing of the relay with the same R_p as in Figure 3.2 but with a different scale. In this case, the noisy peaks duration is approximately 300 µsec but their amplitudes are different from the noisy peaks in Figure 3.2. On the other hand, they are 1 msec apart.

As illustrated by these two figures, although different bouncing of the relay looks similar, they can still show a difference under identical test conditions. The reason is that even for the same relay with identical load and activating voltage, some of the test parameters cannot be controlled as a practical solution to the problem. These parameters are such as contact pressure on the switch which activates the relay, metal fatigue of the relay's structure and the aging of its components especially its spring. So the prediction of bouncing

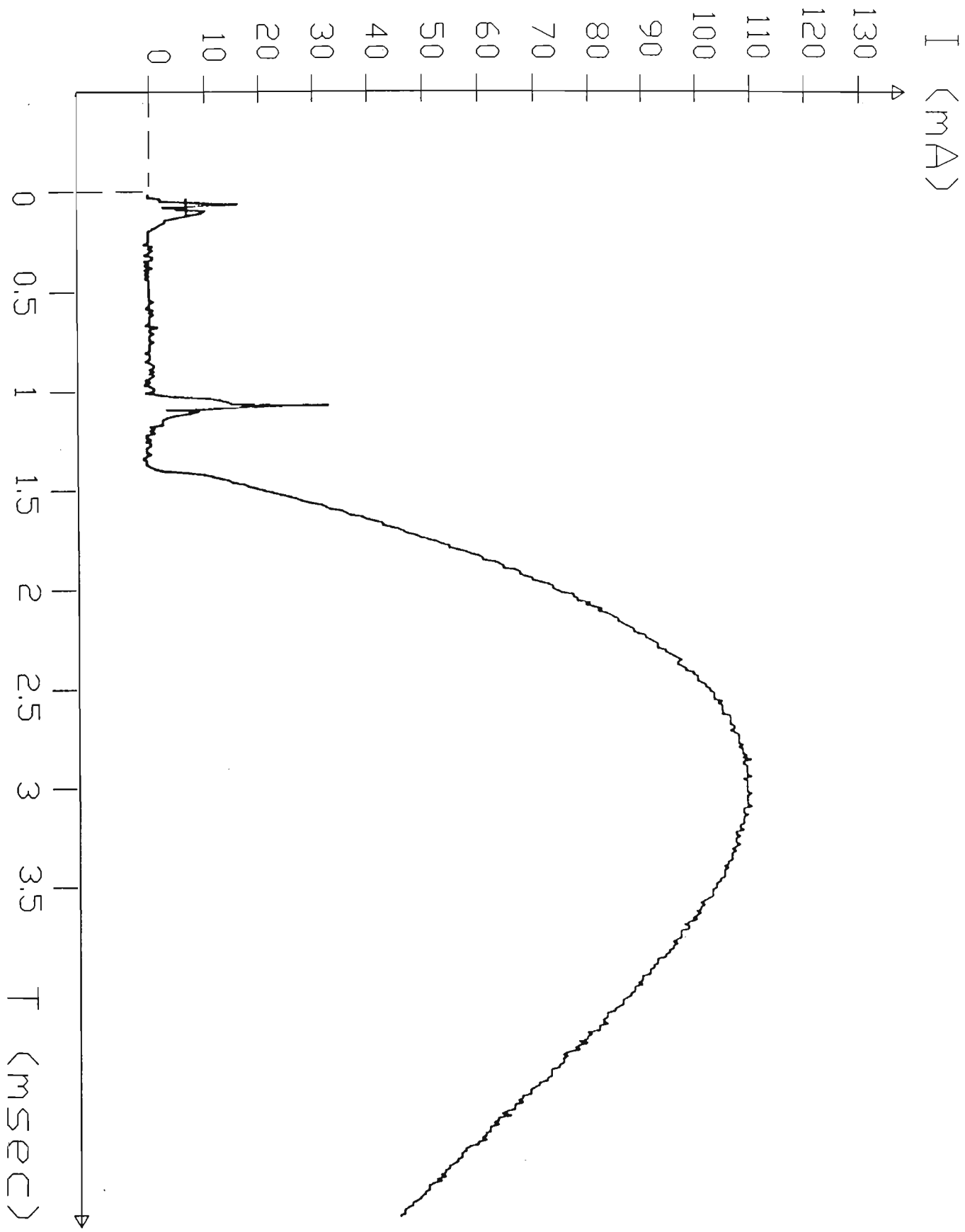

Figure 3.2 Bouncing of the relay.

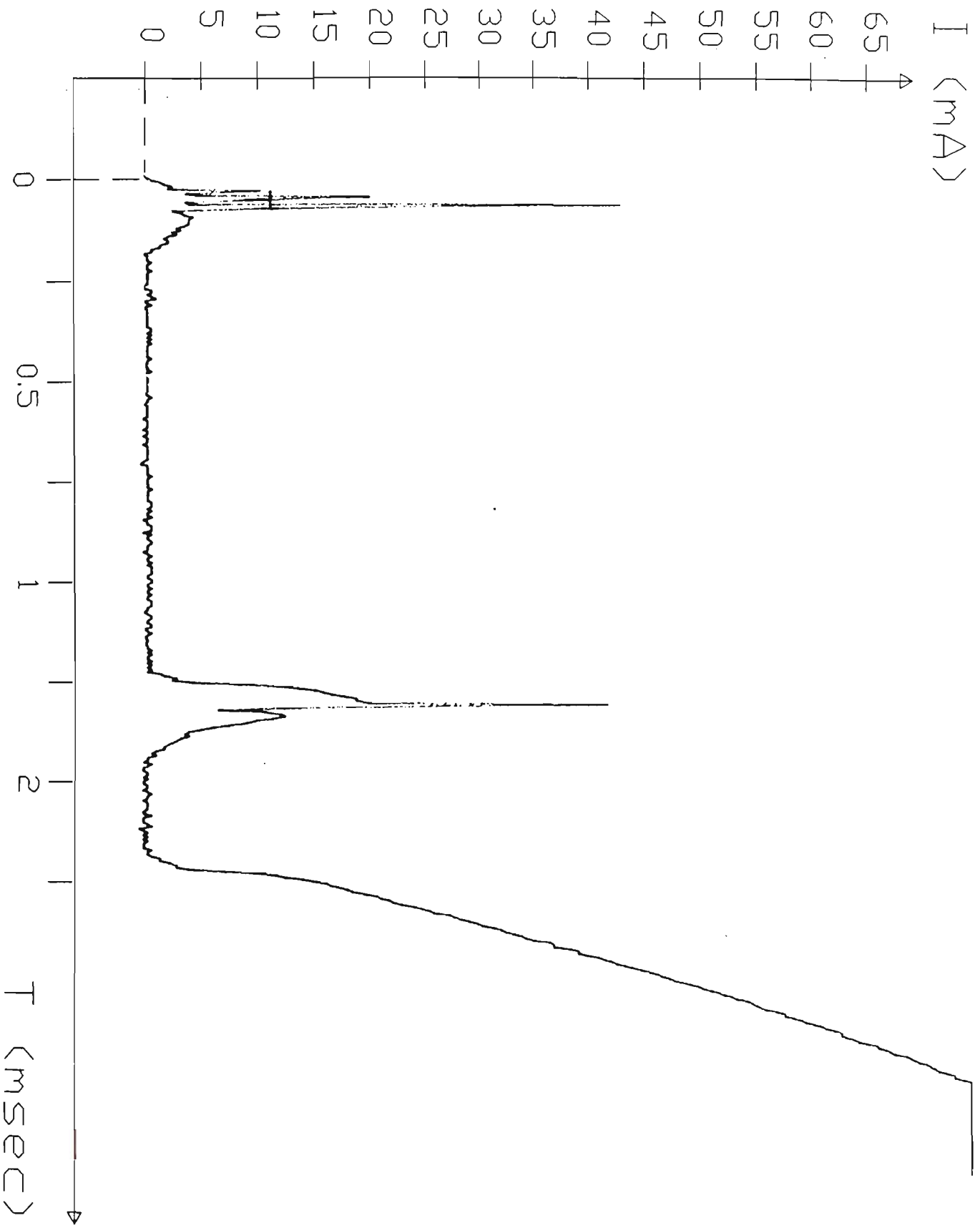

Figure 3.3 Bouncing of the relay.

occurrence in time after the defibrillator is started is impossible and methods like the Sample Comparison Method must be used to predict the TTR. Other methods based on comparison of amplitude, duration and rise time can also be used to differentiate between noisy peaks and Lown waveforms. Similar methods are commonly used to detect, display and analyse signals such as ECG in a noisy environment [42]. The data acquisition system for such signal processing must be very fast.

3.2.3 SAMPLE COMPARISON METHOD FOR DETERMINATION OF THE TTR

To overcome the bouncing problem, it was necessary for the controller to calculate TTR by comparing the current at two sampling times. These two times can be seen in Figure 3.4 (T_{s1} and T_{s2}).

The value of measured current at the first sampling time has to be larger than the amplitude of the spikes generated by the bouncing of the relay (I_n). After 100 µsec, the current in the circuit is sampled again. From the difference in the measured currents at the two times, the controller calculates the TTR. After calculating the TTR, the rest of the algorithm is similar to the one described in the previous section.

3.3 CALCULATION OF THE TIME FOR THE BY-PASSING NETWORK TO OPERATE

Originally, it had been proposed that a network of resistors and switches could be paralleled with the patient's TTR in order to by-pass some of the energy and so limit the current flow through the patient. This method was not practical as many components (usually bulky) were required. The delayed switching was then proposed.

This method utilizes just one resistor and one switch and is described in the following paragraphs.

After calculating the TTR, the controller determines the relationship between the time and the current in the circuit because there is only

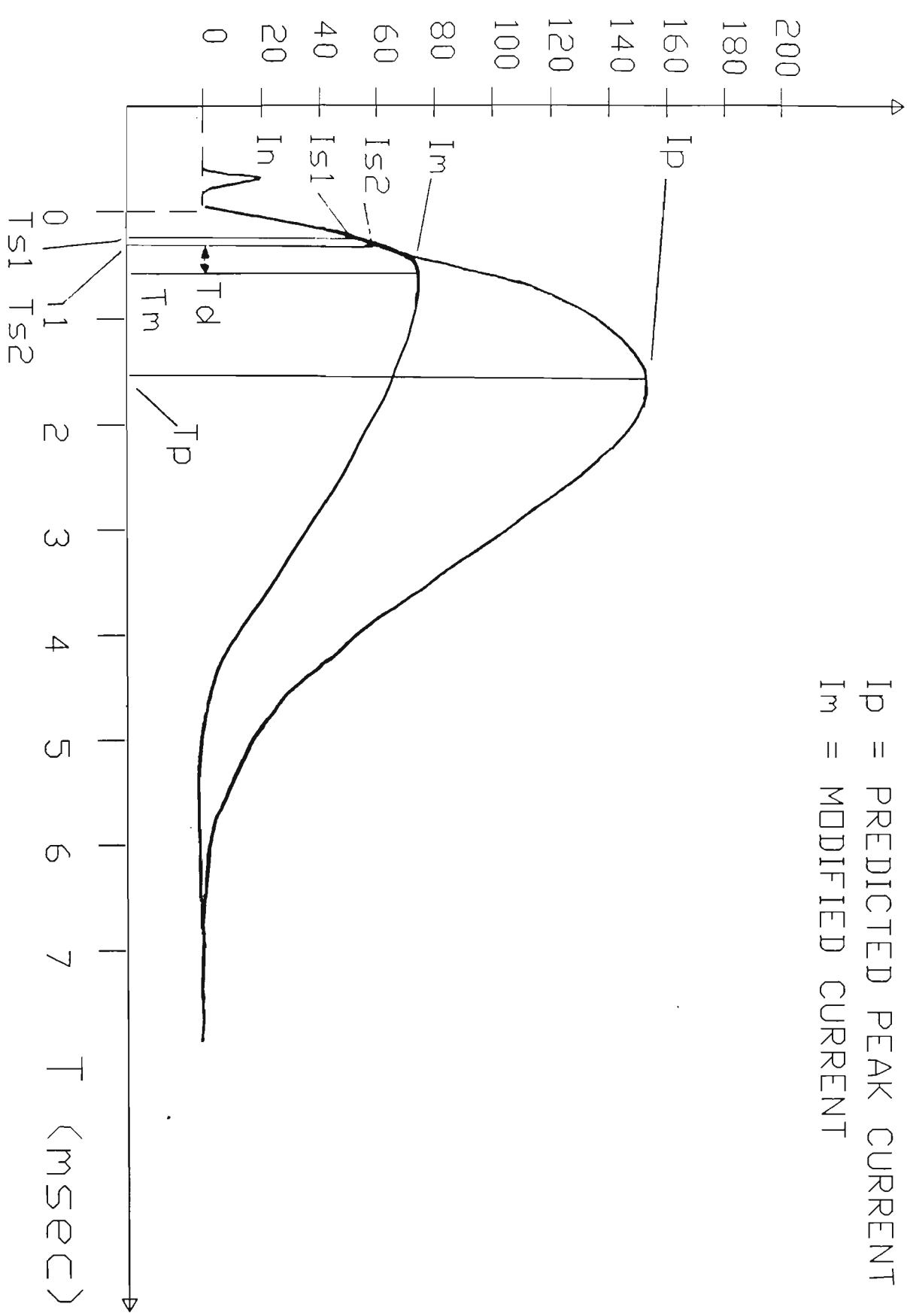

Figure 3.4 Modification of the current in the circuit of the hardware simulator.

one value of TTR that can result in a specific value of current at a specific time, (monolithic solution of the differential equation, Equation 3.1). Refer to Figure 3.4, the threshold current is I_m (the current that the adaptive defibrillator must achieve). I_{s1} is a current value which is larger than the noisy peak currents (I_n) generated by relay bouncing. The scaled value used for the hardware simulation of the defibrillator, I_{s1} was selected as 50 mA because it was larger than the amplitude of the noisy currents generated by the bouncing of the relay. I_{s2} is the current which is sampled 100 µsec after T_{s1}- the sampling time of I_{s1}. I_p will be the peak defibrillator current if the by-passing network does not operate.

For a given TTR, at a short time (calculation time required by microprocessor) after T_{s2}, the controller determines the following:

a) The time T_{s1}, at which the current reached I_{s1} (50 mA, tabulated in Table 3.2).

b) The current (I_{s2}) which occurs 100 µsec after the first sampling time, T_{s2} (tabulated in Table 3.4).

c) The time the current reaches the threshold current, T_m (tabulated in Table 3.3). I_m (72 mA for hardware simulator), the current occurring at T_m, is the threshold current and the defibrillator must be able to deliver this amount of current to a patient with the highest TTR (e.g., 125 ohms, Table 3.1).

d) The by-pass network switching time, T_s (i.e., the time required for the switch to turn on).

Knowing T_m, T_{s2} and T_s from the tables, the time that the controller must wait and then switch in the by-passing resistor can be calculated from, $T_d = T_m - (T_{s2} + T_s)$. For example, after calculating the TTR, if the patient resistance is high, the time delay will be long to allow the current to reach the threshold value. If the TTR is low, the delay will be short to limit the current before it exceeds the threshold.

The flowchart of the operation of the adaptive defibrillator is shown in Figure 3.5.

Referring to Figure 3.1, assume that the load resistance (the unknown TTR) is 25 ohms . As shown in Table 3.2, if R_p = 25 ohms, it takes just 245 µsec (T_{s1}) for the current to reach 50 mA.

For a threshold current of 72 mA (I_m), corresponding to the defibrillation threshold current, Table 3.3 shows the time at which the current becomes 72 mA for resistances from 25 to 125 ohms. It is observed that it takes 374 µsec (T_m) for the current to reach 72 mA if the load resistance (TTR) is 25 ohms.

The second sampling point (T_{s2}) is selected to be 100 µsec after the first sampling, so it is necessary to calculate the current at that time for load resistances from 25 to 125 ohms. This has been shown in Table 3.4.

At this point, if the processor finds the second sampled value of current (I_{s2}) to be between 67.1 and 67.6 mA, it knows the position of the waveform in time (e.g., T_{s2}, 245 + 100 = 345 µsec), the value of the load resistance (25< TTR <30) and hence, the time at which 72 mA (defibrillation threshold current) occurs (I_m, 374 µsec).

So the processor knows how much time is required for the switch to be delayed thus allowing current to reach but not exceed the threshold current, 72 mA (374 - 345 = 29 µsec). If there are time delays in the circuit elements (switching time, A/D conversion and look-up table calculations), they can be taken into account.

Table 3.5 shows the delay required for the switching network to by-pass the energy. Other numbers in Table 3.5 are related to the delay subroutine and the corresponding voltages in the C language program. The description of these values is given in Appendix F.

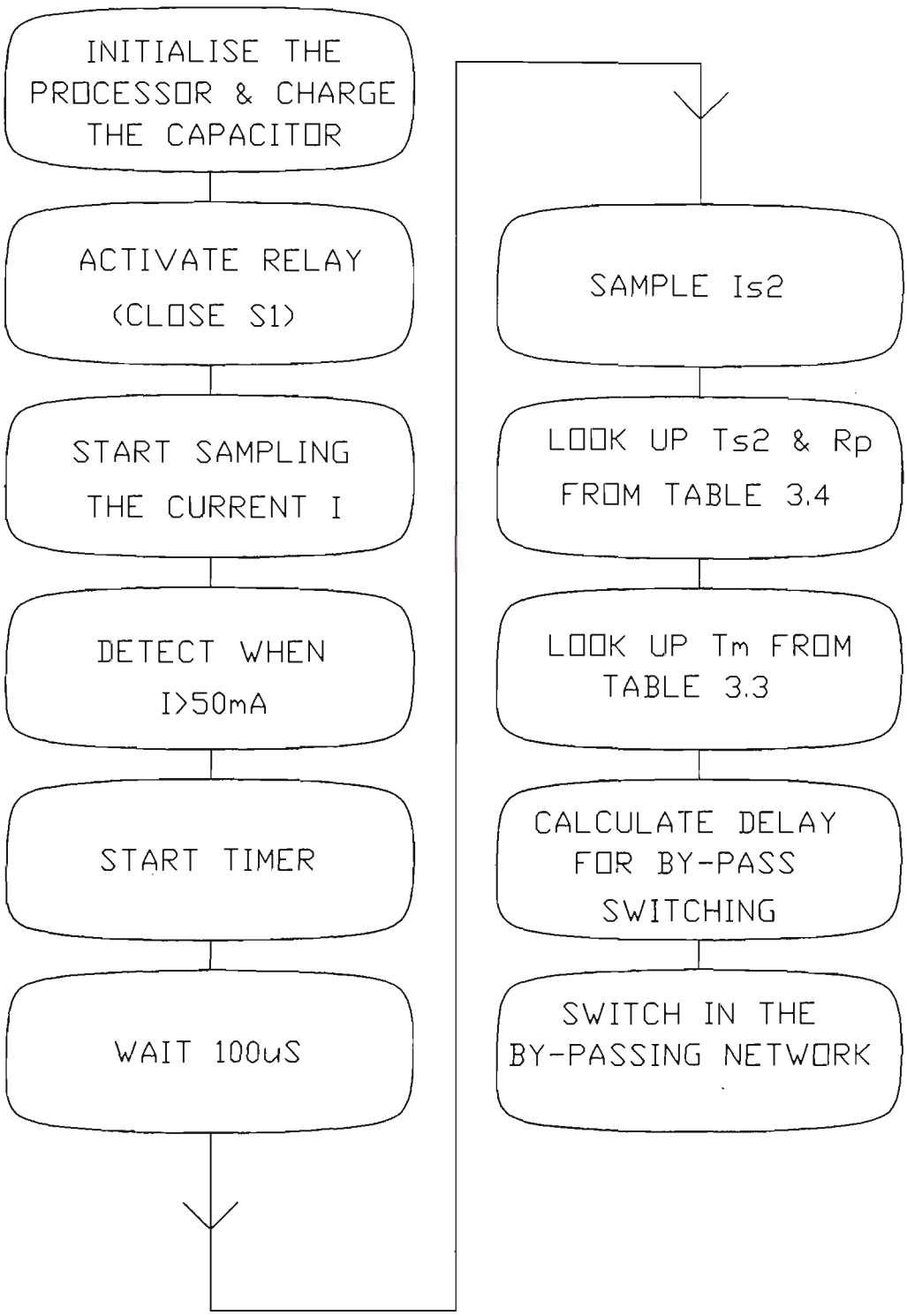

Figure 3.5 Flow chart of the adaptive controller's operation.

Table 3.1 Peak current in the circuit.

R_p (ohms)	I_p (peak, A)	t (μsec)	V_c (volts)
25	.1594378	1546	6.376024
30	.1507667	1507	6.780985
35	.142942	1470	7.143047
40	.1358412	1435	7.467677
45	.129375	1402	7.759086
50	.1234659	1371	8.021083
55	.1180454	1341	8.260711
60	.1130583	1313	8.476601
65	.1084555	1286	8.674744
70	.1041957	1261	8.853394
75	.1002428	1236	9.021103
80	.09656607	1213	9.172423
85	.09314014	1191	9.311887
90	.08993697	1170	9.440614
95	.08693799	1149	9.562364
100	.08412645	1130	9.672043
105	.08148244	1111	9.776124
110	.0789934	1093	9.872371
115	.07664642	1076	9.961386
120	.07442979	1059	10.04616
125	.0723335	1043	10.12461

THE SIMULATOR PARAMETERS ARE:

C = 30 μF, L = 53.3 mH, R_S = 15 Ω, V(0) = 12 V

TABLE 3.2 Calculation of R_p.

R_p (ohms)	I_{s1} (A)	t_{s1} (µsec)	V_c (volts)
25	5.009159E-02	245	11.78933
30	5.007727E-02	248	11.78591
35	5.004499E-02	251	11.78251
40	5.016387E-02	255	11.7775
45	5.009119E-02	258	11.7742
50	5.000152E-02	261	11.77095
55	5.005037E-02	265	11.76606
60	5.007378E-02	269	11.76125
65	5.007229E-02	273	11.75649
70	5.004641E-02	277	11.75177
75	5.013272E-02	282	11.74544
80	5.005557E-02	286	11.74087
85	5.008282E-02	291	11.73468
90	5.007888E-02	296	11.72857
95	5.004489E-02	301	11.72253
100	5.009432E-02	307	11.71492
105	5.010583E-02	313	11.70739
110	5.008113E-02	319	11.69995
115	5.002150E-02	325	11.69263
120	5.002107E-02	332	11.68373
125	5.006710E-2	340	11.67331

THE SIMULATOR PARAMETERS ARE:

C = 30 µF, L = 53.3 mH, R_s = 15 Ω, V(0) = 12 V

TABLE 3.3 The time at which the current in the circuit becomes 72.3335 mA (I_m, threshold current).

R_p (ohms)	I_m = 7.233E-02 A	t (μsec)	V_C (volts)
25	7.238444E-02	374	11.52536
30	7.243520E-02	382	11.51146
35	7.241328E-02	390	11.49775
40	7.246067E-02	399	11.48191
45	7.242615E-02	408	11.46632
50	7.243951E-02	418	11.44863
55	7.236336E-02	428	11.43123
60	7.242690E-02	440	11.40939
65	7.238134E-02	452	11.38792
70	7.242815E-02	466	11.36206
75	7.234898E-02	480	11.33668
80	7.240189E-02	497	11.30465
85	7.237889E-02	515	11.27079
90	7.233597E-02	535	11.23288
95	7.236491E-02	559	11.18616
100	7.234083E-02	586	11.13324
105	7.235216E-02	619	11.06712
110	7.236511E-02	660	10.98332
115	7.234685E-02	713	10.87276
120	7.235107E-02	793	10.70031

THE SIMULATOR PARAMETERS ARE:

C = 30 μF, L = 53.3 mH, R_S = 15 ohm, V(0) = 12 V

TABLE 3.4 The value of current at 100 μsec after the first sampling.

R_p (ohms)	I_{s2} (A)	t_{s2} (μsec)	V_c (volts)
25	6.761632E-02	345	11.59296
30	6.706625E-02	348	11.59045
35	6.650518E-02	351	11.58799
40	6.608193E-02	355	11.58345
45	6.549371E-02	358	11.58121
50	6.489638E-02	361	11.57909
55	6.442323E-02	365	11.57487
60	6.393185E-02	369	11.57082
65	6.342320E-02	373	11.56689
70	6.289840E-02	377	11.56307
75	6.246995E-02	382	11.55729
80	6.191122E-02	386	11.55377
85	6.144177E-02	391	11.54829
90	6.095051E-02	396	11.543
95	6.043924E-02	401	11.53786
100	5.999729E-02	407	11.5309
105	5.952848E-02	413	11.52413
110	5.903522E-02	419	11.51755
115	5.851940E-02	425	11.51119
120	5.805167E-02	432	11.50307
125	5.762109E-02	440	11.4933

THE SIMULATOR PARAMETERS ARE :

C = 30 μF, L = 53.3 mH, R_S =15 Ω, V (0) = 12 V

TABLE 3.5 The delay required for the by-passing network.

CCED = C Compiler Equivalent Delay

CCEC = C Compiler Equivalent of the Current

R_p	I_{s2} (A)	T_{s2}	T(I=72mA)	T_d	CCED	CCEC
25	6.761632E-02	345	374	29	17	11675
30	6.706625E-02	348	382	34	20	11580
35	6.650518E-02	351	390	39	23	11484
40	6.608193E-02	355	399	44	26	11410
45	6.549371E-02	358	408	50	29	11309
50	6.489638E-02	361	418	57	33	11206
55	6.442323E-02	365	428	63	37	11124
60	6.393185E-02	369	440	71	41	11039
65	6.342320E-02	373	452	79	46	10951
70	6.289840E-02	377	466	89	51	10861
75	6.246995E-02	382	480	98	57	10787
80	6.191122E-02	386	497	111	64	10690
85	6.144177E-02	391	515	124	72	10609
90	6.095051E-02	396	535	139	80	10524
95	6.043924E-02	401	559	158	91	10436
100	5.999729E-02	407	586	179	103	10360
105	5.952848E-02	413	619	206	119	10289
110	5.903522E-02	419	660	241	139	10194
115	5.851940E-02	425	713	288	166	10105
120	5.805167E-02	432	793	361	209	10024
125	5.762109E-02	***	***	***	***	9950

THE SIMULATOR PARAMETERS ARE :

C = 30 μF, L = 53.3 mH, R_s = 15 Ω, V(0) = 12 V

3.4 HARDWARE DESIGN

3.4.1 MICROPROCESSOR SELECTION

At the beginning of the hardware design, an MC6809 was selected as the microprocessor for the adaptive controller. The reason for this choice was the availability of the software and hardware facilities in the Footscray campus for development of an MC6809 based controller.

A description of this microcomputer along with the assembly language programs which were developed for this project is given in Appendix D.

To establish that the speed of the microcomputer was enough for the purpose of this project, a look-up table was developed and an A/D was connected to the parallel port of the MCU6809 card. The circuit is shown in Appendix E. In this circuit the processor, using the SYNC instruction, waits for an interrupt from the parallel port (initiation of the pulse and the beginning of the A/D conversion) and then based on the algorithm described in section 3.1 , switches the output FET (by-passing network) from the peripheral port B. No sample and hold was used with the MC6809 board as the only purpose of the test was to estimate the timing of the circuit and a large tolerance for error had been allowed (the A/D IC of the Analogue Interface Board which was eventually used had an on-chip sample and hold circuit).

As described earlier, the bouncing of the relay made it impossible to identify the beginning of the pulse and it was necessary to select another microprocessor with a faster instruction execution cycle.

The software development system for the Digital Signal Processor TMS320C25 with an execution cycle of 100 nsec was available at VUT. Also, an analogue interface board developed in VUT with an A/D and a D/A on board seemed encouraging enough to select this system for hardware simulation of the adaptive defibrillator. The reason was that the hardware simulator needed an input A/D for processing the current and an output port for turning on the by-passing network switch. Since

a TTL port was not available on board the fast D/A outport was used.

As mentioned earlier in section 2.3, the TTR could be calculated from the division of the voltage and current values of the paddles. The TTR calculated in this way, would then be the basis for specifying a delay for the operation of the switching network. The advantage of this approach is that the TTR at any time could be calculated and no assumptions based on the previous work made for linearity of the TTR.

In this project it has been assumed that 200 µsec after the initiation of the pulse there is negligible variation in the value of the TTR. The disadvantage of this approach is that it requires two A/Ds while the isolation of the circuit from the patient and the Electro-Magnetic Interference must be considered as well. The reason is that with the voltage and current measurement, at two different points isolation with the high voltage circuit is required; one for current measurement and the other for the voltage measurement. Also, this technique results in a slower process as the division routine takes a long time (MC6809 is not suitable for this technique).

Although this approach was not used, the selection of the TMS320C25 for the project provides flexibility in development and continuation of this work, based on other approaches or as an evolution of this work would cause no difficulties. Also due to the fast instruction execution cycle of TMS320C25 (100 nsec), it became possible to use a C compiler for generation of the assembly language codes. This may not be possible for real time applications and in small hardware memory assignments, because the C compiler does not use the codes in an efficient way. However, it was found that because of the efficient algorithm, using the C compiler was not generating unexpected performance even without consideration of the instruction cycle timing. A description of the Software Development System (SWDS) for TMS320C25, the C compiler, the C programs developed in the project and the analogue interface board is given in Appendix F.

During the development of the hardware simulator, a few problems were encountered. One of them was that , a delay of 50 µsec was required after any output port instruction as the analogue interface board was not fast enough compared to a PC based Software Development System board which can execute codes at a full speed of 40 MHz.

Another problem was the specification of the analogue input and output ports on the interface board. To extract the data, it was necessary to use the outport function available in the C compiler to find the resolution of the D/A or A/D devices and the way they were read or written to the internal registers of the SWDS board. For instance the C function outport(0,10000) is equivalent to 1.533 volts at port 0 of the analogue interface board measured by a digital voltmeter at the output port.

Also, to extract the timing information with regard to the analogue interface board, it was necessary to refer to the data sheet of each component on the board. It was found that the A/D was an eight bit, 25 µsec conversion time device with the facility of having 4 multiplexed inputs. The schematic diagram of the Analogue Interface Board is given in Appendix G.

3.4.2 CIRCUIT DESIGN

After becoming familiar with the TMS320C25 facilities and the input and output functions, the defibrillator simulator was designed in detail and then connected to the analogue interface board. The circuit diagram is shown in Figure 3.6

Describing the way the circuit operates, the processor first turns off the power FET (Q_2) which represents the by-passing circuit.

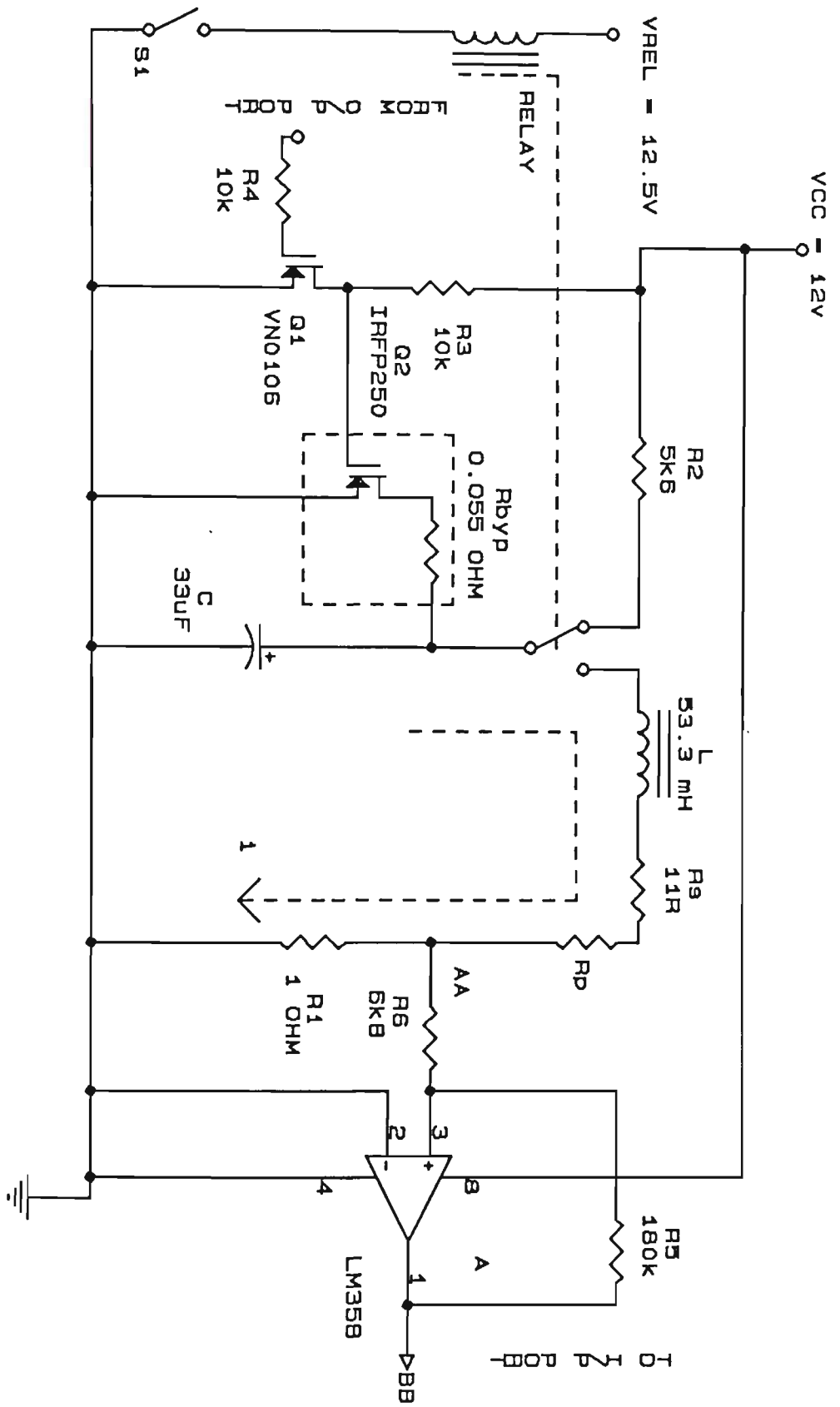

Figure 3.6 The schematic diagram of the hardware simulator circuit.

The command for turning on or off the FET, comes from the output port of the analogue interface board. The voltage across the resistor R_1 represents the current because its value is 1 ohm. On the other hand, as $R_1 << R_p + R_s$, there is negligible error in the calculation if R_1 is ignored.

From Table 3.1, the maximum current that might flow in the circuit is 160 mA when the load resistance (Rp which corresponds to TTR) is 25 ohms. To achieve a good signal to noise ratio and full scale A/D conversion an amplifier was used. The gain was selected so that at maximum current the amplifier provided a voltage of 5 volts for the analogue interface board. Maximum current was selected as 190 mA to provide flexibility in simulation of the circuit when the TTR was less than 25 ohms.

With reference to Figure 3.6, when the current in R_1 is 190 mA, to have 5 volts at the input port of the Analogue Interface Board, the gain of the amplifier, A_v, can be calculated as follows:

$I \times R_1 \times A_v = 5$ if $R_1 = 1$ and $I = 190$ mA then $A_v = 26.4$

If the patient resistance is low (depending on the type of the defibrillator and the energy selected), the current in the circuit can have negative polarity. This negative polarity, which occurs in underdamped conditions, can be observed in Figure 2.2 (and also in Figure 4.2 which is discussed in chapter 4). This negative part of the waveform has no effect in defibrillation. So, for simplicity of the circuit, the negative part of the amplified signal was truncated. The reason is given in the following paragraph.

In Figure 3.6, when the voltage at point AA becomes negative, the output of the operational amplifier clamps to zero volts. To amplify the negative portion of the waveform, a negative supply for the operational amplifier is required which unnecessarily complicates the circuit.

When the circuit was finally tested, no satisfactory results were obtained and no modification in the hardware simulator current was observed. Look-up tables were checked, and were all correct. It was finally found that the inductor was saturating. It was necessary to add an air gap and increase the number of turns to increase the current level at which the saturation occurred. The saturation current level was selected to be 200 mA at 100 °C.

3.4.3 INDUCTOR DESIGN

When a maximum current of I, flows through the winding of a given type of core, an air gap is usually required to ensure that the inductance remains constant and the core does not saturate.

The current at which a core saturates (slope of the BH curve drops, i.e., μ decreases), depends on the ampere-turns, material of the core and, physical characteristics of the core such as the centre pole area and the magnetic path length.

In general, the relationship governing the inductance architecture is:

$N \times I = B \times A_{min}/A_l$

where

N is number of turns

I is maximum current in the winding

A_{min} is the minimum center pole area of the core

B is the saturation flux density

and $Al = L/N^2$

Using this formula and based on the data sheet for the Pot Core 3622:

for the original choke

$N = 100$, $A_l = 8500$ nH/N^2, $B = 0.28G$, $A_{min} = 2.01$ cm^2

$N \times I = 6.59$ A.T

It means that it is allowed to flow 6.59 A through a one-turn winding and as the original winding had 100 turns the core was saturating at 65.9 mA.

Adding a 0.16mm air gap, decreases A_l to 1000 and the new Amp.Turn is:

N x I = 56.28 A.T

To have an inductance of 50mH:

$L = Al \times N^2$ then for L = 50mH and Al = 1000 nH/N^2

N = 224 Turns.

To check the current saturation level:

I = 56.28/224 = 250 mA

which is more than the maximum current in the circuit under the worst case condition. This is when the load resistance R_p is equal to 25 ohms. The current for this resistance is 160 mA.

A gap of 0.15 mm was selected and the turns had to be increased to 230 for an inductance of 50 mH. The measured inductance was 53.3 mH which was well inside the tolerance of the inductor design. This tolerance is due to the variation of the ferrite relative permeability which is usually +/-25% for commercially graded ferrites.

Also, in order to differentiate between the core saturation of the inductor and the bouncing of the relay which appeared as similar effects (sharp break-down of waveform), a response test was performed on the relay in order to investigate its bouncing.

3.5 MINIMISING THE RELAY BOUNCING

During the experiments, it was found that the bouncing of the relay can be minimised by applying a contact energisation voltage of 12.5 volts. Bouncing of the relay is due to the mechanical oscillations of the contact actuator. The frequency of these oscillations depend on the relay's physical size, the nominal voltage and currents in the relay's

bobbin and the characteristics of the relay's spring. The best operation of the relay is at no oscillation (critically damped). This can be compromised with the application of a voltage to the bobbin of the relay which, with overall parameters of the relay (fixed parameters such as spring constant and physical size) generates minimum oscillation of the contacts.

Dc voltages with different amplitudes were applied to the relay and by observation of the Lown waveform generated by the hardware simulator, it was found that for a voltage of 12.5 volts the effect of bouncing was minimal and as the activation voltage of the relay increased or decreased from this level, the bouncing of the relay significantly increased.

An additional technique used by some manufacturers of defibrillators, such as Hewlett-Packard, is that the relays are enclosed in a high pressure capsule to minimise the bouncing effect.

3.6 CIRCUIT OPERATION

Refer to Figure 3.6, S_1 activates the simulator's relay (e.g. firing defibrillator by operator). When S_1 is open circuit , capacitor C is charged through R_2 (e.g. charging main capacitor in defibrillator by flyback converter) and the output port of the Analogue Interface Board (AIB) (D/A port) is high (+5v). As the gate of Q_1 is high, it is ON and hence, Q_2 is OFF. When S_1 is closed, the relay is activated and the capacitor discharges through L and the series resistors, R_p and R_1. As R_1 = 1Ω, the voltage across R_1 is the current passing through R_p (e.g. defibrillator current). The positive section of the current is amplified and then converted to a digital value by the A/D port of the AIB. From the look up tables and based on the Sample Comparison method, the processor calculates R_p and the delay required to achieve 72 mA current in the circuit (e.g. defibrillator threshold current). Then it turns Q_1 OFF by writing 0 to the D/A port. Q_2 is then turned on by R_3

and the excess energy in the capacitor C is by-passed through R_{byp}. The value of R_{byp} is 0.055 ohm and it is inherent in Q_2. The time constant $T = R_{byp}.C$ must be less than the minimum delay required for the power switch to operate. It means that the by-passing network has to be able to discharge the capacitor faster than R_p.

In this project, as the Analogue Interface Board had only an analogue output port, it was used for controlling the power switch. The speed of the D/A port was fast enough for this application (100nsec range). However, for other controllers, a TTL output port must be used because it is cheaper and faster.

Power MOSFETs usually require a voltage above 10 volts to turn on completely. So, it was necessary to use Q_1 to generate a level shift from 5 to 12 volts to turn on Q_2. The total switching time of Q_1 and Q2 is in the 50 nsec range and can be ignored. However, for larger systems the switching time of the power switch increases and it must be included in the calculation of the delay look-up table.

In Figure 3.6, it was possible to use extra hardware to perform some of the operations which were implemented by software. For example, after S_1 is closed, the signal processor starts sampling and when the value of current in R_p reaches 50mA it acts as a timer by going into a loop. This task can be achieved by a comparator and a timer. After the current in R_p reaches 50mA the comparator triggers the timer. After 100µsec the processor takes a sample and from the look-up tables it obtains the delay for the by-passing switch.

Q_2 must withstand an approximate peak current equivalent to $V_c(0)/R_{byp}$ and a drain-source breakdown voltage of $V_c(0)$. Worst case condition is when $R_p = 25\Omega$ as the capacitor voltage is almost at $V_c(0)$ (Table 3.3, $V_c = 11.52536V$) and the peak drain current of Q_2 is $V_c(0)/R_{byp}$. R_{byp} must have an approximate peak power rating of $[V_c(0)]2/R_{byp}$. In a defibrillator, a wire wound resistor with 100 watts average power rating can easily dissipate this amount of power.

CHAPTER 4

EXPERIMENTAL METHODS AND RESULTS

4.1 TEST PROCEDURE OF THE MODEL

The defibrillator model was initially tested for correct operation. While the controller was disabled, the electrical current waveforms in the circuit were checked to be identical to the values in the tables described in chapter 3. For each test resistor (R_p), each experiment was repeated many times to verify the correct operation of the model.

Before data collection, each section of the circuit in the model was tested individually to observe the expected signals. For example, various software routines were written to test the operation of the processor (e.g. signals were applied to the A/D port, processed and written to the D/A port).

After each section was operating correctly, they were connected together and tested. Repeated tests were performed for various test resistors and consistent and satisfactory results were obtained.

Due to the use of a high quality storage oscilloscope, it was possible to plot the current in R_p (Figure 3.6) on a single sheet both with the controller disabled and enabled.

The triggering signal of the oscilloscope was selected higher than the noisy peaks of the relay bouncing to obtain consistant plots.

For each test resistor (R_p), the controller was disabled and the current in R_p was plotted. Then for the same oscilloscope triggering level, the current in R_p was recorded when the controller was enabled.

From Figures 4.8 to 4.12, it can be seen that in both cases (e.g. with

and without controller operating) the traces of the current in R_p are identical until switching of the by-passing network. This showed consistency in obtaining identical results for a test resistor.

In Figure 4.10 it can be seen that although the modified and unmodified traces are identical, the noisy spikes are slightly different in amplitude and time difference with respect to the Lown waveform, thus confirming the discussion (section 3.5) that the bouncing of the relay must be regarded as a random process.

Figures obtained from the plotter (e.g. Figure 4.8) show noisy envelopes which are due to the oscilloscope signal sampling. Some of the noisy ripples are due to interference from the TMS320C25 development board and the Analogue Interface Board for the digital storage oscilloscope. These ripples could be minimised by adding capacitors to the oscilloscope leads. However, adding extra capacitors in the circuit changed the operation of the RLC circuit and it was decided to record the plots with noisy ripples which were just part of the plotted signal not the current in R_p.

4.2 RLC CURRENT WAVEFORMS

Figures 4.1 to 4.4 are photographs of the waveform at point AA of the circuit in Figure 3.6 when the by-passing switch is disabled. These illustrations show the scaled waveform of a typical defibrillator current. The timing and the values of the waveforms match well with the values calculated by computer numerical methods.

In Figure 4.1, the underdamped condition can be observed from the negative portion of the waveform.

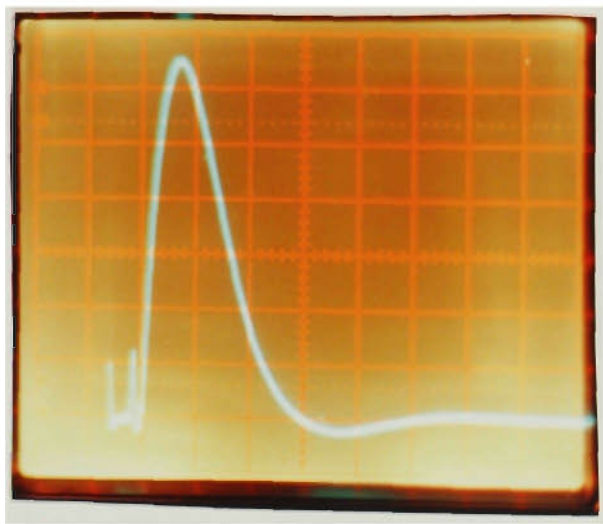

Figure 4.1 R_D = 27 ohms, 2 msec/div, 20 mV/div (not calibrated for full screen display), underdamped condition.

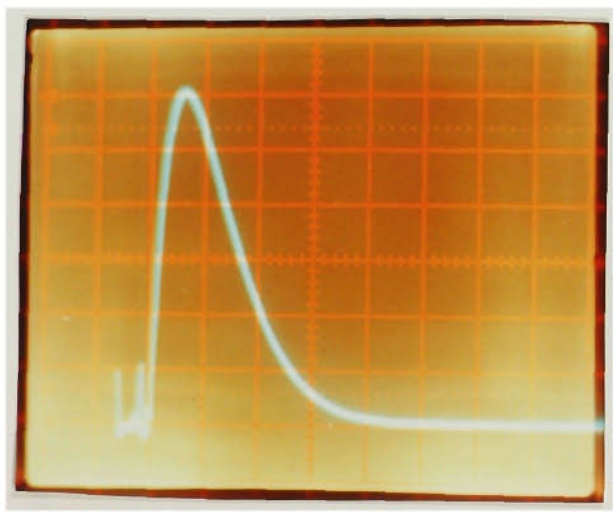

Figure 4.2 R_D = 47 ohms, 2 msec/div, 20 mV/div, critically damped condition.

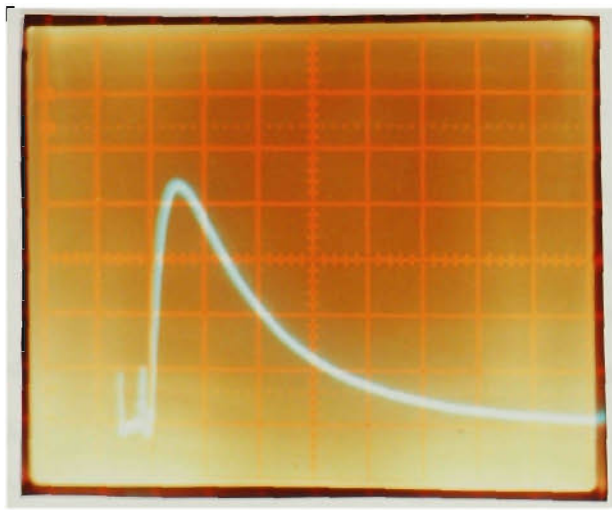

Figure 4.3 R_p = 100 ohms, 2 msec/div, 20 mV/div, overdamped condition.

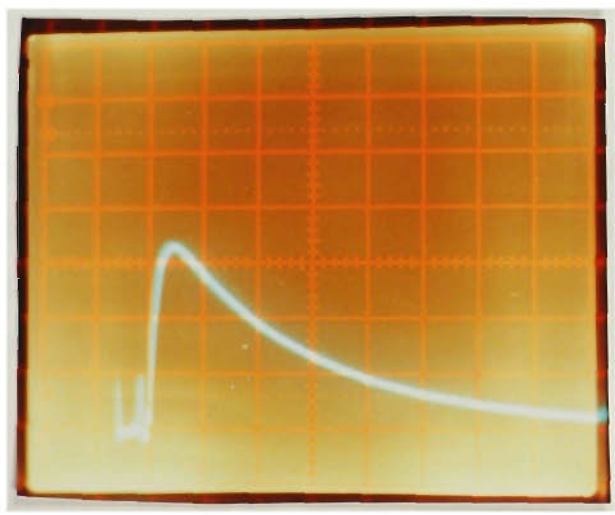

Figure 4.4 R_p = 150 ohms, 2 msec/div, 20 mV/div, overdamped condition.

It is also observed that the peak current occurs earlier if the TTR is higher. This is confirmed by comparing different peak current occurrences and different TTR values, as given in Table 3.1.

Relay bouncing is also shown in these photographs.

In Figure 4.5, the waveforms for different TTR values at the output of the operational amplifier are shown. They represent the current in Rp multiplied by the gain of the amplifier. Also it is observed from the plots that the negative part of the waveforms have been truncated for the under damped condition. The hardware used and developed in this project is shown in Figure 4.6 and Figure 4.7.

4.3 DISCUSSION OF THE RESULTS

Figures 4.8 to 4.12 show the current passing through R_p (TTR) while the controller is enabled (circuit of Figure 3.6). These Figures show the operation of the adaptive controller for the resistance values (TTR), 27, 47, 68, 100 and 120 ohms.

For Figure 4.8, the operation of the model is explained in the following paragraph.

Refer to Figure 3.6, when S_1 is closed, the capacitor C (which had been charged to 12 volts when S_2 was an open circuit) discharges through the circuit. The controller constantly samples the current in R_p. This sampling is performed in the main loop, "start", by the function inport(port0,&datain) (refer to the C language program in Appendix F).

At the beginning of the loop, by writing a high logic at the output port0 (function outport(port0,20000)) , it is assured that the by-passing switch is off.

When the current in R_p reaches 50mA (a current threshold larger

than the noisy peaks), the processor waits for 100μsec. This is performed by function delay(57). Then the processor takes a final sample and based on the algorithm described earlier, finds the value of Rp from the look-up tables. This part is performed by a series of "if" statements. If the condition of a particular "if" statement is met, the processor waits for the delay required (which was described in the algorithm) and then turns on Q_2 (the by-passing switch) by writing a low logic at output port (function outport(port0,0)).

In Figure 4.8, the time between the occurrence of the 50mA level (the first sample) and the modified peak current is approximately 180μsec. With no error and negligible switching time, this value should be 132μsec which is due to the 100μsec waiting period plus 32μsec (Table 4.5, R_p = 27Ω). This 48μsec (180-132) difference is due to different factors which are explained in the following paragraphs.

When the controller was on, it was observed that, not only the peak current was limited, the energy transfer to the TTR was also reduced. As shown in the circuit of Figure 3.6, no external resistor was used in series with the switch. The energy in the TTR could be controlled by adding a resistor in series with the switch (Q_2). The requirements for such a resistor were discussed in chapter 3. Alternatively, a switch and a resistor could be used in series with the TTR to limit the current in the TTR.

By comparing Figures 4.8 to 4.12, it is also observed that there are minor differences in the modified currents for various TTRs. These differences are due to the following reasons:

a) Error due to digitised look-up table (e.g. for TTR of 25 and 29 ohms, just one time delay is used for the switching circuit operation).

b) Error due to the difference in R_1/R_p.

c) Error due to the processor calculation time.

d) Error in A/D conversion and sample & hold.

e) Error due to the numerical solution of the differential equation of the circuit in Figure 3.1.

These errors can be minimised by increasing the calculated values in the look-up table and taking the other differences into account when the time delay is calculated for each TTR. Using a current transformer minimises the error described in (b). Using a faster A/D IC reduces the major source of error which is resulted from (d). This error can be high especially if the threshold detection (e.g. 50mA) is performed by the constant sampling method other than by a comparator. The reason is that the defibrillator current increases rapidly in a short period of time from the noise threshold (e.g. 50mA) to the defibrillation threshold (e.g. 72mA). The worst case condition is for the TTR = 25Ω (374 - 245 = 129μsec).

Calculating look-up tables directly by the classical methods minimises the error described in (e) as the numerical method described in Appendix C generates cumulative errors in the calculated values of the look-up tables.

In Figure 4.13, a comparison between the unmodified current in the TTR and the modified current in the TTR is given. This figure shows the current in the TTR for 27 ohms and 120 ohms. It is observed that the difference in the peak current and energy delivery for the unmodified current is substantial.

When the adaptive controller is enabled, however, it is observed that the difference in energy and peak current is reduced (e.g., constant current, constant energy waveform). The minor differences in peak current and energy of the waveform can be reduced by minimising the sources of errors in calculation of the look-up tables, given earlier in this section.

Figures 4.8 to 4.12 show that it is possible to design an adaptive defibrillator based on this algorithm.

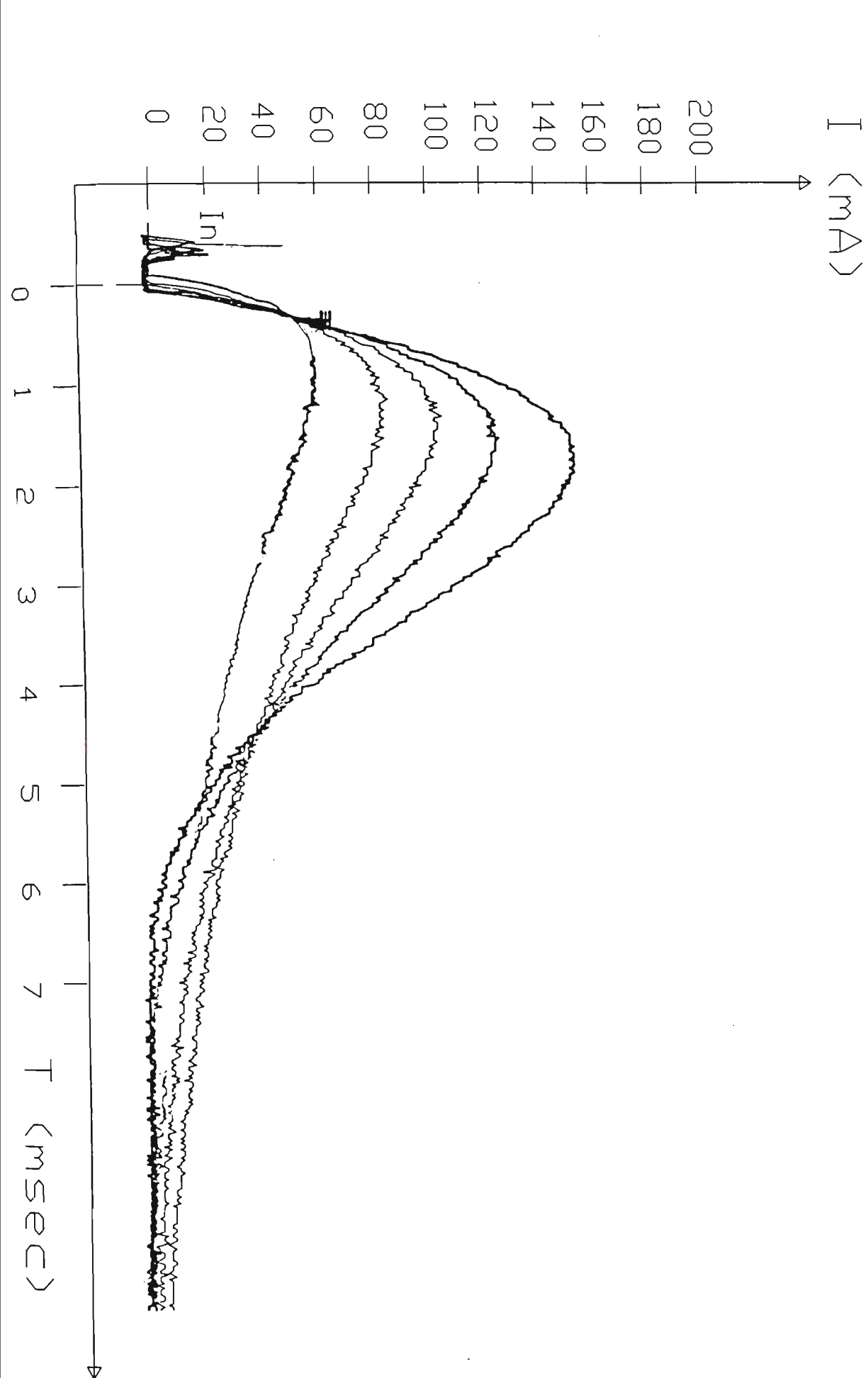

Figure 4.5 The waveforms at point BB of circuit diagram in Figure 3.6 when the controller is disabled.

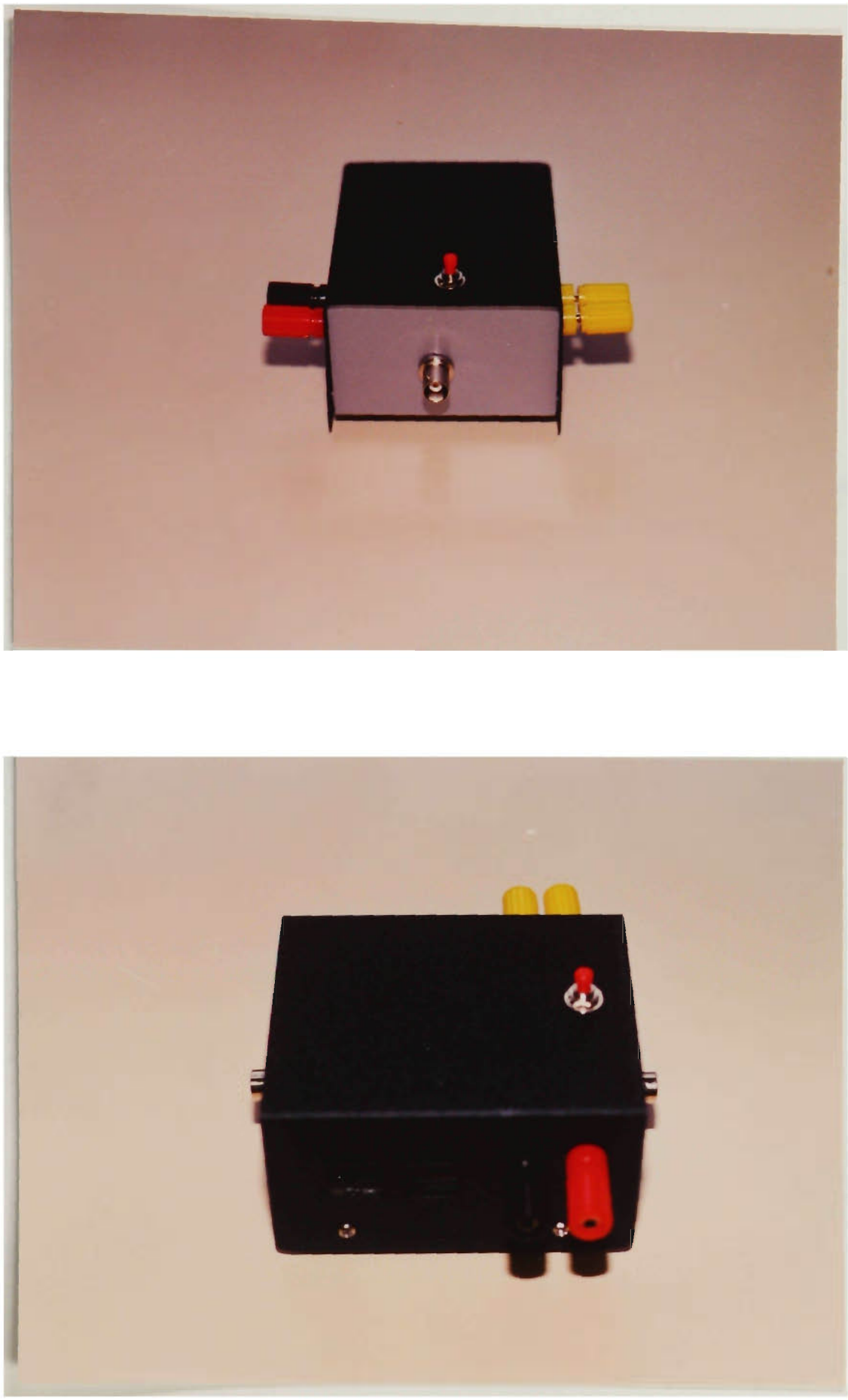

Figure 4.6 Hardware simulator.

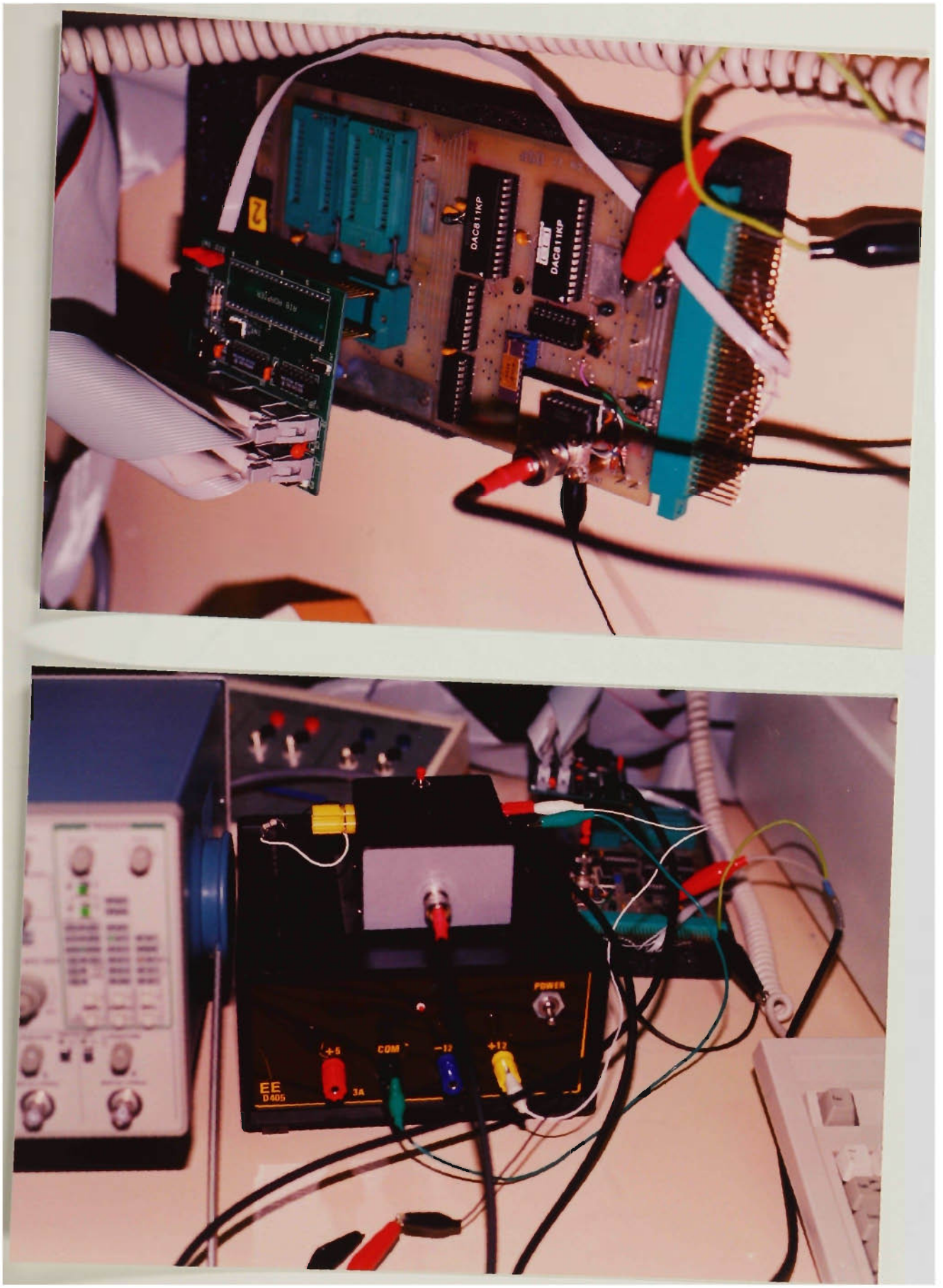

Figure 4.7 Hardware simulator and analogue interface board.

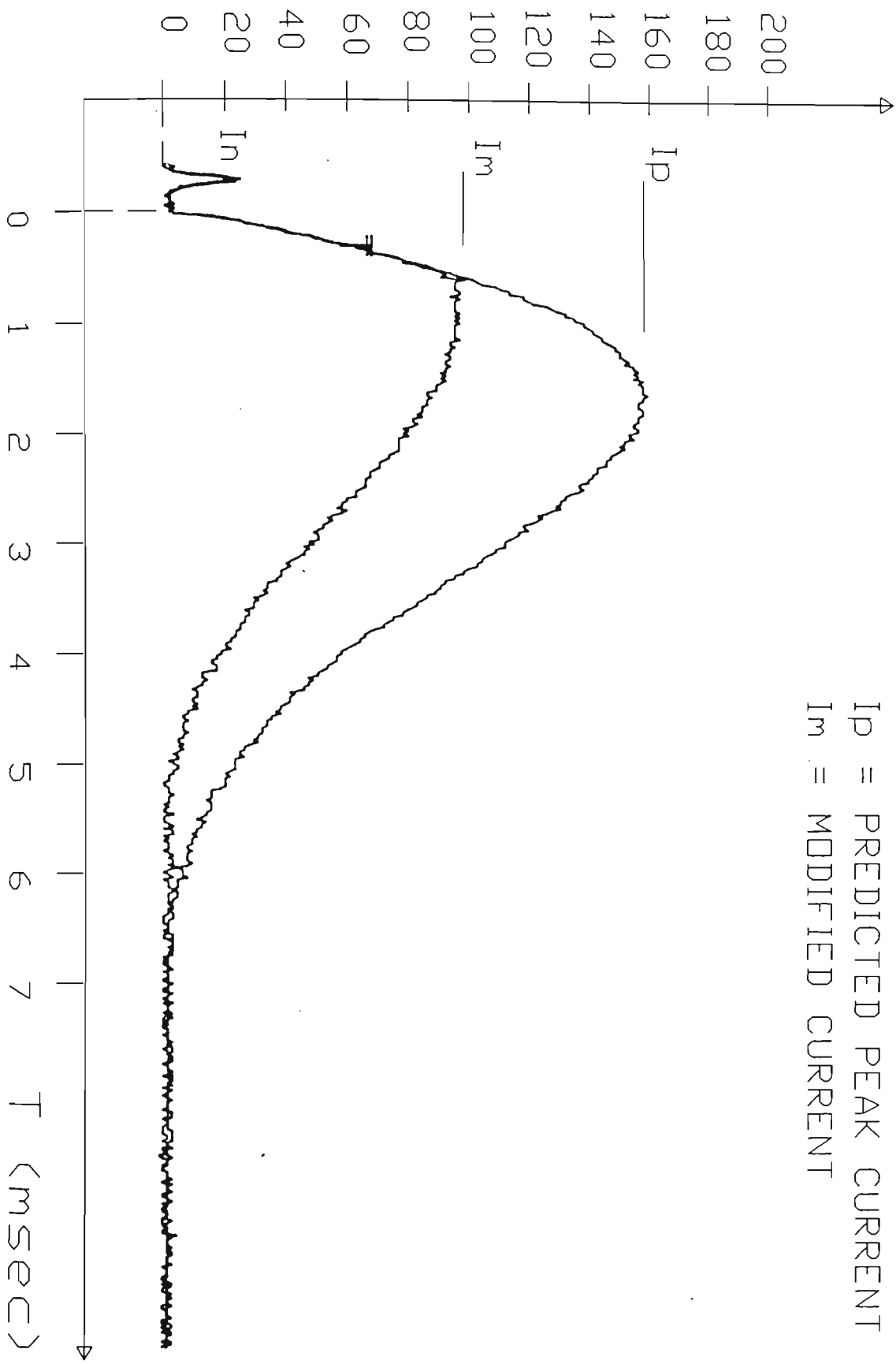

Figure 4.8 The modified current for TTR = 27 ohms.

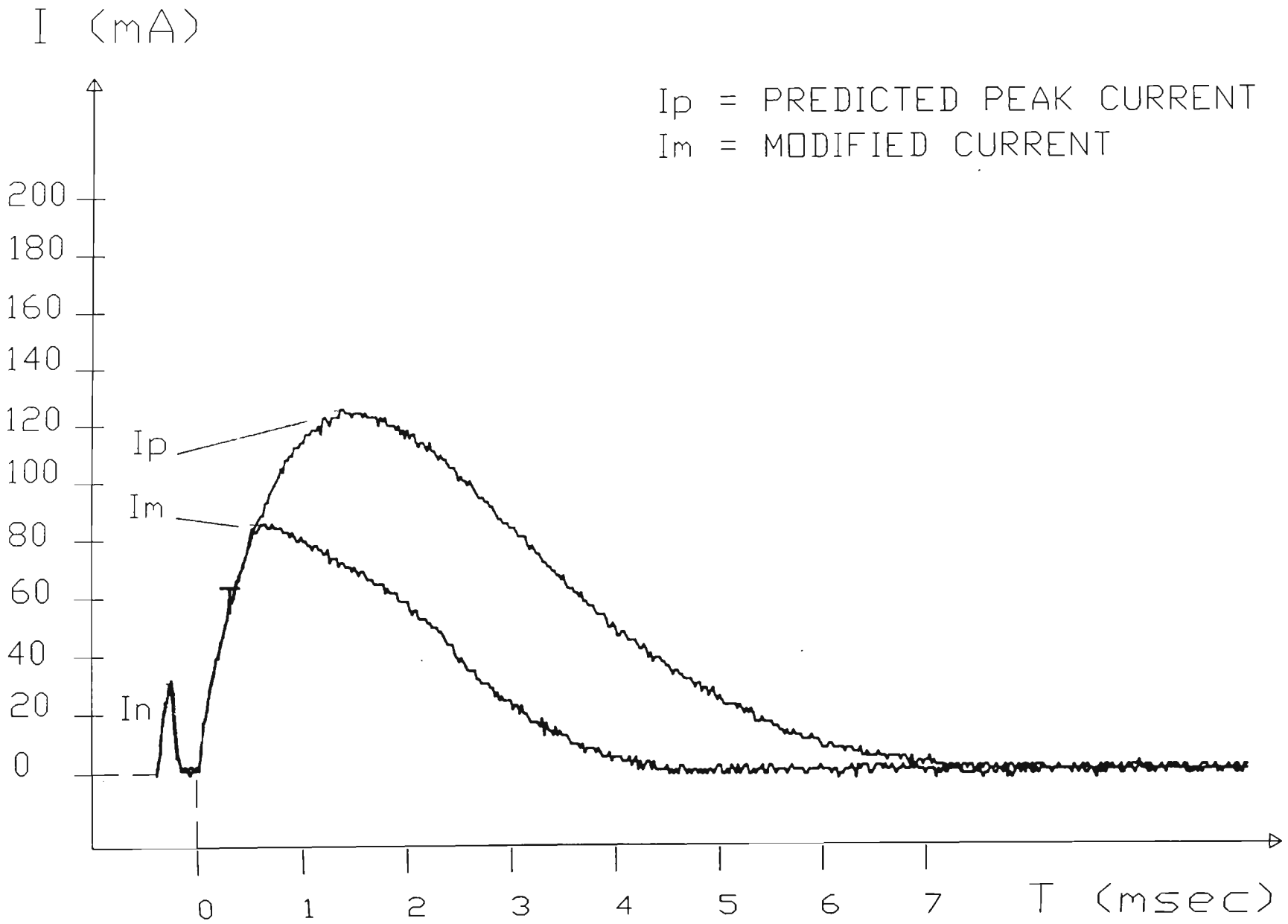

Figure 4.9 The modified current for TTR = 47 ohms.

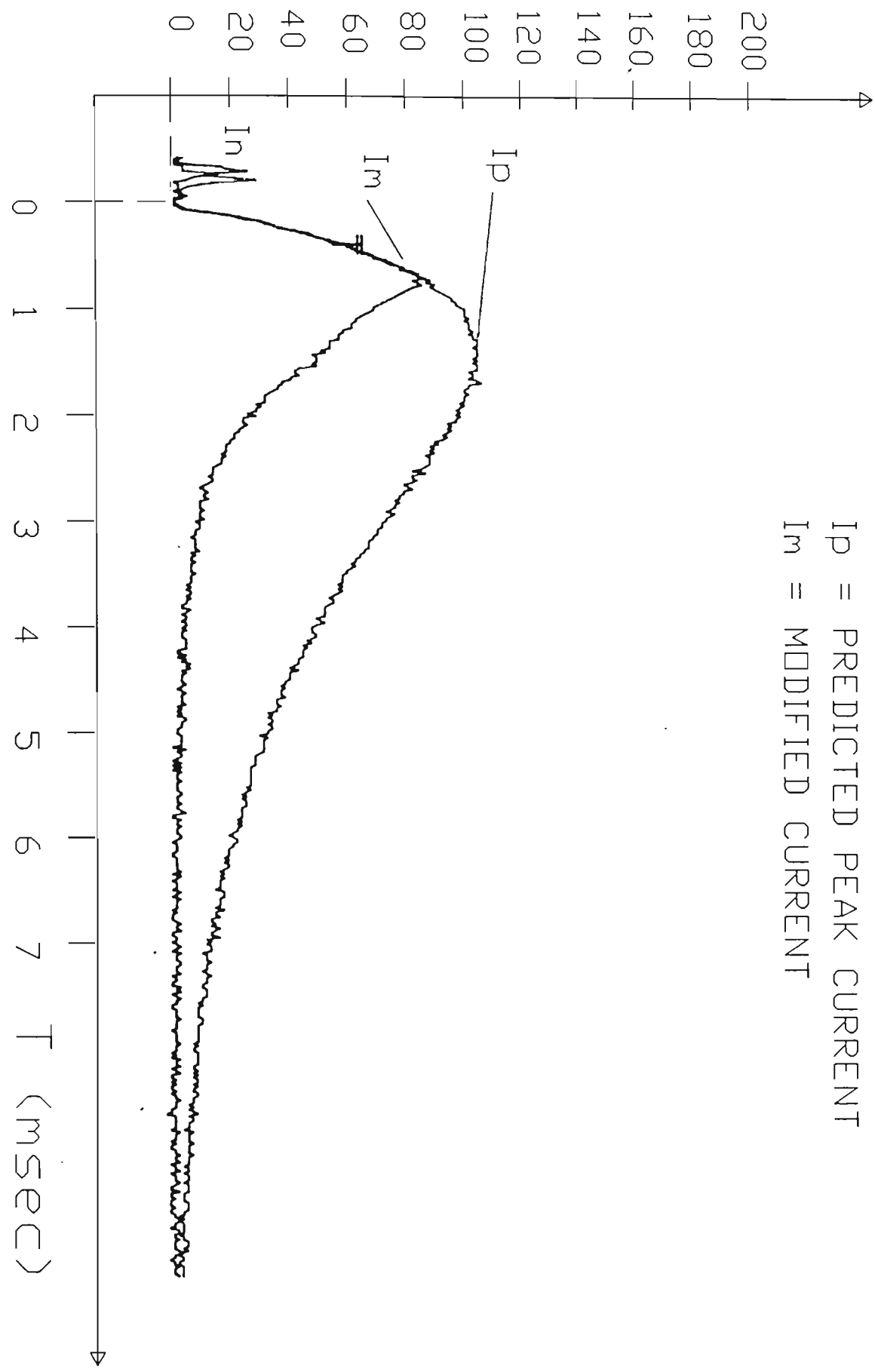

Figure 4.10 The modified current for TTR = 68 ohms.

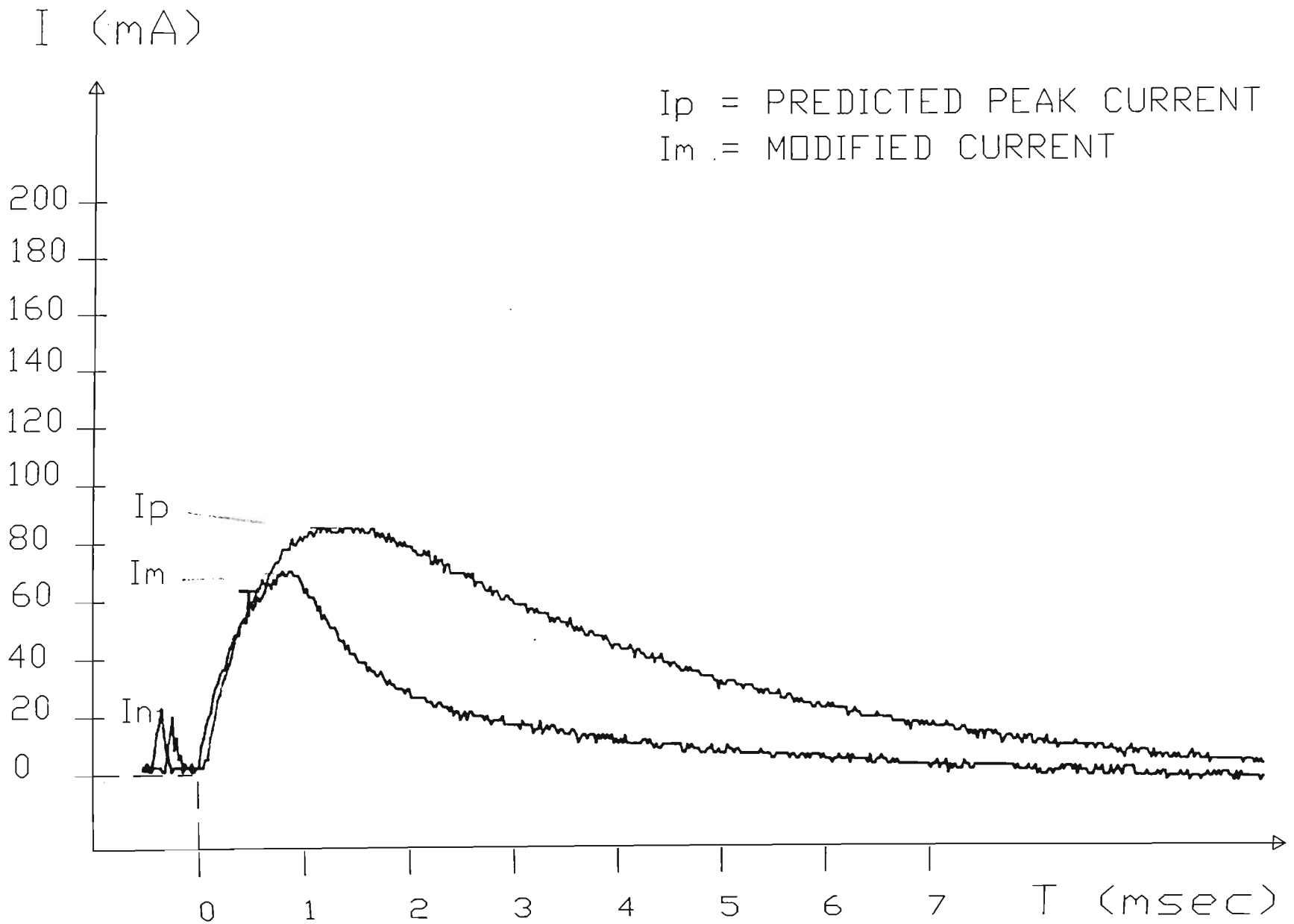

Figure 4.11 The modified current for TTR = 100 ohms.

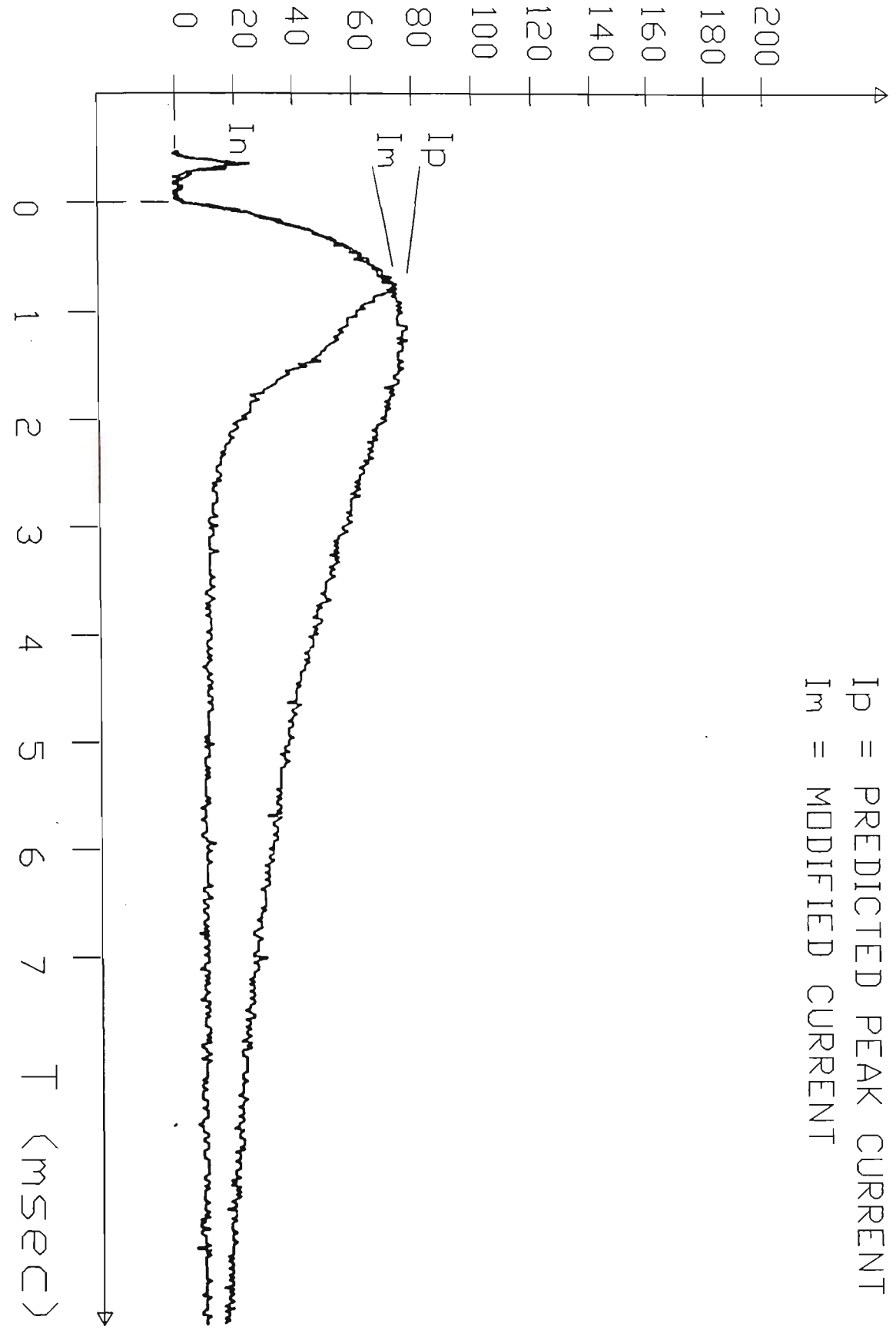

Figure 4.12 The modified current for TTR = 120 ohms.

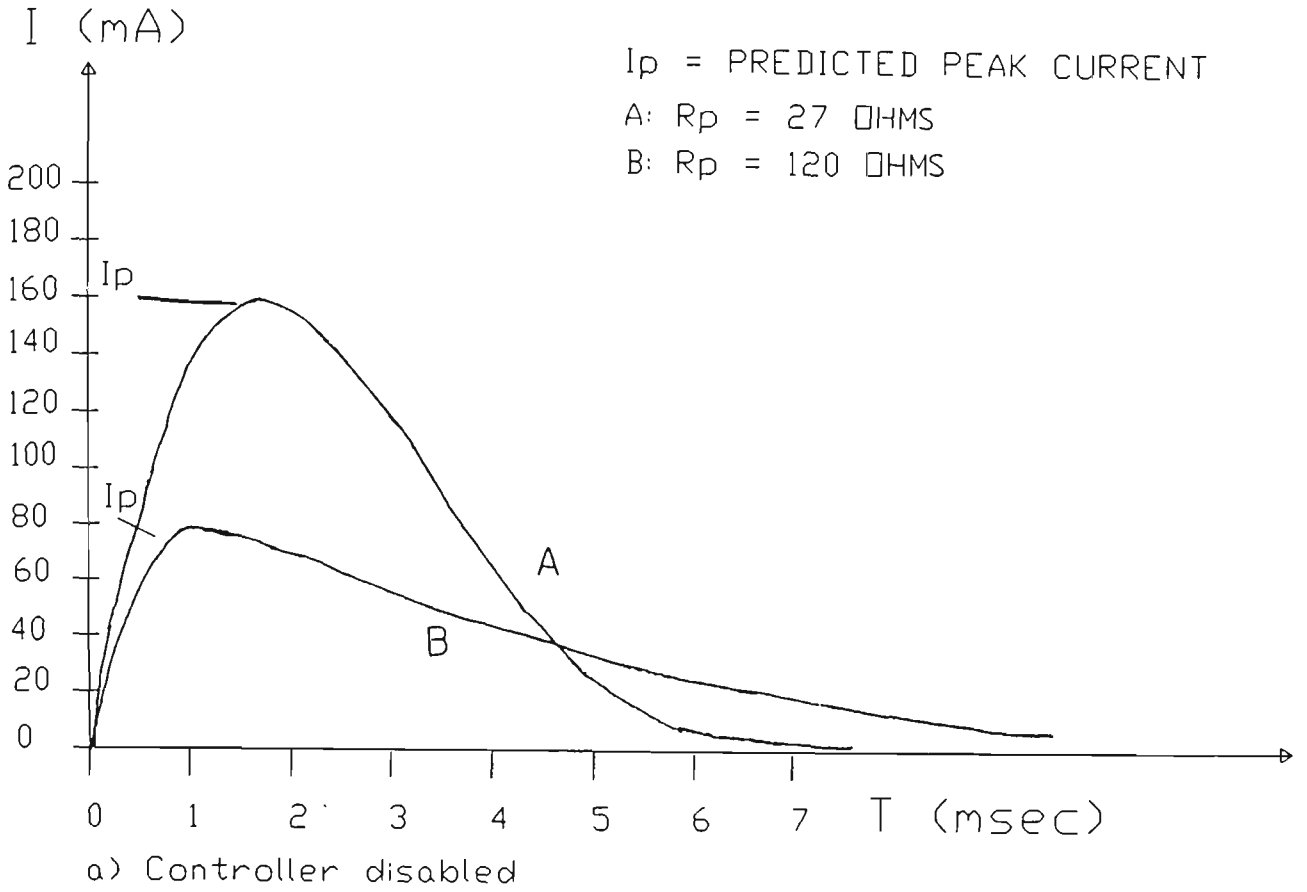

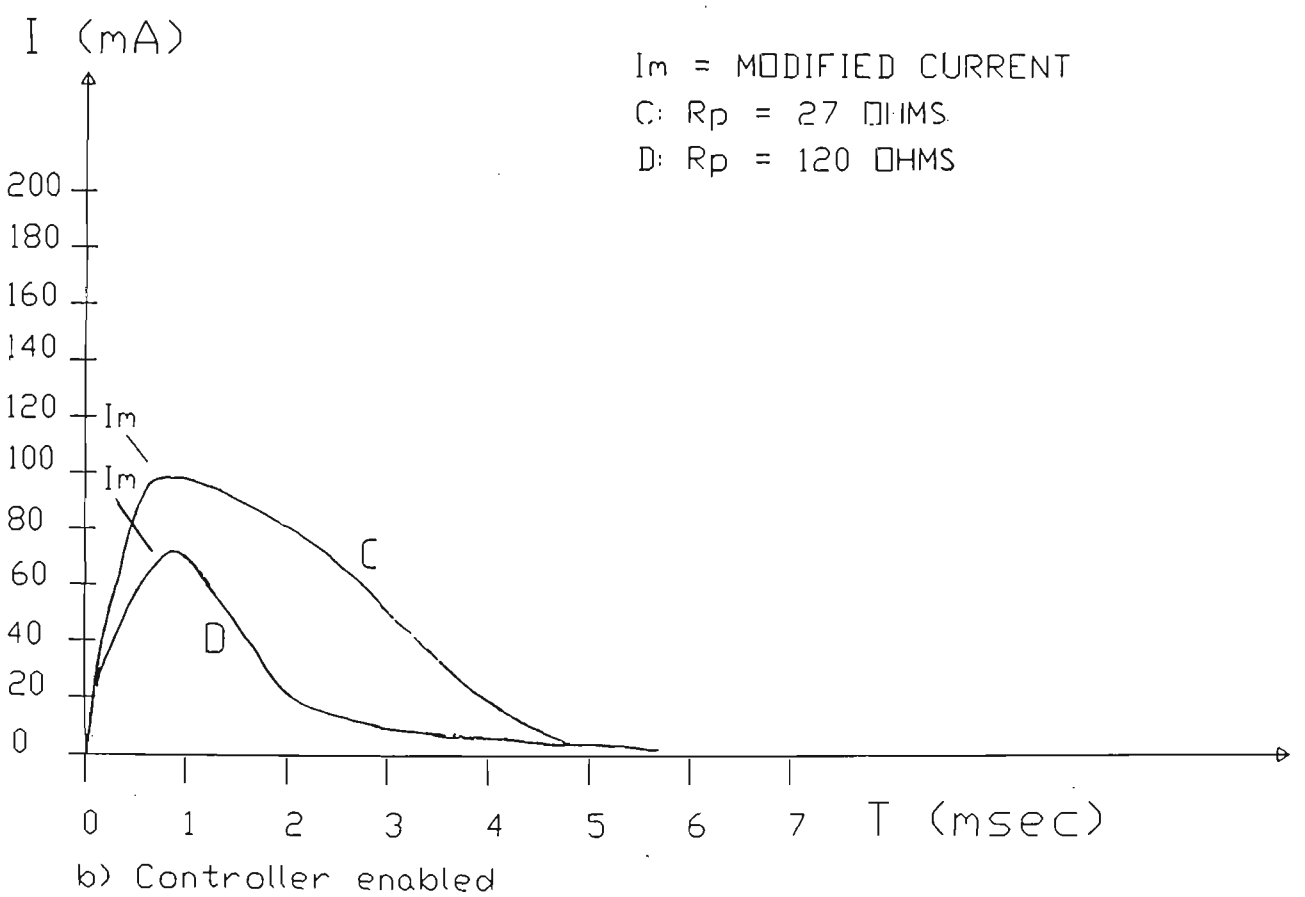

Figure 4.13 Comparison of the TTR current for TTR = 27 ohms and TTR = 120 ohms, a)controller disabled, b) controller enabled.

CHAPTER 5

CONCLUSION

5.1 DISCUSSION OF THE PROJECT

In this research work, a method was described for implementing an adaptive defibrillator. This defibrillator, at the early stages of the defibrillation pulse, calculates the TTR and adjusts its current by switching in a by-passing network, in order to achieve a predetermined current and energy in the TTR. To verify the feasibility of the proposed method, an experimental model was designed and tested and satisfactory results were obtained.

In this research work the problems involved in designing such a defibrillator were identified and solved. Some of these problems and solutions are given in the following paragraphs.

Originally, an MC6809 microprocessor was used for the adaptive controller. This microprocessor was slow for this task, so a TMS320C25 Digital Signal Processor which is 10 times faster than the MC6809 was used. One reason for this selection was the contactor relay bouncing. This bouncing resulted in the Sample Comparison method for the measurement of the TTR which was slower than the single sampling method.

The relay's bouncing had to be minimised by optimisation of the energising voltage of the relay. Electrical voltage applied to the bobbin of the relay had to be selected in such a way that the bouncing was minimised. Some additional mechanical techniques might also be employed to decrease the bouncing further. These techniques are : the use of a high pressurised enclosing of the relay and mechanical dampers to decrease mechanical oscillation of the contact activator.

To measure the TTR, a Sample Comparison method was developed in this research work. This method had to be employed because the bouncing of the relay could not be eliminated completely, so it was impossible to calculate the TTR by the single sampling method.

The defibrillator inductor had to have an air gap, otherwise its core

would saturate. For a defibrillator the magnetic core of the inductor must have high saturation flux densities.

Defibrillator energy had to be by-passed using a high power switch and a power resistor. A time delay method was introduced in this research work in order to maintain the size of the defibrillator and to eliminate the switching problems.

As discussed in the next section, high voltage and high current devices for the by-passing network were not available at the beginning of the experimental work of this research program. At that time it had been predicted that this technological problem would be solved in future. During the writing of this thesis, it was found that some manufacturers have started marketing high power devices specifically for the defibrillator's applications. A short form catalogue for such devices is given in Appendix H. The ramification of the availability of such a device (Isolated Gate Transistor) for the new generation of defibrillators, is discussed in section 5.3.3.

Finally, during this project, it was found that a better technique for the measurement of the TTR is the use of two analogue to digital converters, one for the patient's current and the other for voltage. TTR is the ratio of the patient's voltage to the patient's current during the defibrillation. Alternatively, one analogue to digital converter for current can be used for the measurement of the TTR, but a correction factor must be considered because of the skin resistance breakdown.

5.2 COMPARISON WITH CONVENTIONAL DEFIBRILLATORS

An adaptive defibrillator has many advantages over a conventional defibrillator. In addition to its capability to work as a constant current source for different TTRs, the effect of loose connection of the paddle or bad preparation of the skin can be minimised as they appear as a resistance in series with the TTR and the defibrillator delivers its energy based on the total resistance.

The required additional circuit (power switch and power resistor) does not occupy a large amount of space (there already exists a power resistor for testing purposes in some modern defibrillators that can be used for the by-passing network) and does not conflict with the portability of the defibrillator. Also, realisation of an adaptive defibrillator, minimises the complexity of the set up by eliminating the discharged energy selection, so it is very advantageous in highly stressful and urgent situations in the treatment of ventricular fibrillation. In this regard, in a survey of the users of defibrillators (technical personnel of hospitals) by Raber and Osman [30], it was found that most of the operators preferred the defibrillators to be standardized in performance and operation (e.g., easy to use). There have been complaints by hospital personnel [1] about the complexity of the training and application of this training in highly stressful circumstances. Realisation of an adaptive defibrillator, minimises the complexity of the set up by eliminating the discharged energy selection.

When the complexity of a defibrillator decreases, and the need for technical training is minimised, the defibrillator can be operated by ordinary residents in populated areas with a high rate of heart failure (as recommended by Aronson and Haggar in 1986) [1].

5.3 LIMITATIONS AND RECOMMENDATIONS

As discussed in the previous sections, at the beginning of the experimental part of this project, specific power switches were not available for the adaptive defibrillator design. However, currently some manufacturers have released preliminary data on Isolated Gate Transistors with specific application in defibrillators. The following paragraphs were written before the release of this data and are given in their original form, as the detailed data on the power devices have not been released and the following recommendations can be used in adaptive defibrillator design.

5.3.1 UTILISATION OF HIGH CURRENT-LOW VOLTAGE DEVICES IN HIGH VOLTAGE APPLICATIONS

At this stage, the only technical limitation in realisation of the adaptive defibrillator is the availability of a high voltage (4000 V) and high current device (70 A peak) to by-pass the excess energy of the circuit. This is not, however, in the author's opinion, a technological problem, as yet, there has not been wide spread demand for such a device and the production of a device with little application does not seem encouraging for investors and manufacturers of semiconductor components. So one should say that, as the specified high voltage and high current device is not commercially available, there is a need for other alternatives. One alternative is, to change the high voltage (4000 V)-high current requirement of the switching device to a medium voltage-very high current requirement (400 V-700 A peak).

This device can easily be built by paralleling commercially available HEXFETs. To achieve such a conversion, the circuit in Figure 5.1 has been proposed. In this circuit, if the turns ratio of the transformer is 10 to 1, the replacement of the high voltage-high current switching device with the medium voltage-very high current can be achieved.

If the parameters of the circuit are such that the voltage at point AA is 4000 V, with turns ratio of 10 to 1, the power switch at the secondary must have a voltage rating of just 400 volts. However, the current that the power switch has to by-pass is 10 times more than the primary side (e.g. 50 x 10 = 500 A). The switching of 500 A peak current of the 5-10 msec Lown waveform can be achieved by commercially available solid state switches.

With regard to the energy transfer of the TTR, as Re (equivalent resistance seen at point AA), R_s and the TTR (R_p) are in series, their energy dissipation is proportional to their resistance.

In designing the circuit of Figure 5.1 , the transformer can be assumed to be an ideal transformer by considering its leakage and magnetising inductances as a part of the inductor L, and its series resistance as a part of R_s.

If a resistor is connected to the secondary of the transformer (switching in the by-passing network), the impedance seen at point AA is $R_e = R_t.(n_1/n_2)^2$. The circuit of Figure 5.1 is then simplified to an RLC circuit with $R = R_s + R_p + R_e$.

The values of the currents and the voltages can be predicted using the BASIC program given in Appendix C. For example, a similar approach which was used in the calculation of Table 5.1 may be employed to establish the effect of adding the resistance R_e in the circuit.

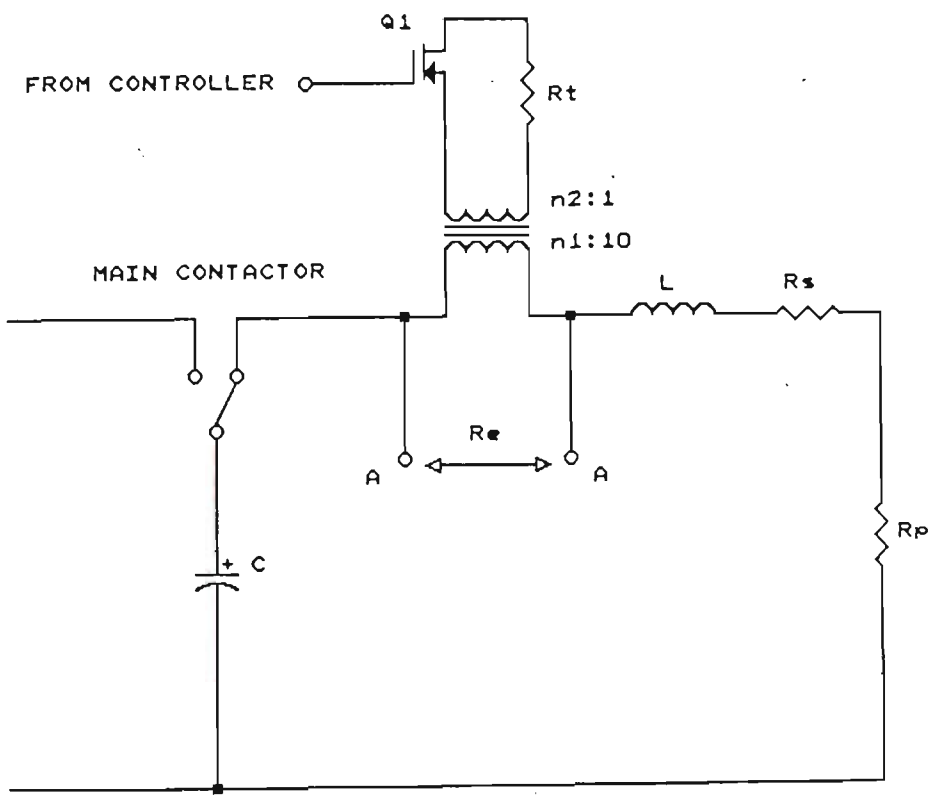

Figure 5.1 Simplified circuit for future work on adaptive defibrillator design.

5.3.2 LINEARITY OF THE TTR

As stated in the previous chapters, Maxwell [22] found that the value of the skin resistance was high before the initiation of the defibrillation pulse and then dropped to a much lower value after the defibrillation current reached a threshold value, a phenomenon known as skin resistance breakdown. The decrease in the skin resistance value occurs in the first 50 µsec after the initiation of the defibrillation pulse. As briefly discussed in section 2.4, a software simulation was developed (Appendix C) to assess the effect of this non-linearity of the TTR due to the skin resistance breakdown in the first 50 µsec of initiation of the pulse. This simulation was achieved by introducing a large resistance value in the software iteration program for the first 50 µsec (e.g. the initial value of patient resistance was assumed to be 5 kΩ for the first 50 µsec).

The peak current of the circuit using this software simulation is shown in Table 5.1. Compared to Table 3.1 where no breakdown was assumed, it is observed that the presence of the skin resistance breakdown, increases the value of TTR calculated by the algorithm employed in this research. For instance, if the breakdown is included in the simulation, for a load resistance of 25 Ω the peak current is 0.1593991 mA at 1588 µsec while if the breakdown is excluded from the simulation, the peak current is 0.1594378 mA at 1546 µsec.

By comparing Table 3.1 and Table 5.1, it can be seen that the difference in the current value for a given TTR, is negligible while occurrence of the peak shifts nearly 50 µsec. This can be expected because, due to the high resistance before and during the breakdown, there is little or no charge transfer from the main capacitor to the circuit. Therefore, the calculated current is less than the actual value, resulting in a higher TTR measurement.

At this point, one can conclude that the measurements of the TTR from the Hewlett-Packard and Cardiac Defibrillators were different because there is a shift in the waveform and also a decrease in the peak

current, so the calculation of the TTR based on the solution of the differential equation results in a false value of the peak current if the skin resistance breakdown is not taken into account in determining the look-up tables. This discussion is supported by Maxwell's results and on this basis, the results from the Cardiac Recorders 61A (Figure 2.5) are more acceptable and in any future work, it is recommended to take the breakdown of the skin into account by addition of a coefficient in the calculation of the look-up table. This coefficient can be obtained from Maxwell's results. Alternatively, Maxwell's measurement technique can be combined with the algorithm presented by this research to design an adaptive defibrillator.

To calculate the values in look-up tables, the differential equation (Equation 3.1) was solved by a numerical method. The numerical method used is advantageous when the TTR varies continuously (non-linear TTR). However, compared with this numerical method which generates cumulative errors, the solution of the linear second order differential equation by standard methods (Appendix B) would result in look-up tables with no error. Hence, a further development would be to generate more accurate look-up tables based on a more realistic model of skin breakdown. The iterative technique which was developed in this research work would be ideal for this purpose.

5.3.3 THE EFFECT OF AVAILABILITY OF HIGH VOLTAGE SEMICONDUCTORS IN DEFIBRILLATOR DESIGN

The following advancements in the defibrillator design are expected if semiconductor power switches with a maximum of 100 µsec switching time and 4000-6000 voltage rating are available:

The contactor relay will be replaced with a semiconductor switch. Due to replacement of the relay, Electro-Magnetic Interference (EMI) will considerably decrease. As the bouncing of the relay is removed, TTR can be calculated much faster so slower power switches can be used. Adaptive defibrillators can be designed based on the technique explained in this research program if the switch has slow turn-off

characteristics. If the power switch has a fast turn-off speed, the by-passing power switch can be removed- the controller turns on the main switch (the switch which replaces the relay) to initiate the defibrillation current pulse. After calculation of the TTR and the required delay (dual sampling method and delayed switching), it then turns off the power switch to modify the current. Availability of high voltage and fast switches results in a new generation of defibrillators which can deliver currents with various shapes and energies.

With regard to the peak value and energy of the defibrillation current, an interesting aspect of the circuit shown in Figure 3.6 is that, various ranges of peak currents and energies can be generated by the adaptive defibrillator proposed in this research work, if Q_2 is turned on and off repeatedly by the processor. This method is similar to Pulse Width Modulation (PWM) techniques. In a PWM circuit, usually a lowpass filter is required for demodulation. However, advantageously, in a defibrillator, this filter is inherent (RLC circuit, Figure 3.1). In this research work the circuit of Figure 3.6 was designed for operation with the optimum value of energy delivered for a given R_p. As discussed earlier, the energy in R_p can be controlled by R_{byp}. The disadvantage of this method is that for a given R_p, the modified current and energy are fixed and hence, further work in development of a PWM by-passing method is recommended . With such a defibrillator, peak current and energy of the defibrillation current can be adjusted independently. The operation of an adaptive PWM type defibrillator is similar to the defibrillator proposed in this work with the difference being that after the processor has calculated R_p and waited (delayed switching), it turns on the by-passing switch and when the current in R_p decreases to a value slightly less than the threshold level (e.g., defibrillation threshold level), the processor turns off the by-passing switch causing the current in R_p to increase again. If the by-passing switch is turned on and off sequentially, a current in R_p is generated with an energy which can be controlled by the speed of this sequence and the duty cycle of the on & off pulse.

TABLE 5.1 The peak current of the circuit if the resistance breakdown is taken into account based on the Maxwell model.

R_p (ohms)	I(peak, A)	t(μsec)	V_C (volts)
25	.1593991	1588	6.371256
30	.15073	1548	6.78127
35	.1429074	1511	7.143158
40	.1358078	1476	7.467588
45	.129344	1443	7.758851
50	.1234354	1412	8.02062
55	.1180169	1382	8.260168
60	.1130306	1354	8.475878
65	.1084287	1327	8.673896
70	.1041702	1302	8.852442
75	.1002185	1278	9.016731
80	.09654235	1254	9.171273
85	.09311737	1232	9.310663
90	.08991505	1211	9.439314
95	.08691672	1191	9.558088
100	.08410575	1171	9.670566
105	.08146249	1152	9.774601
110	.07897409	1134	9.870771
115	.07662775	1117	9.959746
120	.07441174	1100	10.04447
125	.07231575	1084	10.12285

THE SIMULATOR PARAMETERS ARE:

C = 30 μF, L = 53.3 mH, R_S =15 Ω, V(0) = 12 V

Feature	Cardiac Recorders 2610	Hewlett-Packard 78670A	Honeywell (Philips) BD 500	Kontron Heartstation 504	Physio-Control Lifepak 6S	Physio-Control Lifepak 7
Manufacturer/supplier	Cardiac Recorders Ltd	Hewlett-Packard Ltd	Honeywell Control Systems Ltd	Kontron Instruments Ltd	Physio-Control Ltd	Physio-Control Ltd
Country of origin	UK	USA	The Netherlands	UK	USA	USA
Cost	£1465 £2460 with CR7 monitor	£6482	£2900	£3800	£4560	£3560
Dimensions of case (h × w × d)	275 × 205 × 295 mm 10·8" × 8" × 11·6"	229 × 311 × 470 mm 9" × 12·3" × 18·5"	160 × 380 × 450 mm 6·2" × 15" × 17·7"	240 × 410 × 520 mm 9·5" × 16" × 20·5"	234 × 305 × 489 mm 9·2" × 12" × 19·24"	234 × 305 × 489 mm 9·2" × 12 ≧ 19·24"
Weight[1]	14 kg (30·8 lb) 21 kg with CR7 monitor (275 × 510 × 305 mm)	12·7 kg (28 lb)	14·5 kg (32 lb)	16 kg (35·2 lb)	15·4 kg (34·3 lb)	13·7 kg (30·3 lb)
Carrying handle	Yes	Yes—exclusive of charger 368 × 575 mm (14·5" × 23")	Yes	Yes	Yes	Yes
Power supply	Mains only	Internal battery mains via separate charger tray	Internal battery mains/ external supply	Internal battery/mains	Internal battery/mains	Internal battery/mains
battery charger	n/a	In separate charger tray	Built-in	Built-in	Built-in each module	Built-in each module
battery condition indicator	n/a	Battery 'low' lamp	Meter	Lamp for each battery	Meter for each battery	Meter for each battery
separate battery for monitor	n/a	No	No	Yes	Yes	Yes
cost of battery set of batteries	n/a	£194·12p	£78·16p	£240	£50 defib., £95 monitor	£50 defib., £90 monitor
Facilities						
ECG recorder	No	Yes	Optional	Yes	Optional	Optional
plug-in paddles	Yes	Yes	No	Yes	Yes	No
internal paddles	Yes	Yes	No	Yes	Yes	No
output automatically limited	Yes	Yes	n/a	Yes	Yes	n/a
synchronization facilities	Yes, with separate monitor	Yes	Yes	Yes	Yes	Yes
indication of synchronized mode	lamp and marker output to monitor	Marker on monitor and lamp	Lamp	Indicator and marker on monitor	Marker on monitor and lamp	Marker on monitor and lamp
automatic reversion to emergency mode on switch-off	Yes	Yes	Yes	Yes	Yes	Yes
Claimed performance characteristics						
charging time to max energy	3 s	< 10 s	< 10 s	< 10 s	< 10 s	< 10 s
max delivered energy 50 Ω load	360 J	360 J	320 J	360 J	400 J	360 J
Controls and indicators						
firing controls	Dual paddle buttons	Dual paddle buttons	Dual paddle buttons	Dual paddle buttons	Dual paddle buttons	Dual paddle buttons
built-in defibrillator tester	No	Yes	Yes	Yes	Yes	Yes
defibrillator charging method[2]	Manual	Automatic	Manual	Automatic	Automatic	Automatic
indication of deliverable energy	Meter	Meter	Meter	Digital read-out on monitor	Selector switch position	Selector switch position
ECG monitor	No used with CR7 monitor	Yes	Yes	Yes	Yes	Yes
size of display (h × w)	100 × 120 mm	45 × 90 mm (1·75" × 3·5")	60 × 78 mm (2·4" × 3")	70 × 90 mm (2·75" × 3·54")	76 × 102 (3" × 4")	76 × 102 mm (3" × 4")
freeze facility	Yes	No	No	Yes	Yes	Yes
trace speed (mm/s)	25 (fixed)	25 (fixed)	25 (fixed)	25 (fixed)	25 (fixed)	25 (fixed)
calibration facility	Yes	Yes	Yes	Yes	Yes	Yes
patient electrode cable	Yes three electrode	Three electrode	Three electrode	Three electrode	Five electrode	Three electrode
lead selector	No	Yes three lead	No	No	Seven-position 12 lead	Three lead
Guarantee	12 months	12 months	12 months	12 months	12 months	12 months
Maintenance provision						
availability of spares	5 years	5 years from last production	7 years minimum	7 years	5 years from last production	5 years from last production
service contracts	Yes, and co-operation with hospital's own maintenance schemes	Yes, and co-operation with hospital's own maintenance schemes	Yes, and co-operation with hospital's own maintenance schemes	Yes, and co-operation with hospital's own maintenance schemes	Yes, and co-operaton with hospital's own maintenance schemes	Yes, and co-operation with hospital's own maintenance schemes
first visit	At user's premises	At user's premises	At user's premises	At user's premises	At user's premises	At user's premises
max. response time	Normally 48 h	Dependent on contract	Normally within 24 h	24 h or 72 h	24 h response	24 h response
loan replacement	Yes	Yes, when available	Yes	Yes, when available	Yes, as appropriate	Yes, as appropriate

Notes. (1) = Including battery but excluding separate charging units; (2) = manual = continuous depression of charge button until the required charge is achieved; automatic = momentary depression to initiate charging after the level of charge has been selected; n/a = not applicable.

APPENDIX B

TIME DOMAIN SOLUTION OF THE DIFFERENTIAL EQUATION OF THE DEFIBRILLATOR CIRCUIT

Equivalent circuit of a cardiac defibrillator is given below:

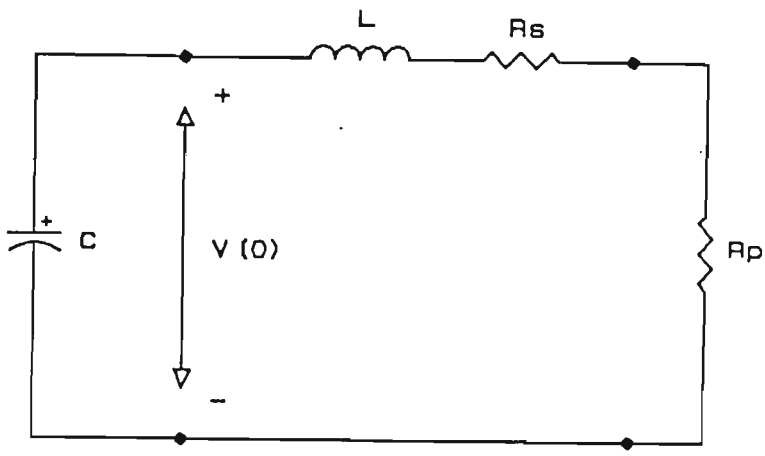

Figure B.1 Simplified circuit diagram of defibrillator.

The time domain equation for the circuit in Figure B.1 is :

$$L\frac{d\,i(t)}{d\,t} + (R_S + R_p)\,i(t) + \frac{1}{C}\int i\,dt = 0 \qquad B.1$$

Laplace transform into the s domain results in:

$$(R_S + R_p)\,I(S) + S.L.I(S) - L.i(0+) + \frac{1}{S.C}\,I(S) - \frac{q(0)}{S.C} = 0 \qquad B.2$$

The initial boundary conditions are:

$i(0) = 0$

$q(0)$ = stored charge on the capacitor.

Let $R = R_s + R_p$ then from B.2:

$$I\left(S^2 + \frac{R}{L}S + \frac{1}{L.C}\right) = \frac{q(0)}{L.C}$$

Let $\frac{R}{2.L} = \sigma$ and $\frac{1}{L.C} = W^2$ then

$$I(S) = \frac{q(0).\,W^2}{S^2 + 2.\sigma.S + W^2} \qquad \text{B.3}$$

Using the method of partial fractions, B.3 can be broken up into fractions of general form:

$$I(S) = \frac{a_1}{S + P_1} + \frac{a_2}{S + P_2} \qquad \text{B.4}$$

The general solution of B.4, using the residue theorem is:

$$i(t) = a_1.\exp(P_1.t) + a_2.\exp(P_2.t) \quad \text{for } t \geq 0 \qquad \text{B.5}$$

where the solution for P_1 and P_2 are:

$$P_{1,2} = -\sigma \pm \sqrt{\sigma^2 - W^2}$$

There are three solutions to B.4 :

$\sigma^2 - W^2 > 0$	overdamped case
$\sigma^2 - W^2 = 0$	critically damped case
$\sigma^2 - W^2 < 0$	underdamped case

OVERDAMPED CASE

$P_1 = -\sigma + \sigma_d$ and $P_2 = -\sigma - \sigma_d$

where

$$\sigma_d = \sqrt{\sigma^2 - W^2}$$

then

$$i(t) = \frac{W^2 \cdot q(0)}{2.\sigma_d} \exp(-\sigma.t) \left(\exp(\sigma_d.t) - \exp -(\sigma_d.t) \right)$$

CRITICALLY DAMPED CASE

$$P_1 = P_2 = \sigma$$

then

$$i(t) = W^2 \cdot q(0) \cdot t \exp(-\sigma.t)$$

UNDERDAMPED CASE

$$P_1, P_2 = -\sigma \pm \sqrt{\sigma^2 - W^2}$$

$$P_1, P_2 = -\sigma \pm i.\sqrt{w^2 - \sigma^2}$$

Let $W_d = \sqrt{W^2 - \sigma^2}$ then

$$I(S) = \frac{q(0).W^2}{(S + \sigma + i.W_d) (S + \sigma - i.W_d)}$$

$$= \frac{1}{Wd} \cdot \frac{q(0).W^2.W_d}{(S + \sigma)^2 + W_d^2}$$

Then

$$i(t) = \frac{q(0).W^2}{W_d} \exp(-\sigma.t)$$

APPENDIX C

The second order differential equation of the defibrillator circuit can be solved by numerical methods. From the equation C.1:

$$L.d^2q(t)/dt^2 + (R_s + R_p).dq(t)/dt + 1/C.q(t) = 0 \qquad C.1$$

the following equations can be derived

$$q(k+1) = q(k) + T\ i(k) \qquad C.2$$

$$i(k+1) = -q(k).T/LC + (1- (R + R_p).T/L).i(k) \qquad C.3$$

based on the definition of the differential equation

$$dq(t)/dt = i(t)$$

or

$$i(t) = \lim_{T \to 0} [q(t+T)-q(t)]/T$$

provided the condition that the sampling rate T is very small.

From initial conditions

$$I(0) = 0$$

$$q(0) = \sqrt{2.C.W}$$

if the initial energy of the capacitor is known, then q(k+1) from equation C.2 can be found and hence i(k+1) from equation C.3 is found and finally using a computer to do the iterations, the current in the circuit can be found at any time.

In the software programs it was found that if the sampling rate is more that 3 µsec STEP, error will occur especially for underdamped conditions. To obtain good accuracy T = 1 µsec has been used.

```
**************************************************************************

       PROGRAM WHICH CALCULATES THE PEAK DEFIBRILLATOR CURRENT.

**************************************************************************

200 DIM A(1990),Q(1990)
206 REM THE INPUT PARAMETERS ARE THE DEFFIBRILLATOR'S.
210 INPUT "ENTER THE SAMPLING RATE IN MICROSECOND:";T
220 INPUT "ENTER THE CAPACITANCE IN MICROFARAD:";C
240 INPUT "ENTER THE INDUCTANCE IN MILIHENRY:";L
250 INPUT "ENTER THE SERIES RESISTANCE IN OHM:";R
255 INPUT "THE ENERGY SETTING OF THE DEFIBRILLATOR IN JOUL:";W
260 INPUT "ENTER THE LOWER VALUE OF PATIENT RESISTANCE";J
280 INPUT "ENTER THE HIGHER VALUE OF PATIENT RESISTANCE";K
281 CLS
282 PRINT " Rp             Im             T             Vc "
283 PRINT
285 T=T*.000001
290 C=C*.000001
295 L=L*.001
320 Q(0)=SQR(2*C*W)
330 RP=J
340 FOR I=0 TO 1899 STEP 1
360 Q(I+1)=Q(I)+T*A(I)
380 A(I+1)=-Q(I)*T/(L*C)+(1-(R+RP)*T/L)*A(I)
410 IF -A(I)>-A(I+1) THEN GOTO 650
600 NEXT
650 PRINT RP,-A(I),T*I*1000000!,Q(I)/C
700 RP=RP+5
900 IF RP<K+1 THEN GOTO 340 ELSE 1000
1000 PRINT "THE DEFIBRILLATOR'S PARAMETERS ARE:"
1100 PRINT "C=";C;"  L=";L;   "  ENERGY=";W
1200 END
```

```
**************************************************************************

PROGRAM WHICH CALCULATES THE TIME AT WHICH THE FIRST SAMPLING CURRENT FLOWS.

**************************************************************************

 200 DIM A(1500),Q(1500)
 206 REM THE INPUT PARAMETERS ARE THE DEFFIBRILLATOR'S.
 210 INPUT "ENTER THE SAMPLING RATE IN MICROSECOND:";T
 220 INPUT "ENTER THE CAPACITANCE IN MICROFARAD:";C
 240 INPUT "ENTER THE INDUCTANCE IN MILIHENRY:";L
 250 INPUT "ENTER THE SERIES RESISTANCE IN OHM:";R
 255 INPUT "THE ENERGY SETTING OF THE DEFIBRILLATOR IN JOUL:";W
 260 INPUT "ENTER THE LOWER VALUE OF PATIENT RESISTANCE";J
 280 INPUT "ENTER THE HIGHER VALUE OF PATIENT RESISTANCE";K
 281 CLS
 282 PRINT " Rp            Im            T             Vc "
 283 PRINT
 285 T=T*.000001
 290 C=C*.000001
 295 L=L*.001
 320 Q(0)=SQR(2*C*W)
 330 RP=J
 340 FOR I=0 TO 1498 STEP 1
 360 Q(I+1)=Q(I)+T*A(I)
 380 A(I+1)=-Q(I)*T/(L*C)+(1-(R+RP)*T/L)*A(I)
 400 IF -A(I)>.05 GOTO 650
 600 NEXT
 650 PRINT RP,-A(I),T*I*1000000!,Q(I)/C
 700 RP=RP+5
 900 IF RP<K+1 THEN GOTO 340 ELSE 1000
1000 PRINT "THE DEFIBRILLATOR'S PARAMETERS ARE:"
1100 PRINT "C=";C;"  L=";L;  "  ENERGY=";W
1200 END
```

```
**************************************************************************

PROGRAM WHICH CALCULATES THE TIME AT WHICH THE THRESHOLD CURRENT FLOWS.

**************************************************************************

200 DIM A(1500),Q(1500)
206 REM THE INPUT PARAMETERS ARE THE DEFFIBRILLATOR'S.
210 INPUT "ENTER THE SAMPLING RATE IN MICROSECOND:";T
220 INPUT "ENTER THE CAPACITANCE IN MICROFARAD:";C
240 INPUT "ENTER THE INDUCTANCE IN MILIHENRY:";L
250 INPUT "ENTER THE SERIES RESISTANCE IN OHM:";R
255 INPUT "THE ENERGY SETTING OF THE DEFIBRILLATOR IN JOUL:";W
260 INPUT "ENTER THE LOWER VALUE OF PATIENT RESISTANCE";J
280 INPUT "ENTER THE HIGHER VALUE OF PATIENT RESISTANCE";K
281 CLS
282 PRINT " Rp             Im             T             Vc "
283 PRINT
285 T=T*.000001
290 C=C*.000001
295 L=L*.001
320 Q(0)=SQR(2*C*W)
330 RP=J
340 FOR I=0 TO 1498 STEP 1
360 Q(I+1)=Q(I)+T*A(I)
380 A(I+1)=-Q(I)*T/(L*C)+(1-(R+RP)*T/L)*A(I)
400 IF -A(I)>.0723335 GOTO 650
600 NEXT
650 PRINT RP,-A(I),T*I*1000000!,Q(I)/C
700 RP=RP+5
900 IF RP<K+1 THEN GOTO 340 ELSE 1000
1000 PRINT "THE DEFIBRILLATOR'S PARAMETERS ARE:"
1100 PRINT "C=";C;"  L=";L;  "  ENERGY=";W
1200 END
```

```
**************************************************************************

PROGRAM WHICH CALCULATES THE VALUE OF THE CURRENT AT THE  SECOND  SAMPLING
                                    TIME.

**************************************************************************

200 DIM A(1990),Q(1990)
206 REM THE INPUT PARAMETERS ARE THE DEFFIBRILLATOR'S.
260 INPUT "ENTER THE LOWER VALUE OF PATIENT RESISTANCE";J
270 INPUT "ENTER TIME LIMIT:";TL
283 PRINT
285 T=.000001
286 R=15
287 W=.00216
290 C=.000001*30
295 L=.001*53.3
320 Q(0)=SQR(2*C*W)
330 RP=J
340 FOR I=0 TO 1899 STEP 1
360 Q(I+1)=Q(I)+T*A(I)
380 A(I+1)=-Q(I)*T/(L*C)+(1-(R+RP)*T/L)*A(I)
410 IF 1000000!*T*I >=TL GOTO 650
600 NEXT
650 PRINT RP,-A(I),T*I*1000000!,Q(I)/C
700 INPUT "more";SIG$
710 J=J+5
750 IF SIG$="y" GOTO 270 ELSE GOTO 1000
1000 PRINT "THE DEFIBRILLATOR'S PARAMETERS ARE:"
1100 PRINT "C=";C;"  L=";L;   "  ENERGY=";W
1200 END
```

```
**************************************************************************

      PROGRAM WHICH SIMULATES THE BREAK DOWN OF THE SKIN RESISTANCE.

**************************************************************************

200 DIM A(1990),Q(1990)
206 REM THE INPUT PARAMETERS ARE THE DEFFIBRILLATOR'S.
210 INPUT "ENTER THE SAMPLING RATE IN MICROSECOND:";T
220 INPUT "ENTER THE CAPACITANCE IN MICROFARAD:";C
240 INPUT "ENTER THE INDUCTANCE IN MILIHENRY:";L
250 INPUT "ENTER THE SERIES RESISTANCE IN OHM:";R
255 INPUT "THE ENERGY SETTING OF THE DEFIBRILLATOR IN JOUL:";W
260 INPUT "ENTER THE LOWER VALUE OF PATIENT RESISTANCE";J
280 INPUT "ENTER THE HIGHER VALUE OF PATIENT RESISTANCE";K
281 CLS
282 PRINT " Rp             Im             T             Vc "
283 PRINT
285 T=T*.000001
290 C=C*.000001
295 L=L*.001
320 Q(0)=SQR(2*C*W)
330 RP=5000
340 FOR I=0 TO 1899 STEP 1
360 Q(I+1)=Q(I)+T*A(I)
380 A(I+1)=-Q(I)*T/(L*C)+(1-(R+RP)*T/L)*A(I)
410 IF -A(I)>-A(I+1) THEN GOTO 650
420 IF I>50 THEN RP=J
600 NEXT
650 PRINT RP,-A(I),T*I*1000000!,Q(I)/C
700  J= J+5
900 IF J<K+1 THEN GOTO 330 ELSE 1000
1000 PRINT "THE DEFIBRILLATOR'S PARAMETERS ARE:"
1100 PRINT "C=";C;"  L=";L;  "  ENERGY=";W
1200 END
```

APPENDIX D

MCU6809 is a fully functional microcomputer system based on the MC6809 microprocessor unit, associated memories and I/O devices.

The basic unit is located on a single module in conjunction with a resident monitor program (firmware) can be used for entering and debugging user programs.

The MCU6809 system features include:

a) 4MHz MC6809 8 bit microprocessor.
b) 2k bytes of static RAM.
c) 4k bytes of EPROM monitor.
d) Two serial communication ports. Both are RS-232C compatible and have programmable rates.
e) Two parallel ports (16 data lines with hand shake for each) which can be used for I/O. One may be used with a manual paper reader or an EPROM programmer.
f) Four 16-bit internal timers.
g) Reset and NMI switches.
h) EPROM programmer.
i) Programs can be down loaded from or up loaded to ahost system.

A modified version of the MCU6809 with one parallel port was used in this research. This unit can communicate with a PC via one serial port. Assembly programs can be prepared on a PC based text editor and be assembled by an assembler and loaded into the internal memories of the MCU6809 for execution.

The following is one of the assembly programs written in this research. The aim of this program was to establish if the speed of the MC6809 was enough for this application or there was a need to select a faster microprocessor.

```
*************************************************************************

    MC6809 ASSEMBLY PROGRAM FOR THE ADAPTIVE DEFIBRILLATOR DESIGN

*************************************************************************

DATA     EQU    $80
  ORG    DATA
TABLE    FCB    $FF,$CF,$BF,$9F,$7F,$5F,$3F,$2F,$0F,$0D,$0A
CODE     EQU    $100          START ADDRESS
  ORG    CODE
  LDA    #$82              INITIALIZE IER
  STA    $E10E
  LDA    #$01              INITIALIZE ACR FOR CA1 LATCH
  STA    $E10B
  LDA    #$EC              INITIALIZE PCR FOR CA1 LOW O/P
  STA    $E10C             AND CA2 HIGH
  SYNC                       WAIT FOR INTRUPT
  LDA    $E101             LOAD ACC A FROM A/D
  LDX    #$007F
  LEAX   1,X           POINT TO THE FIRST DATA
  CMPA   ,X+               COMPARE A/D RESULT WITH TABLE
  BHS    LOOP1
  CMPA   ,X+
  BHS    LOOP2
  CMPA   ,X+
  BHS    LOOP3
  CMPA   ,X+
  BHS    LOOP4
  CMPA   ,X+
  BHS    LOOP5
  CMPA   ,X+
  BHS    LOOP6
  CMPA   ,X+
  BHS    LOOP7
  CMPA   ,X+
  BHS    LOOP8
  CMPA   ,X+
  BHS    LOOP9
  CMPA   ,X+
  JMP    LOOP10
LOOP1    LDB    #$03              START DELAY1 FOR RP1
  JMP    FIND
LOOP2    LDB    #$3E              START DELAY2 FOR RP2
  JMP    FIND
LOOP3    LDB    #$3C
  JMP    FIND
LOOP4    LDB    #$3A
  JMP    FIND
LOOP5    LDB    #$38
  JMP    FIND
LOOP6    LDB    #$36
  JMP    FIND
LOOP7    LDB    #$34
  JMP    FIND
LOOP8    LDB    #$32
  JMP    FIND
LOOP9    LDB    #$30
  JMP    FIND
LOOP10   LDB    #$2E              START DELAY10 FOR RP10
  JMP    FIND
FIND     DECB
  CMPB   #$01
  BHS    FIND
  LDB    #$FF              LOAD VIA, PORT B TO
  STB    $E102             SWITCH THE HIGH VOLTAGE
  SWI                        FET
```

After initialisation of the parallel port and internal registers, the microprocessor waits for an interrupt signal (SYNC instruction) from the VIA (initiation of the defibrillation pulse).

After reading the value of the current from the A/D, the microprocessor finds the R_p from a look-up table and then provides the required delay for the by-passing network to operate. The schematic of the circuit has been given in Appendix E.

For further information refer to [23] and [26].

APPENDIX E

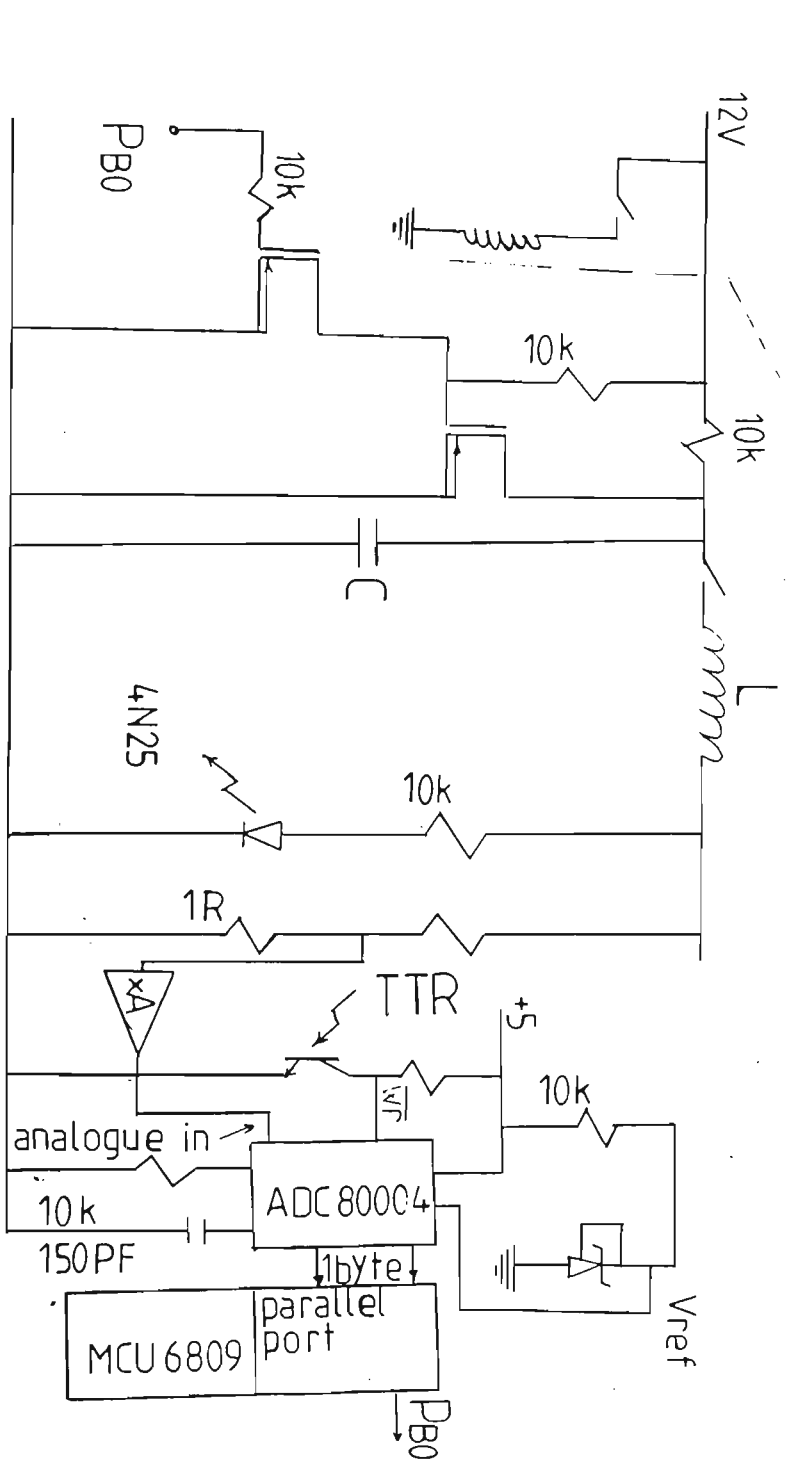

Figure E.1 Schematic diagram of the simulator using MCU6809.

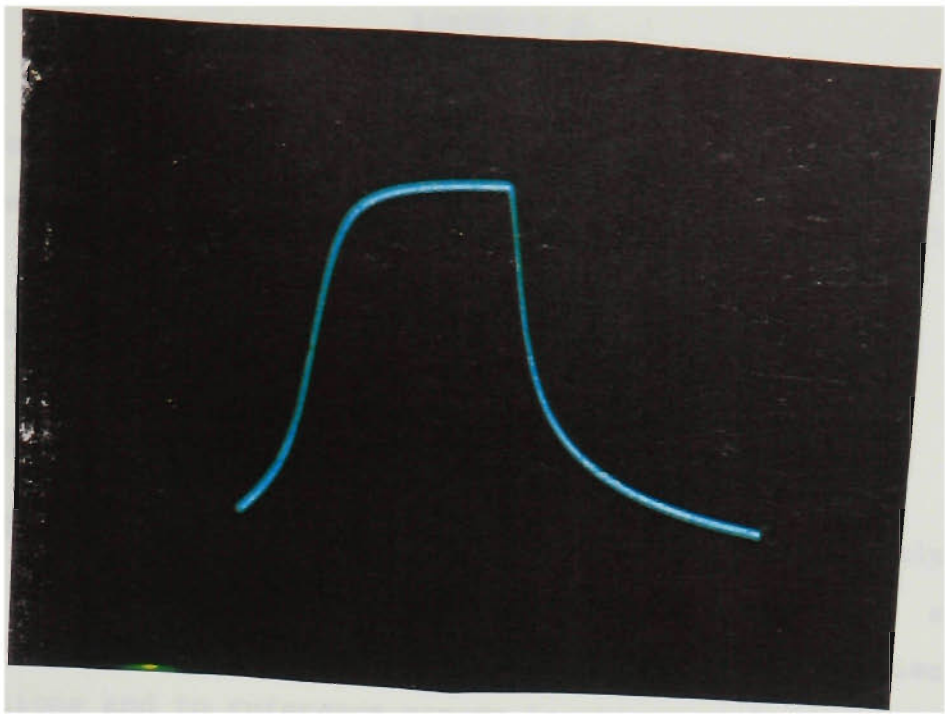

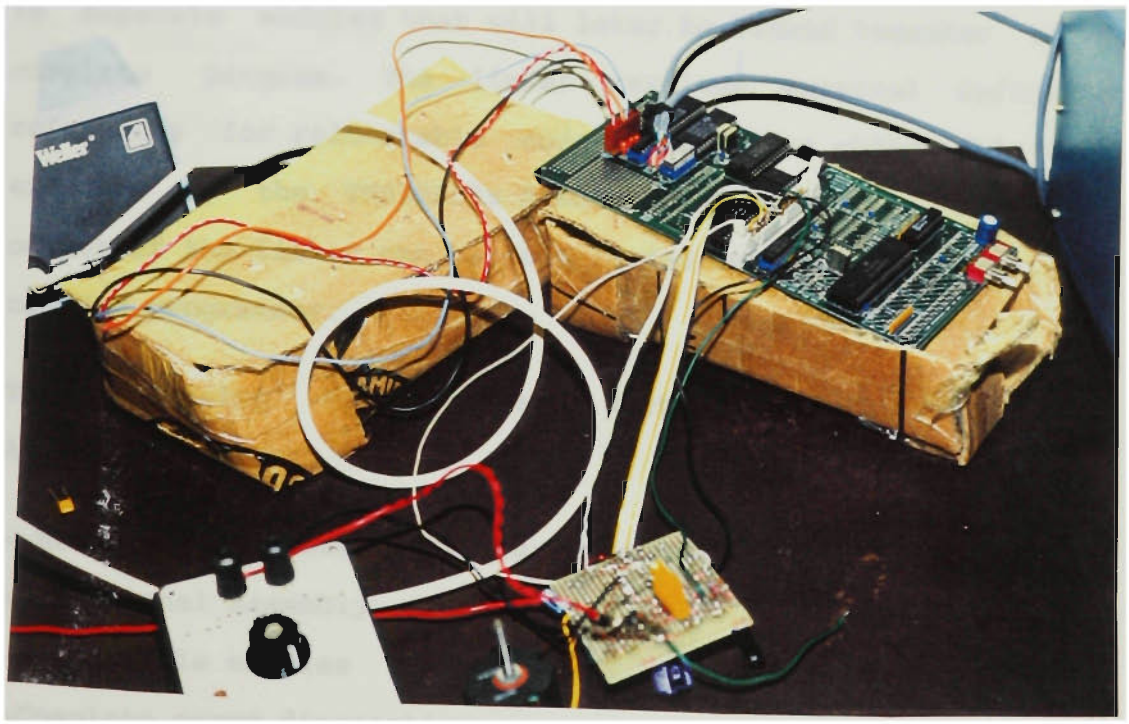

Figure E.2 Illustration of the simulator, using MCU6809.

APPENDIX F

In this appendix the software development tools of the TMS320C25 is explained and the C program used in the project is also discussed.

SECTION 1

TMS320C2x MACRO ASSEMBLER/LINKER

The TMS320C2x Macro Assembler translates TMS320C2x assembly language source code into executable object code. The assembler allows the programmer to work with mnemonics rather than hexadecimal machine instructions and to reference memory locations with symbolic addresses. The macro assembler supports macro calls and definitions along with conditional assembly.

The TMS320C2x Linker permits a program to be designed and implemented in separate modules that will later be linked together to form the complete program. The linker resolves external definitions and references for relocatable code, creating an object file that can be executed by the TMS320C2x Simulator, Emulator, or DSP device. The output of the linker can be down loaded into the simulator, XDS, SWDS, or PROM programmer.

The following key features distinguish the TMS320C2x Macro Assembler/Linker:

- Macro capabilities and library functions
-Conditional assembly
-Relocatable modules
-Complete error diagnostics
-Symbol table and cross reference.

The macro assembler/linker is currently available for the VAX/VMS and MS/PC-DOS operating systems.

SECTION 2

TMS320C2x SOFTWARE DEVELOPMENT SYSTEM (SWDS)

The SWDS is a PC resident tool that allows software simulation in real time for the TMS320C2x. The SWDS provides the system interface necessary to write, assemble/link, load, and debug the TMS320C2x code on a PC workstation. The SWDS is capable of single stepping through the code or setting software breakpoints for monitoring register or memory contents during execution. It can also associate files with I/O ports so that specific I/O values may be used during test and debug.

The SWDS consists of three parts:

1) A circuit board, resident in the PC, that contains the TMS320Cx and program and data memory.

2) Two small cable adaptor boards situated outside the PC and are connected to the SWDS via two 40-conductor ribbon cables. The cable adaptor boards included with the system are:

a) The PGA Adaptor Connector that connects the SWDS to a TMS320C2x target system via a 68-pin grid array footprint.
b) The Analogue Interface Board (AIB) Adaptor Connector that connects the SWDS directly to the TMS320 AIB.

3) Software that includes TMS320C2x assembler/linker software, the DSP Software Library, and SWDS monitor software.

The SWDS is designed to function in the IBM-PC/AT and compatible environment and the operating system MS-PC DOS version 2.0 or later is required.

The development system occupies 64K bytes of the PC memory. It is equipped with 24K words (48 Kbytes) of static RAM, and allows the TMS320C2x to execute at full speed. SWDS does not address target memory.

The SWDS is configured to emulate the TMS320C25 upon shipment; i.e., a TMS320C25 and a 40 MHz oscillator are on-board.

SECTION 3

TMS320C25 C COMPILER[1]

A full Kernigan and Ritchie C compiler is provided for the TMS320C25. The compiler accepts a digital signal processing program written in the widely used C language and outputs TMS320C2x assembly language source code. The TMS320C2x mnemonics are then converted to object code by a TMS320Cx assembler.

The high-level language compiler allows time-critical routines written in assembly language to be called from within the C program. The converse is also available: assembly routines may call C functions. The output of the compiler can be edited prior to assembly/link to further optimise the performance of the code. The compiler is also capable of accepting other programs written in C.

The compiler is currently available for the VAX/VMS and MS/PC-dos operating systems.

SECTION 4

In this section the command file, C program, and the command lines saved in batch file are given. More information on the linker command file can be obtained by referring to the TMS320C1x/TMS320C2x Assembly Language Tools User's Guide from the Texas Instrument company.

---

1. For further information refer to [33] and [41].

```
*************************************************************************

                                C PROGRAM

*************************************************************************


 /*  This  program  has been developed for hardware  simulation  of  */

/*  an adaptive defibrillator. This program requires the FIT developed*/

/*  run board for the digital signal processing applications.*/


#include "ioports.h"
#include "math.h"
#include "stdlib.h"
#define port0 0
#define port4 4
#define clamp 8824      /* first sampling level (50mA)*/


main()

{

int dataout;
int datain;
int j,i;
i=0;
j=0;

  start:

        outport(port0,20000);             /* turn off the FET */

              delay(25);

              inport (port0,&datain);      /* sample the first data  */

        if  (datain>clamp)  /* check if it is larger than 50 mA  */

    {
              delay(57);              /*delay 100usec*/

              inport (port0,&datain);       /*take the second sample*/

              dataout=datain;

         /* check if the sample diferences are larger than */
                    /*the look-up table values*/

   if(dataout >= 10024 && dataout < 9950)
         {
              delay(209);
              outport(port0,0);
              delay(25);      /* if yes, turn on the FET */
         }

   if (dataout >=10105 && dataout < 10024 )
         {
              delay(166);
              outport(port0,0);
              delay(25);
         }
```

```
if (dataout >= 10194 && dataout < 10105 )
      {
            delay(139);
                  outport(port0,0);
            delay(25);
      }

if (dataout >= 10289 && dataout < 10194)
      {
            delay(119);
                  outport(port0,0);
            delay(25);
      }

if (dataout >= 10360 && dataout < 10289)
      {
            delay(103);
                  outport(port0,0);
            delay(25);
      }

if (dataout >= 10436 && dataout < 10360)
      {
            delay(91);
                  outport(port0,0);
            delay(25);
      }

if (dataout >= 10524 && dataout < 10436)
      {
            delay(80);
                  outport(port0,0);
            delay(25);
      }

if (dataout >= 10609 && dataout < 10524)
      {
            delay(72);
                  outport(port0,0);
            delay(25);
      }

if (dataout >= 10690 && dataout < 10609)
      {
            delay(64);
                  outport(port0,0);
            delay(25);
      }

if (dataout >= 10787 && dataout < 10690)
      {
            delay(57);
                  outport(port0,0);
            delay(25);
      }

if (dataout >=10861 && dataout < 10787 )
      {
            delay(51);
                  outport(port0,0);
            delay(25);
      }
```

```
if (dataout >= 10951 && dataout < 10861 )
      {
            delay(46);
                  outport(port0,0);
            delay(25);
      }

if (dataout >= 11039 && dataout < 10951)
      {
            delay(41);
                  outport(port0,0);
            delay(25);
      }

if (dataout >= 11124 && dataout < 11039)
      {
            delay(37);
                  outport(port0,0);
            delay(25);
      }

if (dataout >= 11206 && dataout < 11124)
      {
            delay(33);
                  outport(port0,0);
            delay(25);
      }

if (dataout >= 11309 && dataout < 11206)
      {
            delay(29);
                  outport(port0,0);
            delay(25);
      }

if (dataout >= 11410 && dataout < 11309)
      {
            delay(26);
                  outport(port0,0);
            delay(25);
      }

if (dataout >= 11484 && dataout < 11410)
      {
            delay(23);
                  outport(port0,0);
            delay(25);
      }

if (dataout >= 11580 && dataout < 11484)
      {
            delay(20);
                  outport(port0,0);
            delay(25);
      }

if (dataout >= 11675 && dataout < 11580)
      {
            delay(17);
                  outport(port0,0);
            delay(25);
      }
```

```
   }
        goto start;
}

delay(j)                    /* delay routine*/
{
int k;
k=0;
        for (k=0;k<j;k++)
              {     k++;
                    k--;
              }
}
```

```
*************************************************************************

    This file is the required command file for the linker.

*************************************************************************

-c
-u RESET
-o hossien.out
-m hossien.map

hossien.obj
-l rts.lib
-l flib.lib

MEMORY

{
   PAGE 0 :VECS (IRX): origin = 0h,      length=030h

           CODE (IRX): origin = 030h,    length=0F90h

   PAGE 1 :POD (WIRX) : origin=00300h , length=10000h

}

SECTIONS

{
   vectors 00000h       :{ } > VECS PAGE 0

   .text                :{ } > CODE PAGE 0

   .data                :{ } > CODE PAGE 0

   .bss                 :{ } > POD PAGE 1
}

*************************************************************************

This section is the batch file written for the assembling, linking and

running the C programs.

*************************************************************************

dspc hossien
del hossien.tag
dspa -l hossien.asm
dsplnk hossien.cmd
dsprom -t hossien.out
swds
```

APPENDIX G

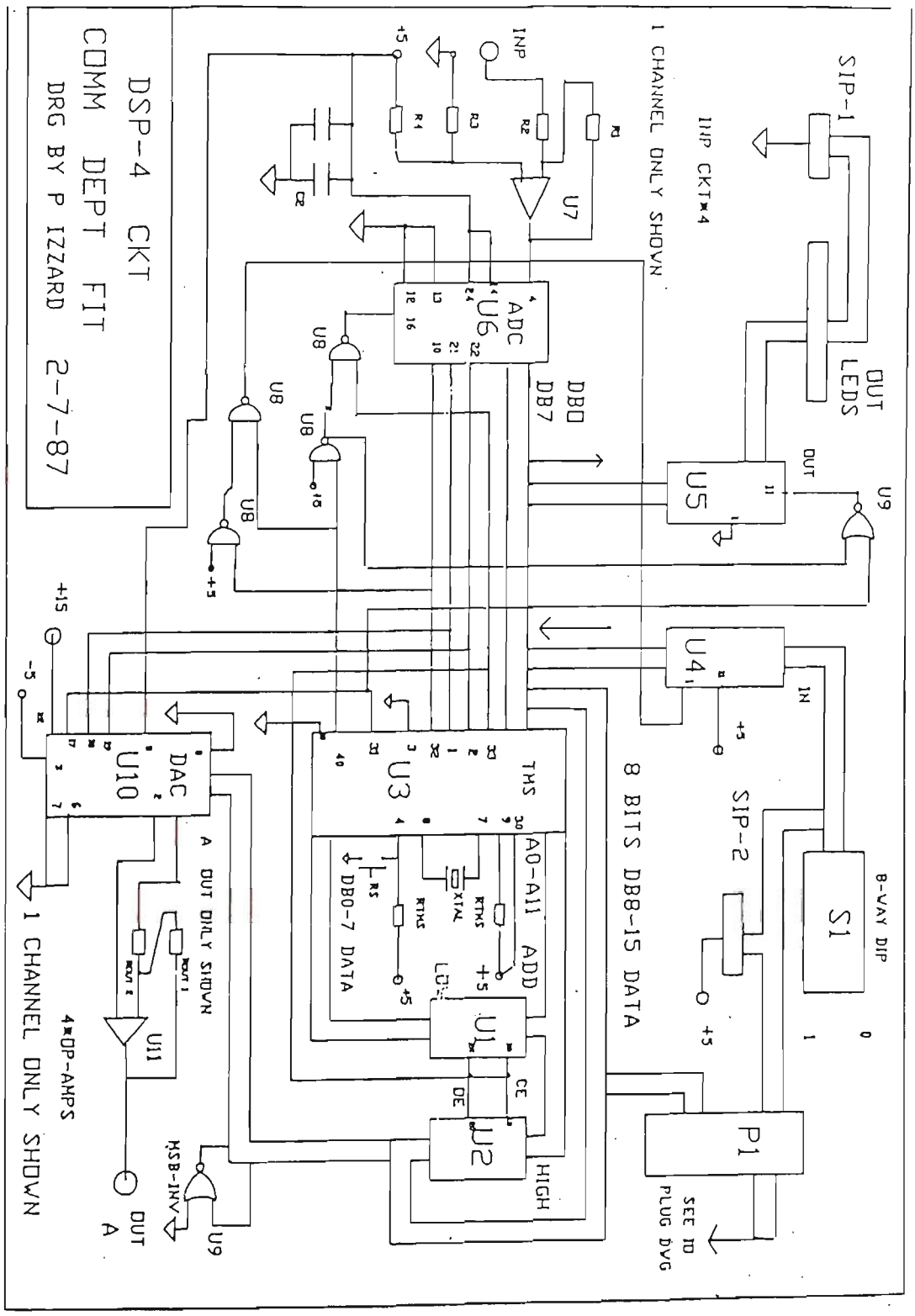

Figure G.1 Schematic diagram of the analogue interface board for TMS320C25 DSP board.

APPENDIX H

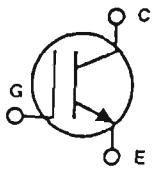

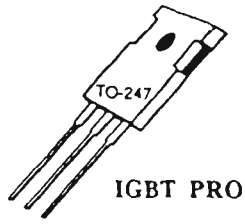

ADVANCED POWER TECHNOLOGY®

IGBT PRODUCT INTRODUCTION

IGBT's have been attracting a tremendous amount of attention lately, in both the trade press and amongst our customers. They represent a huge market opportunity for APT, at very attractive prices.

Advantages of IGBT vs Bipolar Darlington

- Drives like a MOSFET
  - Voltage controlled device
  - Simpler drive circuit design
  - Lower power losses in drive circuitry
- Lower Switching Losses
  - Fast turn-on speed
  - Comparable turn-off speed
  - Max switching frequency ~ 30 KHZ
- Better Turn-Off Safe Operating Area (RBSOA)

Advantages of IGBT vs MOSFET

- Lower conduction losses
- Greater current handling capability per unit chip size
- Lower cost per amp

Target Applications

Frequency Inverters
Uninterruptible Power Supplies
Low Frequency Switching Power Supplies
Defibrulators
Welding Equipment
Motor Control Circuits
Linear Amplifiers

Initial Product Offering: See attached for detail.

Die Size: 204 & 205
Package: Plastic TO-247
Voltages: 600V and 1000V

Future Products

In late 1991 and early 1992 will be expanding our offering into larger die sizes in TO-247 Isotops, modules and military packages and eventually in voltages up to 1200V.

Pricing

No price sheets are available yet, but in general we are seeing prices that are 2 or 3 times the price of an equal die size and voltage MOSFET.

Competitive Analysis: See the attached sheets.

In general we believe that our IGBT devices will offer the same competitive advantages as our MOSFETs.

BIBLIOGRAPHY

1. Aronson, A. L., Haggar, B. , (1986); ' The automatic external defibillator-pacemaker: Clinical rationale and engineering design', Medical Instrumentation, V20, N1, 27-35, Jan-Feb.

2. Bennett, P. I., Jones, V.C. (1982); 'Portable defibrillator monitor for cardiac resuscitation', Hewlett-Packard, J 22-28.

3. Cameron, J. R., Skofronick, J. G., 1978, ' Medical Physics ', Wiley & Sons, Inc..

4. Church, T. R., Martinson, M. S., Watson, W. S., Kallok, M. J., (1988); ' Determination of Individual Defibrillation Thresholds From Population Data and Limited Interaoperative Trials', Medical Instrumentation, V22, N6, 293-297, Dec.

5. Dahl, F., Ewy, G., Ewy, D., Thomas, D. (1976) ; ' Transthoracic impedance to direct current discharge: Effect of repeated countershocks', Medical Instrumentation, V10, N3, 151-154.

6. Ewy, A., Hellman, D. A., McClug, S., Taren, D., (1980); ' ' Influence of ventilation phase on transthoracic impedance and defibrillator effectiveness', Crit. Care Med., 8, 3, 164-166.

7. Ewy, A. , Taren, D., (1978) ; 'Impedance to transthoracic direct current discharge: A model for testing interface material', Medical Instrumentation, V12, N1, 47-48, Jan-Feb.

8. Ewy, A. , Taren, D. , Bangert, G., Clungs, S., Hellman, A. (1980); ' Comparison of myocardial damage from defibrillator discharge at various voltages' , Medical Instrumentation, V14, N1, Jan-Feb.

9. Ganong, W. F. , (1989) ; 14th Ed. Review of Medical Physiology, Prentice-Hall International Inc..

10. Geddes, L. A. , (1972); ' Electrodes and the Measurement of Bio-electric Events', Wiley Interscience.

11. Geddes, L. A. (1976) ; ' William Kowenhoven, a pioneer Biomedical Engineer', Medical Instrumentation, V10, N3, May-June.

12. Geddes, L. A., Niebauer, M. J., Babbs, F. , Bourland, J. D. (1985); ' Fundamental criteria underlying the efficacy and safety of defibrillating current waveform', Medical & Biological Eng & Computing 23,122-130, March.

13. Geddes, L. A., Tacker, W. A., McFarlane, J., Bourland, E. E., (1970); ' Strength-duration curves for Ventricular Defibrillation in dogs, Cir. Res. 27, 551-650.

14. Geddes, L. A., Tacker, W.A., Schoenlein, W., Minton, M., Grubbs, S., Wilcox, P. , (1976); ' The prediction of the impedance of the Thorax to defibrillate current', Medical Instrumentation, V10, N3, 159-162, May-June.

15. Guyton, A. C., (1981); 6th Ed. Textbook of Medical Physiology, W.B. Saunders.

16. Holmes, (1980), ' Hemodynamic response to two defibrillator trapezoidal waveforms ', Medical Instrumentation, 14, 47-50.

17. Holmes, R. , Bourland, D. , Tacker, A., Geddes, L. A., (1980); ' Hemodynamic response to two defibrillating trapezoidal waveforms' Medical Instrumentation, V14, N1, 47-50, Jan-Feb.

18. Kavakami, K., Kira, S., (1973); 'Associated change of transthoracic electrical impedance with regional ventilation of the lung', Medical and Biological Engineering, 469-478, July.

19. Lappin, L. A., (1974); ' Ventricular Defibrillation in Heavy Patients ', N. Engl., J. Med., 291, 153.

20. McDaniel, W. C., Schuder, J. C., (1988); ' An Up-Down Algorithm for Estimation of the Cardiac Ventricular Defibrillation', Medical Instrumentation, V22, N6, 286-292, Dec.

21. Machin, J. W., Briwnhill, J. (1987); ' Thoracic impedance during defibrillation- a curious discrepancy', Medical & Biological Eng & Computing, 25, 679-683, November.

22. Maxwell , R. F. , (1985) ; ' Skin resistance changes during electrocution', M. Eng. Sc. Thesis, University Of Melbourne, Australia.

23. MC6809 Assembler reference manual, FIT., 1986.

24. Miyamoyo, Y., Takahashi, M., Tamura, T., Nakamura, T., Hiura, T., Mlkami, M., (1981); ' Continuous determination of cardiac output during exercise by the use of impedance plethysmography. Medical & Biological Eng & Computing, 19, 638-644, Sept.

25. Monzon, E., Guiller, G., (1985); ' Current defibrillator: New instrument of programmed current for research and clinical use' IEEE transactions on Biomedical Engineering, Vol. BME-32 No11, Nov.

26. Motorola MC6800 series Handbook, Motorola Co., 1982.

27. Niebauer, M. J., Babbs, C. F., Geddes, L. A., Bourland, J. D. (1984); 'The efficacy and the safety of the defibrillation with the 10 msec trapezoidal waveforms of different tilts, Medical Instrumentation V18, N2, 119-121, March-April.

28. Packer, J., Zayegh, A. (1987); 'Adaptive Control of defibrillator energy delivery using Digital Signal Processor', proceeding of the ISSPA87 , Signal Processing, theories, implementations and application, 799-802.

29. Peleska, B., (1965); ' Cardiac arrhythmias following condenser discharges fed through an inductance- comparison with effects of pure condenser discharges', Circ. Res. 16:11-18.

30. Raber, M. B., Osman, F. S. (1986); 'User views on standards for defibrillators', Medical Instrumentation, V20, N6, 316-319.

31. Ruiz, V. , Rosso, A. , Savino, V. , Valentiuzzi, E. , (1985); ' Ventricular fibrillation threshold in the dogs determined with the defibrillator paddles ', Medical & Biological Eng & Computing, May .

32. Schuder, J. C., Mcdaniel, W. C., Stoeckle, H., Yerkovich, D., (1988); ' Comparison of Effectiveness of Relay-Switched, One-Cycle Quasisinusoidal Waveform with Critically Damped Sinusoid Waveform in Transthoracic Defibrillation of 100-Kilogram Calves', Medical Instrumentation, V22, N6, 281-280, Dec.

33. Second-Generation TMS320 User's Guide, Texas Instrument Co., 1988.

34. Tacker, W. A., (1968); 'Defibrillation without A-V block using capacitor discharge with added inductance', Circ. Res. 22:633-638.

35. Tacker, W. A. (1976); 'Defibrillation research: Search for the shocking truth', Medical Instrumentation, V10, N3, May-June.

36. Tacker, W. A. , Galioto, F. M. , Guiliani, E., Geddes, L. A., McNamara, D., (1974); ' Energy Dosage for Human Trans-chest Electrical Ventricular Defibrillation ', N. Engl. J. Med. 290, 214-215.

37. Tacker, W. A., Geddes, L. A. (1980); ' Electrical Defibrillation' , CRC Press, Boca Raton, Florida.

38. Tacker, W. A., McNamara, D., Guiliani, E., Geddes, L. A., (1974); ' An Energy Dose for Human Ventricular Defibrillation ', Amer. J Cardiol. 33, 172.

39. Tacker, W. A. , Paris ,R. , (1983); ' Transchest defibrillation effectiveness and electrical impedance using disposal conductive pads', Heart & Lung,12 510-513.

40. Thomas, E. D., Ewy, G. A., Dahl, C. F., Ewy, D., (1977); ' Effectiveness of Direct Current Defibrillation: Role of Paddle Electrode Size', Amer. Heart J. 93: 463-467.

41. TMS320C1x/TMS320C2x Assembly Language Tools User's Guide, Texas Instrument. Co., 1988.

42. Trahanias, P., Skordalakis, E., (1989); ' Bottom-up approach to the ECG pattern-recognition problem', Medical & Biological Eng & Computing, 27, 221-229, May.

43. Tulloh, A. M., (1983) ; ' Transthoracic Resistance during cardiac defibrillation', M. Eng. Sc. Thesis, University Of Melbourne, Australia.

READING BIBLIOGRAPHY

1. Bipolar Power Transistor Data Book, Motorola Co., 1984.

2. Bourland, D., Babbs, F., Tacker, W. A., Geddes, L. A., (1980); ' An animal model for testing automatic defibrillators', Medical Instrumentation, V14, N1, 15-17, Jan- Feb.

3. Bourland, B., Tacker, W. A., Wessal, L., Kallok, J., Graf, E., Geddes, L. A., (1986); ' Sequential pulse defibrillation for implantable defibrillators, Medical Instrumentation, V20, N3, 138-142, May-Jun.

4. Burne, R. M., Levy, M. N., (1981); ' Cardiovascular Physiology', 4th Ed., C.V. Mosby Company.

5. Carr, J. J., Brown, J. M., 1981, ' Introduction to Biomedical Equipment Technology', John Wiley & Sons, Inc..

6. Cathinol, D., Fourcade, C., Jossinet, J., Lavandier, R., (1978); ' Interface of pulmonary exploration by the real-time treatment of curves obtained by thransthoracic impedance', Medical & Biological Eng & Computing, 16, 459-470, Sept.

7. Eiken, O., Segerhammer, P., (1987); ' Elimination of breathing artifacts from impedance cardiograms at rest and during exercise', Medical & Biological Eng & Computing, 26, 13-16, April.

8. Ewy, G., Horan, W. (1976); ' Electrode catheter for transvenous defibrillation', Medical Instrumentation, V10, N3, 155-158.

9. Gold, H., Schuder, J., Stoeckle, H., (1980); ' Ventricular defibrillation with myocardial electrodes in the dog, calf, pony, and pig', Medical Instrumentation, V14, N1, 19-21, Jan-Feb.

10. Gray's Anatomy, (1980); 36th Ed. Churchill Livingstone, Williams & Warwick.

11. Khan, M., Tandon, S., Guha, S., Roy, S., (1977); ' Quantitative electrical-impedance plethysmography for pulmonary oedema', Medical & Biological Engineering & Computing, 15, 627-633, Nov.

12. Konrad, P. E., Tacker, W. A., Bourland, J. D., Geddes, Hood, D., (1988); ' A New Implantable Arterial Pulse Sensor For Detection of Ventricular Fibrillation', Medical Instrumentation, V22, N6, 304-311.

13. Langer, A., Heilman, M. S., Mower, M. M., Mirowski, M., (1976); ' Considerations in the development of the automatic implantable defibrillator', Medical Instrumentation, V10, N3, 163-167.

14. Linear data book, National semiconductor Co., 1984.

15. Linear Products Databook, Analogue Devices, 1988.

16. Luceri, R. M., Castellanos, A., Myerburg, R., Myerburg, R.J.,(1986); ' Implantable devices for the Treatment of Cardiac Arrhythmias', Medical Instrumentation, V20, N5, ,277-289, Sept-Oct.

17. Maijer, H., Reulen, H., Oe, L., Allon, W., Thijs, L., (1982); ' Differential impedance plethysmography for measuring thoracic impedances', Medical & Biological Eng & Computing, 20, 187-194.

18. O'Dowd, J., (1983); ' Defibrillator design and development review', Journal of Medical Engineering & Technology, V7, N1, 5-15, Jan-Feb.

19. Panerai, B., Neto, G, (1982); ' Surface mapping of transthoracic impedance Cardiogram', Medical & Biological Engineering & Computing, 20, 274-280, May.

20. Power Mosfet Transistor Data Book, Mortorola Co., 1989.

21. Ruffy, R., Schwartz, D. J., Hieb, B., (1980); ' Influence of acute coronary artery occlusion on direct ventricular defibrillation in dogs', Medical Instrumentation, V14, N1, 23-26, Jan-Feb.

22. Rushmer, R., 1976, 'Cardiovascular Dynamics', W. B. Saunders Co..

23. Turbo C reference Guide, Borland, 1987.

24. Turbo C User's Guide, Borland, 1987.

25. Van Boxtel, A., (1977); ' Skin resistance during square wave electrical pulses of 1 to 10mA', Med. Biol. Eng. Compt., 17, 679-687.

PUBLISHED WORK

Proceedings Intern. AMSE Confer. "Applic. of Signals, Data, Systems Methodologies to Engineering Problems", Alexandria (Egypt), Dec. 28-30, 1992, AMSE Press, Vol. 2, pp. 215-223

ADAPTIVE DEFIBRILLATOR: NEW APPROACH TO IMPLEMENTING AN AUTOMATED DEFIBRILLATOR ENERGY DELIVERY

A. ZAYEGH, J. S. PACKER*, H. MAHDAVIAN

Department of Electrical & Electronic Engineering
Victoria University of Technology

* Department of Electrical & Electronic Engineering
University of Melbourne

Melbourne, Victoria, Australia

ABSTRACT It is well established that successful defibrillation depends on the energy selected and the transthoracic resistance (TTR) of the patient. To achieve an effective and safe defibrillation, the TTR should be measured accurately during the defibrillator pulse where the breakdown phenomenon of the skin resistance occurs, followed by the adjustment of the defibrillator parameters to ensure the correct current flow through the heart to completely depolarise all myocardial cells without any associated tissue damage being caused by heating.

In this paper, an online technique is described which determines the dynamic TTR and adjusts the defibrillator current to ensure safe operation regardless of patient variability.

INTRODUCTION

Defibrillation is a well established technique for terminating a potentially fatal malfunction of the heart characterised by onset of irregular high frequency contractions. This is achieved by discharging a capacitor through the thoracic cavity including the heart. In defibrillation, current flow depends on the energy selected and the transthoracic resistance. If transthoracic resistance is high, current flow may be inadequate to defibrillate. For the most effective use of a defibrillator, sufficient current must be delivered to the heart to completely depolarise all myocardial cells without any associated tissue damage being caused by heating (Packer et al 1987).

It is universally accepted that for the successful defibrillation, the electrical current passing through the heart has to reach a threshold level. Geddes et al (1985) have shown that for a damped sinusiodal waveform of 4-6 ms duration an average minimum current density of 55 mA/cm2 is required for defibrillation of the myocardial tissue. Since only a relatively small portion of the current delivered by an external

defibrillator actually passes through the heart, peak current delivered by the defibrillator circuit must be of the order of 40-60 A if defibrillation is to be achieved. (Geddes et al 1974) have suggested that 1 A/Kg of body weight is required for defibrillation.

Currently, available defibrillators offer a range of stored energy levels for providing a stimulus to a patient. However, usual practice is to apply the maximum energy level available (360 joules) on the first application and repeat if successful defibrillation is not achieved. This procedure gives a high recovery rate on the first application but leads to excessive tissue damage in many patients. For these patients lower energy levels would probably have achieved defibrillation without significant tissue destruction.

Efforts are being made to overcome this problem by measuring the patient resistance using low voltage measurement of resistance prior to initiation of the defibrillation pulse (Kerber et al 1985). The difficulty of this approach is that low voltage measurement of resistance does not cause the breakdown phenomenon of skin resistance which occurs during the high voltage pulse. This may result in inaccurate estimates of the resistance and unsatisfactory adaptation of the defibrillator parameters.

Maxwell (1985) has shown that during the first 50 micro sec. of the defibrillation the TTR value drops from KΩ range to 100Ω range when the skin resistance breakdown occurs see figure 1.

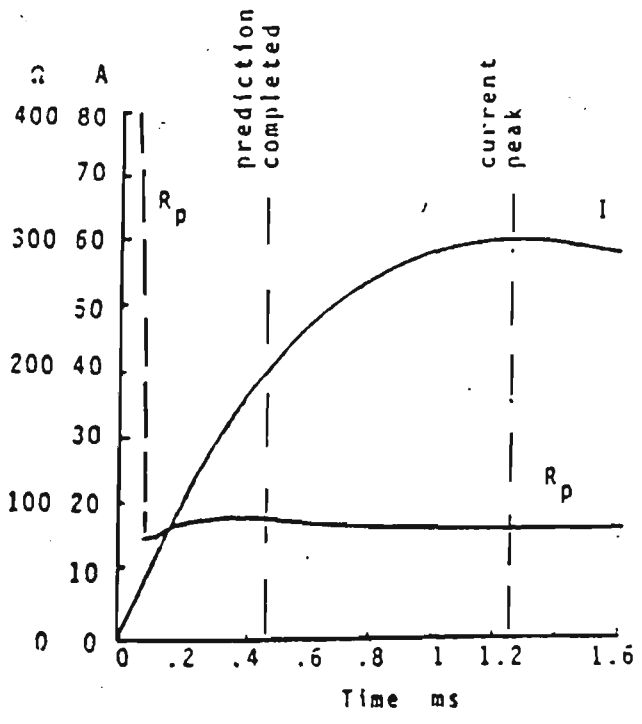

Figure 1 Variation of Rp and I for first 1.6 ms of the defibrillation pulse. Rp = TTR values derived from (Maxwell 1985).

He showed that by 100 micro sec. after the initiation of the current pulse, the resistance was within 20% of its final value. It is this final value of resistance which determines the magnitude of the current peak occurring at typically 1.2 ms from initiation of the pulse. For different patients transthoracic resistance may vary over the range of 25 - 125 ohms. The fact that an estimate of patient breakdown resistance can be obtained after 100μs provides the possibility of predicting the current peak before it occurs. If this prediction can be made then it should be feasible to adapt the defibrillator parameters during the discharge to ensure that safe and effective current levels are achieved for all patients regardless of their physical characteristics.

Packer et al (1987) have shown that it is possible to measure the patient TTR during the discharge of the defibrillation pulse but after the skin resistance breakdown occurrence (using high speed controller) , and adjust the current peak to the patient by switching the necessary by-pass network to the defibrillator circuit.

This paper details a new approach for implementing an adaptive defibrillation technique which can measure the patient thransthoracic resistance during the discharge of the defibrillator current and adjust the defibrillator parameters to ensure satisfactory defibrillation and safe operation regardless of the patient variability.

MATERIALS AND METHODS

Measurement of the TTR

It is well know that a variety of current waveforms can achieve ventricular defibrillation (Tacker et al 1980). To date Lown or damped Sinusoidal current waveform is most currently used in defibrillators. The circuit used to generate this waveform is shown in figure 1. The capacitor is charged to the required energy level (e.g. 400 joules) and then discharged through the inductor and the patient via the two electrodes.

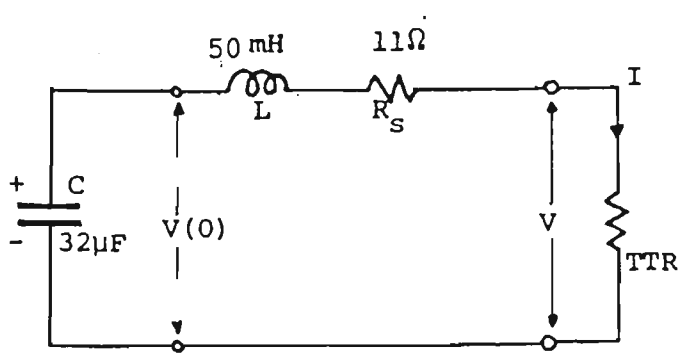

Rs = internal resistance of the defibrillator
TTR = transthoracic resistance of the patient
I = current delivery to patient
V = electrode to electrode volltge
V(0) = the initial voltge across the capacitor

Figure 2 Typical defibrillator/patient circuit.

The governing equation of Lown current generated by the defibrillator is an integro-differential equation of the following form

$$L\frac{di(t)}{dt} + \frac{1}{C}\int i(t)dt + V(0) + i(t)(R_s + TTR) = 0 \qquad (1.1)$$

To determine the peak current during defibrillation discharge, it is necessary to solve the above equation for a specific value of the patient resistance. The patient TTR varies during the discharge due to the breakdown of skin resistance during the first 50νs of the defibrillation pulse, Therefore the first measurement of TTR should not start before 100 vs (TTR value should be within 20% of its final value (Maxwell 1985)). The measurement of TTR requires the measurement of V (electrode to electrode voltage) and I (the circuit current) after 100νs of the pulse current starting.

Method:

In Lown (damped sinusoidal) waveform defibrillator circuit shown in figure 2, if the parameters of the circuit are known (e.g. L, C, Rs, and V(0)) and TTR is linear, therefore by measuring the current in the circuit, the value of TTR can be found by solving the differential equation 1.1 . Alternatively, this equation can be solved to calculate the current i(t) for different TTR values and a constant energy setting. This energy must be large enough to defibrillate the heart of the patient with expected TTR = 125 (360 joules). A look-up table can be established with the values of the current i(t) for TTR range of 25 to 125 ohms in increments of say 5 ohms (depending on the required accuracy of the system).

Now, if the current i(t) is measured during the defibrillation, the value of TTR can be found from the look-up table, because the solution of the above differential equation is monolithic and there is just one specific value of current which can result in one specific TTR value.

Due to the skin resistance breakdown, a correction factor must be used for the calculation of the look-up tables. For example, in numerical methods for the solution of the above differential equation, TTR can be assumed as a function of time, for which its value is high during the first 50-100νs of the defibrillation pulse and low otherwise.

The use of the look-up table technique for for the prediction of TTR values, threshold values, instead of on-line calculation of these values, provides two advantages:

a) it greatly reduces the required calculation time of the controller, which should be much less than the peak current time
b) it provides more time for the controller to improve the adaptive algorithm.

Hardware Implementation

To investigate the validity of this concept practically, a simulated defibrillator was built with low energy level. The parameters of this simulated circuit were selected similar to the real defibrillator parameters. (e.g. C=30νF, L= 53.3 mH, Rs =15, V(0) = 12 V).

The adaptive controller is based on a high speed microprocessor The TMS32025 Digital Signal Processor with an Analog Interface Board (AIB) and high speed switching by-pass circuit. A schematic diagram of the adaptive defibrillator is shown in figure 3. As in the commercial defibrillator a relay was used to discharge the energy stored in the capacitor C in the TTR.

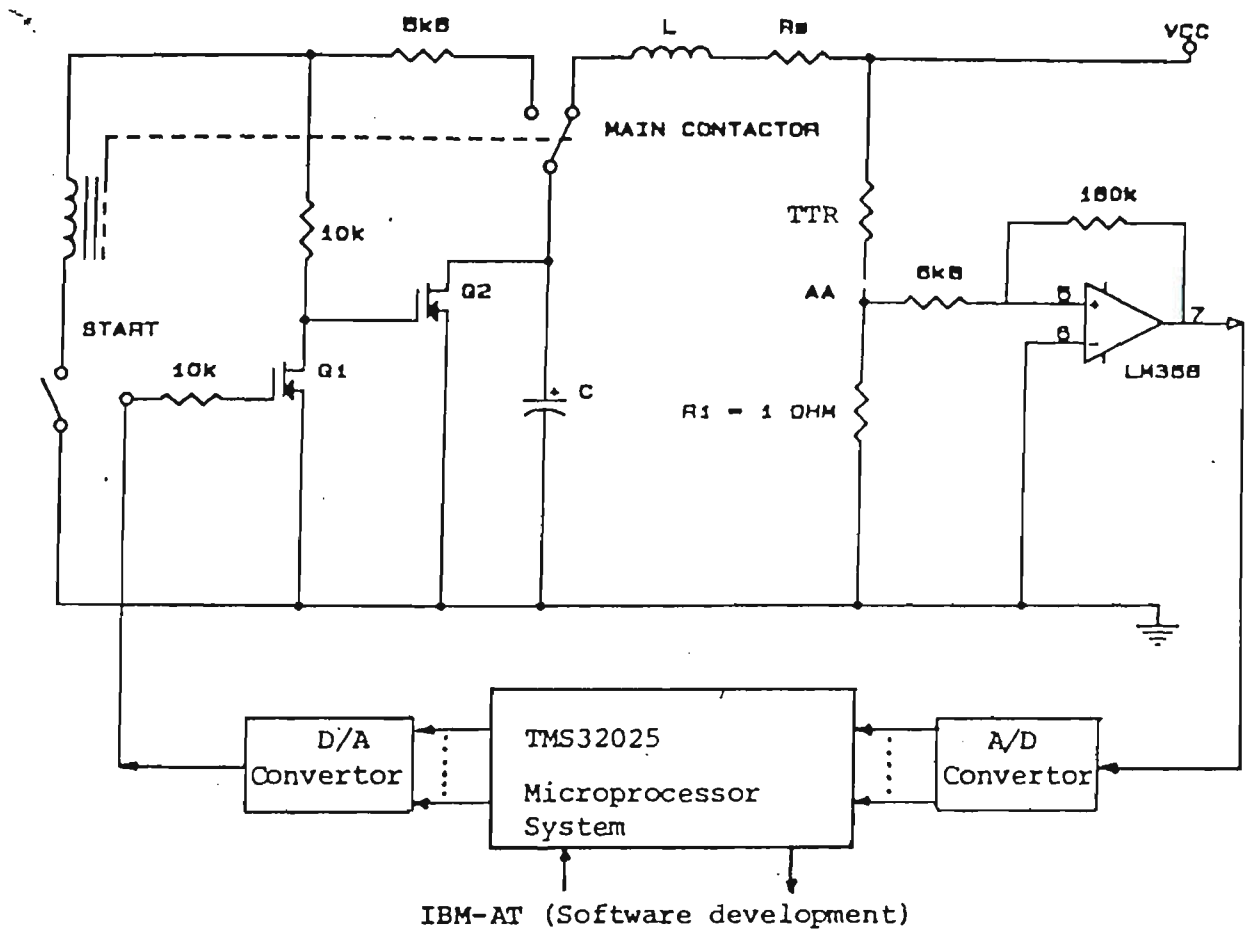

Figure 3 The schematic diagram of the adaptive defibrillator.

Bouncing of the relay generates large spikes reported by several sources as a major problem in TTR measurement (Tulloh 1983) and (Maxwell 1985). The spikes make it impossible for the controller to start sampling the current after the relay is activated. Also the Lown waveform is not generated exactly until the relay bouncing is stopped and its contacts are firmly closed. Several techniques are used to minimise the current spikes due to the relay bouncing, this includes high pressure encapsulation, use of mechanical damper, and activating the relay at an optimum voltage

which results in minimum mechanical oscillation of the relay's actuator (HP 1987).

SYSTEM FUNCTION

The function of the adaptive controller shown in figure 3, can be summarised as follows:

1. Initiate the defibrillation pulse.
2. Measure the current at a time greater than 50 vs (the TTR breakdown time) after the initiation of the pulse.
3. Obtain TTR values for the measured current in step 2 from the look-up table.
4. Calculate the time at which the peak current occurs and the time that the controller must wait for the current to reach the threshold value.
5. switch the by-pass network to modify the peak current.

Due to the bouncing of the relay, it was not possible to identify the initiation of the pulse immediatly after closing-on the relay. To overcome this problem, it was necessary for the controller to calculate the current by comparing two samples at a specified time interval as shown in figure 4. The first sampling

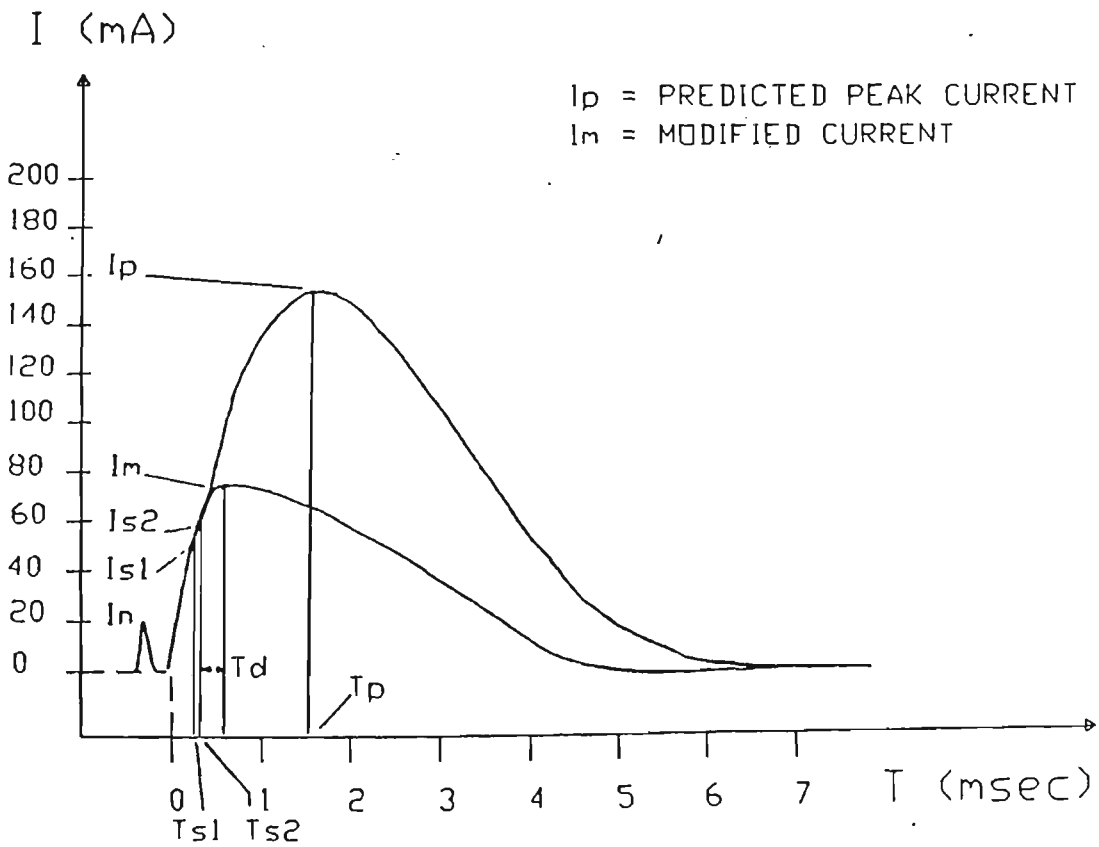

Figure 4 The dual sampling method, the threshold detection and current modification.

time should be after the current reaches to a level higher than the spikes, the second is after a specified time (100μs). From these two samples the controller can then find the related TTR, because there is just one waveform that can pass through these two sampling points for a particular TTR. Then the controller proceeds with the following steps of the operation algorithm to predict the necessary threshold current for such TTR and adjust the energy source to produce the necessary threshold current as shown in figure (4).

RESULTS

The adaptive hardware simulator system shown in figure (3) has been tested for the standard set of TTR values (25 to 125 ohms) to ascertain whether the adjustment of energy set (by inserting by-pass resistance to the circuit) would produce the required threshold current predicted by the controller. The result of the two extreme values of TTR are shown in figure (5.a & b) . Curve A indicates the current peak expected with a fixed set of energy delivery and Patient TTR = 27 ohms, where the controller is disabled. Curve B shows the adjusted current after the enabled controller has predicted the necessary threshold current and switches on the by-pass circuit at the required time.

In this work the set of the threshold currents for TTR values from 25 to 125 ohms (the range accepted for TTR) have been tested with increment of 5 ohms. This increment can be decreased to achieve better accuracy of the process. However, the prediction time will be longer as the look-up table will be larger. Therefore a faster controller must be used.

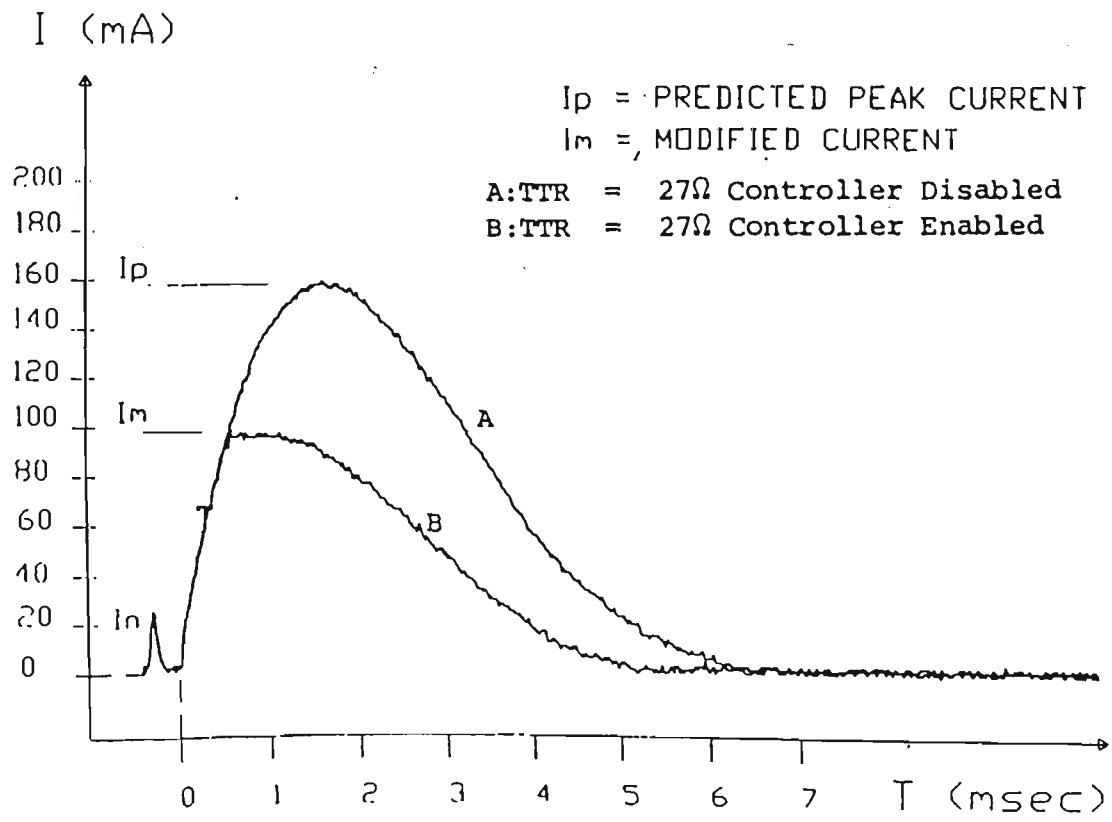

(5.a)

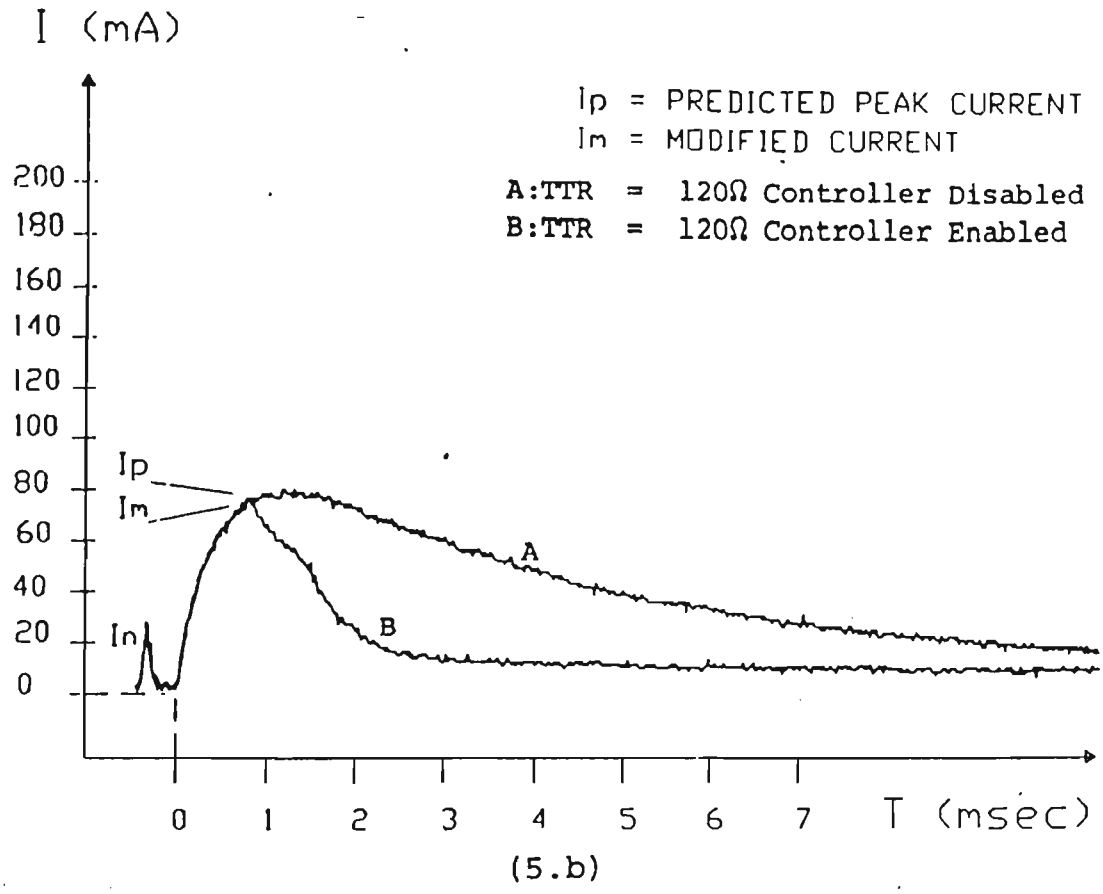

Figure 5 Adaptive modification of the defibrillator current (energy delivery) to the patient for different TTR.

CONCLUSION

In this work a prototype of an adaptive simulator is developed. The system demonstrates that the principle of an automated defibrillator energy delivery proposed in previous work by (Packer et al 1987) is feasible. The system shows quite encouraging result, which is based on a new approach in implementing the adaptive algorithm.

Several important points can be drawn from the results of this study:

1. It is possible to measure the breakdown value of the patient transthoracic resistance and predict the resultant current peak, the threshold current and then modify the energy delivery to the patient during the defibrillator discharge.

2. The principle of measuring only the current in the defibrillator circuit provide an advantage for the hardware design, where only one current transformer is necessary. This reduces the size, cost, and the isolation required between the digital controller and the high power circuit.

3. The use of look-up table technique for the prediction of TTR, and the threshold values for the measured current during the defibrillation process, has greatly reduced the controller calculation time. Therefore the adaptive algorithm became easy to implement.

This work provides clear evidence that the implementation of an adaptive defibrillator is possible. Some other technological problems might be considered. For example, the power switching for the by-pass network, bouncing of the relay, the speed of the controller, and isolation of the digital circuit from the high power circuit. Practical solutions were presented in this work for most of these problems. The rapid development of semiconductor technology for high power and low power devices will overcome all the rest of the obstacles.

REFERENCES

Geddes,L.A., Niebauer,M.J., Bourland,J.D. (1985); 'Fundamental criteria underlying the efficiency and safety of defibrillation current waveforms', Medical and Biological Engineering and Computing 23, 122-130.

Geddes,L.A., Tacker,W.A., Rosborough,J.P., Moore,A.G., Cabler,P.S. (1974); 'Electrical dose for ventricular defibrillation of large and small animals using periodical electrodes', J. Clin. Invest. 53, 310-319.

Kerber,R.E., McPherson,D., Charbounier,F., Kieso,R., Hite,P. (1985); 'Automated impedance based energy adjustment for defibrillation: experimental studies', Circulation 71, No 1, 136-140.

Maxwell,R.F. (1985); 'Skin resistance change during electrocution', M.Eng.Sc. Thesis, University of Melbourne, Australia.

Packer,J.S., Zayegh,A. (1987); 'Adaptive control of defibrillator energy delivery, using a digital signal processor', Proceeding of the ISSPA89, Signal processing, theories, implementations and applications, 799-802.

Tacker,W.A., Geddes,L.A. (1980); 'Electrical defibrillation', CRC Press, Boca Raton, Florida.

Tulloh,A.M. (1983); 'Transthoracic resistance during cardiac defibrillation', M.Eng.Sc. Thesis, University of Melbourne.